

Biosynthesis of Vitamin B₂ (Riboflavin).
Studies on the Reaction Mechanism of Riboflavin Synthase.

Dissertation

Zur Erlangung des Doktorgrades
des Fachbereiches Chemie
der Universität Hamburg

Institut für Lebensmittelchemie

Vorgelegt von

Ryuryun Kim

Hamburg, im März 2012

Die vorliegende Arbeit wurde in der Zeit von January 2008 bis September 2011 unter der wissenschaftlichen Betreuung von Prof. Dr. Markus Fischer und Dr. Boris Illarionov an Institut für Lebensmittelchemie der Universität Hamburg angefertigt.

1. Gutachter der Dissertation: Prof. Dr. Markus Fischer
2. Gutachter der Dissertation: Prof. Dr. Ulrich Hahn

Tag der Disputation: 11. Mai 2012

Dedicated to my parents

Publications

Haigney, A., Lukacs, A., Zhao, R. K., Stelling, A. L., Brust, R., **Kim, R.R.**, Kondo M., Clark. I., Towrie, M., Greetham, G. M., Illarionov, B., Bacher, A., Römisch-Margl, W., Fischer, M, Meech, S. R., and Tonge, P. J. (2011) Ultrafast Infrared Spectroscopy of an Isotope-Labeled Photoactivatable Flavoprotein. *Biochemistry*, 50, 1321-1328

Kim, R.R., Yi, J.H., Nam, K.S., Ko, K.W., and Lee, C.Y. (2011) Spectrofluorometric Characteristics of the N-terminal domain of riboflavin synthase. *The Korean Journal of Microbiology*, 47, 14-21

Kim, R.R., Illarionov, B., Joshi, M., Cushman, M., Lee, C.Y., Eisenreich, W., Fischer, M., Bacher, A. (2010) Mechanistic Insights on riboflavin Synthase Inspired by Selective Binding of the 6,7-dimethyl-8-ribityllumazine Exomethylene Anion, *J. Amer. Chem. Soc.*, 132(9), 2983-2990

Kim, S.Y., **Kim, R.R.**, Choi, J.S., Kim, Y.D., and Lee C.Y. (2010) Purification and characterization of the Amino-terminal domain of Lumazine protein from *Photobacterium leiognathi*, *Bulletin of the Korean chemical society*, 31, 1017-1020

Poster Presentations

Kim, R.R., Illarionov, B., Haase, I., Bacher, A., Fischer, M. (2011) Preparation of selectively deuterated riboflavin, *40th Deutscher Lebensmittelchemikertag 2011*

Kim, R.R., Illarionov, B., Joshi, M., Eisenreich, W., Bacher, A., Lee, C.Y., Haase, I., Fischer, M. (2008) NMR studies on the interaction of 6,7-dimethyl-8-ribityllumazine with the N-terminal domain of riboflavin synthase. *37th Deutscher Lebensmittelchemikertag 2008*

Abstract

Riboflavin synthase catalyzes the transfer of a 4-carbon fragment between two molecules of the substrate, 6,7-dimethyl-8-ribityllumazine, resulting in the formation of riboflavin and 5-amino-6-ribitylamino-2,4(1*H*,3*H*)-pyrimidinedione. Earlier, a pentacyclic adduct formed from two substrate molecules was shown to be a catalytically competent intermediate, but the mechanism of its formation is still poorly understood. The present study shows that the recombinant N-terminal domain of riboflavin synthase from *Escherichia coli* interacts specifically with the exomethylene-type anion of 6,7-dimethyl-8-ribityllumazine but not with any of the tricyclic adduct-type anions that dominate the complex anion equilibrium in aqueous solution. Whereas these findings can go along with previously published mechanistic hypotheses, we also present a novel, hypothetical reaction sequence that starts with the transfer of a hydride ion from the 6,7-dimethyl-8-ribityllumazine exomethylene anion to an electroneutral 6,7-dimethyl-8-ribityllumazine molecule. The pair of dehydrolumazine and dihydrolumazine molecules resulting from this hydride transfer is proposed to undergo a 4+2 cycloaddition affording the experimentally documented pentacyclic intermediate. In contrast to earlier mechanistic concepts requiring the participation of a nucleophilic agent, which is not supported by structural and mutagenesis data, the novel concept has no such requirement. Moreover, it requires fewer reaction steps and is consistent with all experimental data.

Kurzfassung

Riboflavinsynthase katalysiert die Übertragung eines Vierkohlenstofffragmentes zwischen zwei 6,7-Dimethyl-8-ribityllumazinmolekülen. Dabei entstehen ein Riboflavinmolekül und ein 5-Amino-6-ribitylamino-2,4(1*H*,3*H*)pyrimidindionmolekül. Wie früher berichtet wurde, entsteht dabei als Reaktionsintermediat ein pentazyklisches Addukt aus zwei Lumazinmolekülen, welches durch Riboflavinsynthase teil zu Riboflavin, teil zu Pyrimidindion umgewandelt wird. Das pentazyklische Addukt wurde vor zehn Jahren entdeckt. Trotzdem blieb die Reaktionssequenz, die zu seiner Bildung führen kann, eher problematisch. In dieser Studie wurde nachgewiesen, dass die rekombinante N-terminale Domäne der Riboflavinsynthase aus *Escherichia coli* das Exomethylenanion, aber keines der trizyklischen Addukten von 6,7-Dimethyl-8-ribityllumazin binden kann, obwohl die letzteren das Aniongleichgewicht in wässrigen Lösungen von Lumazin dominieren. Basiert auf dieser Erkenntnis wird eine neue hypothetische Reaktionssequenz für Riboflavinsynthase vorgeschlagen. Diese fängt mit der Übertragung eines Hydridions von 6,7-Dimethyl-8-ribityllumazinexomethylenanion auf elektroneutrales 6,7-Dimethyl-8-ribityllumazinmolekül an. Das dadurch entstandene Molekülpaar, Dehydrolumazin und Dihydrolumazin, gehen in eine 4 + 2 Zyклоaddition ein das zu einem experimentell nachgewiesenen pentazyklischen Reaktionsntermediat führen kann. Im Unterschied zu den früheren Hypothesen über den Reaktionsablauf braucht der vorgeschlagene Reaktionsmechanismus die Beteiligung eines Nukleophils nicht. Übrigens, die Hypothese über Existenz eines solchen Nukleophils fand trotz zahlreicher Daten über räumlicher Struktur des Enzyms noch keine Unterstützung. Das neue Konzept braucht eine solche Anforderung nicht, ist wesentlich einfacher und steht in Einklang mit allen vorhandenen experimentellen Daten.

Table of Contents

<i>Publications</i>	i
<i>Poster Presentations</i>	ii
<i>Abstract</i>	iii
<i>Table of Contents</i>	v
<i>Acknowledgements</i>	ix
1 Introduction	1
1.1 Riboflavin	1
1.1.1 Overview of the biosynthesis of riboflavin	2
1.1.2 Riboflavin synthase	5
1.1.3 Flavokinase and FAD synthetase	8
1.2 Isotope-labeled riboflavin and 6,7-dimethyl-8-ribityllumazine	9
1.2.1 Random isotopologue mixtures of 6,7-dimethyl-8-ribityllumazine and riboflavin by <i>in vivo</i> biotransformation	9
1.2.2 Rapid one-pot enzyme-assisted synthesis of riboflavin	10
1.3 Flavoproteins	12
1.3.1 Blue-light receptors using flavin chromophores	12
1.3.1.1 LOV domains	13
1.3.1.2 BLUF domains	15
1.3.2 DNA photolyase.....	16
2 Materials and Methods	19
2.1 Materials	19
2.1.1 Chemicals	19
2.1.2 Substrates and cofactors	20
2.1.3 Enzymes	20
2.1.4 Culture medium.....	21
2.1.5 Buffers.....	22
2.2 Instruments	25
2.3 Methods	26
2.3.1 Cloning and mutagenesis.....	26

2.3.1.1	PCR.....	26
2.3.1.2	DNA Restriction enzymes	27
2.3.1.3	Isolation of PCR fragments or plasmids.....	28
2.3.1.4	Ligation of insert into the vector	29
2.3.1.5	Transformation	29
2.3.1.6	PCR screening	30
2.3.1.7	Expression constructs for bifunctional flavokinase/ FAD synthetase	31
2.3.1.8	N-terminal domain of riboflavin synthase from <i>Escherichia coli</i>	32
2.3.1.9	DNA photolyase from <i>Thermus thermophilus</i>	33
2.3.2	Transformation and expression	34
2.3.2.1	Riboflavin biosynthesis enzymes	34
2.3.2.2	N-terminal domain of riboflavin synthase from <i>Escherichia coli</i>	36
2.3.2.3	LOV2 domain from <i>Avena sativa</i> phototropin	36
2.3.2.4	BLUF domain of AppA protein from <i>Rhodobacter sphaeroides</i>	37
2.3.2.5	DNA photolyase from <i>Thermus thermophilus</i>	37
2.3.3	SDS polyacrylamide gel electrophoresis.....	37
2.3.4	Protein purification.....	38
2.3.4.1	Purification of enzymes for riboflavin biosynthesis.....	38
2.3.4.1.1	Ribose kinase of <i>Escherichia coli</i>	38
2.3.4.1.2	3,4-Dihydroxy-2-butanone 4-phosphate synthase of <i>Escherichia coli</i>	39
2.3.4.1.3	Lumazine synthase of <i>Bacillus subtilis</i>	39
2.3.4.1.4	Riboflavin synthase of <i>Escherichia coli</i>	40
2.3.4.1.5	Flavokinase of <i>Schizosaccharomyces pombe</i>	40
2.3.4.2	Bifunctional flavokinase/FAD synthetase of <i>Enterococcus faecalis</i>	40
2.3.4.3	N-terminal domain of riboflavin synthase of <i>Escherichia coli</i>	41
2.3.4.4	LOV2 domain of <i>Avena sativa</i> phototropin.....	41
2.3.4.5	BLUF domain of AppA of <i>Rhodobacter sphaeroides</i>	42
2.3.4.6	DNA photolyase of <i>Thermus thermophilus</i>	42
2.3.5	Enzyme-assisted synthesis of riboflavin isotopologues	43
2.3.5.1	Preparation of a random isotopologue mixtures of 6,7-dimethyl-8-ribityllumazine by <i>in vivo</i> biotransformation.	43
2.3.5.2	Preparation of deuterium-labeled riboflavin by enzyme-assisted synthesis	43
2.3.5.2.1	[6,8 α - ² H ₂]riboflavin.....	43
2.3.5.2.2	[6,7 α ,8 α ,9- ² H ₈]riboflavin.....	44
2.3.5.2.3	[7 α ,9- ² H ₄]riboflavin.....	44
2.3.5.2.4	[6,8 α - ² H ₄]riboflavin.....	44
2.3.5.3	Enzyme-assisted synthesis of FMN.....	45

2.3.5.4	Enzyme-assisted synthesis of FAD	45
2.3.6	Determination of protein and flavin cofactor concentration.....	46
2.3.7	Reconstitution of protein with cofactors	47
2.3.7.1	N-terminal domain of riboflavin synthase from <i>Escherichia coli</i>	47
2.3.7.2	LOV2 domain from <i>Avena sativa</i>	47
2.3.7.3	DNA photolyase from <i>Thermus thermophilus</i>	47
2.3.8	Spectroscopic methods.....	48
2.3.8.1	Optical spectroscopy.....	48
2.3.8.2	CD spectroscopy.....	48
2.3.8.3	NMR spectrometry	48
2.3.8.4	Mass spectrometry.....	48
3	Results and Discussion	49
	Studies on the reaction mechanism of riboflavin synthase	
3.1	Preparation and reconstitution of N-terminal riboflavin synthase domain.....	49
3.1.1	Optical spectroscopy of the N-terminal riboflavin synthase domain	51
3.1.1.1	Characterization of the recombinant N-terminal riboflavin synthase domain by UV-VIS spectroscopy	51
3.1.1.2	Photometric titration of recombinant N-terminal riboflavin synthase domain	52
3.1.2	NMR spectroscopy of recombinant N-terminal riboflavin synthase domain.....	55
3.1.2.1	Preparation of isotopologue libraries by biotransformation of ¹³ C-Glucose	55
3.1.2.2	¹³ C-NMR spectroscopy of isotopologues of 6,7-dimethyl-8-ribityllumazine and riboflavin in complex with recombinant N-terminal riboflavin synthase domain.....	55
3.1.2.3	Characterization of recombinant N-terminal riboflavin synthase domain under neutral and alkaline conditions by ¹³ C, ¹⁵ N-NMR spectroscopy.....	60
	Hyperfine mapping of FMN bound to the LOV photoreceptor domain of phototropin	
3.2	Enzyme-assisted synthesis of riboflavin isotopologues and flavocoenzymes.....	70
3.2.1	Preparation of enzymes for enzyme-assisted flavin biosynthesis.....	71
3.2.1.1	Ribose kinase of <i>Escherichia coli</i>	71
3.2.1.2	3,4-Dihydroxy-2-butanone 4-phosphate synthase of <i>Escherichia coli</i>	72
3.2.1.3	6,7-Dimethyl-8-ribityllumazine synthase of <i>Bacillus subtilis</i>	72
3.2.1.4	Riboflavin synthase of <i>Aquifex aeolicus</i>	74
3.2.1.5	Flavokinase of <i>Schizosaccharomyces pombe</i>	75
3.2.1.6	Bifunctional flavokinase/FAD synthetase of <i>Enterococcus faecalis</i>	75
3.2.1.7	Enzyme storage.....	76
3.2.2	Preparation of 5-amino-6-ribitylamino-2,4(1 <i>H</i> ,3 <i>H</i>)-pyrimidinedione	77

3.2.3	One-pot synthesis of riboflavin	78
3.2.4	Preparation of deuterated riboflavin.....	80
3.2.4.1	Attempted synthesis of [6,8 α - ² H ₂]riboflavin	81
3.2.4.2	Preparation of [6,7 α ,8 α ,9- ² H ₈]riboflavin	82
3.2.4.3	Preparation of [7 α ,9- ² H ₄]riboflavin	83
3.2.4.4	Preparation of [6,8 α - ² H ₄]riboflavin	84
3.3	LOV2 domain from <i>Avena sativa</i>.....	88
3.3.1	Isolation and reconstitution of LOV2 domain from <i>Avena sativa</i>	89
3.3.2	Optical spectroscopy of LOV2 domain from <i>Avena sativa</i>	90
3.3.3	ENDOR spectroscopy of LOV2 domain from phototropin of <i>Avena sativa</i>	91
Assigning the vibrational spectra of free and protein-bound FAD in the ground state and the optically excited S1 state		
3.4	BLUF domain from <i>Rhodobacter sphaeroides</i>.....	92
3.4.1	Isolation of BLUF domain.....	92
3.4.2	Time-resolved infrared spectroscopy of FAD and BLUF domain	93
3.5	DNA photolyase from <i>Thermus thermophilus</i>.....	95
4	References	97
	<i>GHS-Grahrstoffkennyeichnus</i>	<i>ix</i>
	<i>Abbreviations</i>	<i>xi</i>
	<i>Curriculum Vitae</i>	<i>xii</i>

Abbreviations

Å	Ångstrom
ADP	Adenosine 5'-diphosphate
AMP	Adenosine 5'-monophosphate
APS	Ammonium persulfate
ATP	Adenosine 5'-triphosphate
bp	Base pair
CD	Circular Dichroism
Da	Dalton
DNA	Deoxyribonucleic acid
dNTP	Deoxynucleotide triphosphate
DTT	Dithiothreitol
EDTA	Ethylenediaminetetraacetic acid
ENDOR	Electron Nuclear Double Resonance
EPR	Electron Paramagnetic Resonance
FAD	Flavin adenine dinucleotide
FMN	Flavin mononucleotide
FTIR	Fourier Transform Infrared Spectroscopy
GTP	Guanosine triphosphate
h	hour
HEPES	4-[2-Hydroxyethyl]-1-piperazineethanesulfonic acid
HPLC	High Performance Liquid Chromatography
Hz	Hertz
IPTG	Isopropyl- β -thiogalactopyranoside
J	Coupling constant
LB-Medium	Luria-Bertani Medium
LOV	Light Oxygen Voltage
min	Minute
NADP	Nicotinamide adenine dinucleotide phosphate
NMR	Nuclear Magnetic Resonance
OD	Optical density
PAGE	Polyacrylamide Gel Electrophoresis
PCR	Polymerase Chain Reaction
PEP	Phosphoenol pyruvate
PMSF	Phenylmethylsulphonyl fluoride
ppm	Parts per million
RT	Room temperature
SDS	Sodium dodecyl sulphate
SDS-PAGE	Sodium dodecylsulphate polyacrylamide electrophoresis
T	Tesla
Taq	<i>Thermus aquaticus</i>
TEMED	Tetramethylethylenediamine
Tris	Tris-(hydroxymethyl)-aminomethane
U	uniform
UV	Ultraviolet
vis	Visible
TLC	Thin layer chromatography

1 Introduction

1.1 Riboflavin

Riboflavin is a water soluble trace nutrient also designated as vitamin B₂. It is stable to heat but sensitive to light. It is a fluorescent yellow crystalline compound that is found naturally in a number of foods including milk and milk products, meat, fish, leafy vegetables, egg and others. The name of riboflavin comes from the combination of “ribose” and “flavus” (yellow color in Latin). It was discovered in 1926 by D. T. Smith and E. G. Hendrick. In 1933, pure riboflavin was isolated from yeast and egg white, and the structure was determined by Richard Kuhn and T. Wagner-Jauregg [1]. After that, it was synthesized in 1935 by Paul Karrer [2]. At the same time, flavoenzymes were discovered by Hugo Theorell [3]. FMN was synthesized by Kuhn and Rudy in 1936 [4]. For their work, the first stable flavin radical was discovered by Kuhn. For their achievements in the area of vitamin chemistry, Karrer and Kuhn were awarded Nobel Prizes in chemistry in 1937 and 1938.

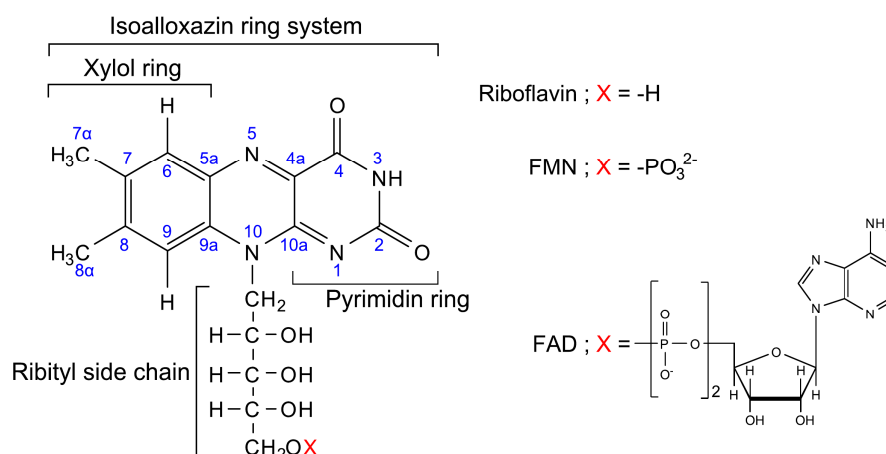


Figure 1.1 Riboflavin and flavoenzymes (FMN and FAD).

Riboflavin is the universal precursor of the flavoenzymes FMN (flavin mono-nucleotide) and FAD (flavin adenine dinucleotide) (Figure 1.1). These two compounds serve as coenzymes in a variety of electron-transfer reactions that occur in energy-producing, biosynthetic, detoxifying and electron scavenging pathways; thus, they are extraordinarily important components in all living organisms. It has been estimated that up to 2 % of all cellular proteins use flavoenzymes. Riboflavin can be biosynthesized by plants and many microorganisms but must be obtained from nutritional sources by humans and animals. The daily recommended allowance for riboflavin is reported to be around 1.3 mg for adults and 0.6 mg for children.

The investigation of the biosynthesis of riboflavin started around the 1950s. Today, riboflavin is produced on a global scale of about 3000 metric tons per year by technically advanced fermentation processes. The manufactured riboflavin is used as a vitamin in human and animal nutrition and as a

food colorant. Since cereals are poor sources of vitamin B₂, virtually all types of compound animal feed must contain vitamin B₂ supplements. Biotechnological aspects were an important driving force for studies on the riboflavin biosynthesis.

Riboflavin biosynthesis has been predominantly studied on microorganisms. The early work was focused on fungi, ascomycetes and yeasts, some of which are naturally flavinogenic. More recently, eubacteria and yeast were involved in the riboflavin biosynthesis research. Plants are the most important primary providers of the vitamin for animals (either directly or via the food chain). However, the pathway in plants has been investigated only relatively recently. The plant pathway shows more similarity with the eubacterial pathway as compared with archaea and fungi. Work on riboflavin biosynthesis in microorganisms has been reviewed repeatedly [5] [6] [7] [8] [9] [10] [11] [12].

1.1.1 Overview of the biosynthesis of riboflavin

Figure 1.2 summarizes the current state of information on riboflavin biosynthesis [10]. The biosynthesis of one riboflavin molecule requires one molecule of GTP and two molecules of ribulose-5-phosphate and some cofactors (NADPH, Mg²⁺, Zn²⁺). The reactions are catalyzed by GTP cyclohydrolase II or III, pyrimidine deaminase/reductase, 3,4-dihydroxy-2-butanone 4-phosphate synthase, lumazine synthase and riboflavin synthase. With the exception of the reductase, these reactions are strongly exergonic. Some of the biosynthesis enzymes have very complex reaction mechanisms.

Consistently, all pathway variants start with GTP (**1**). The imidazole ring of GTP (**1**) is opened by GTP cyclohydrolase III (**A**) or GTP cyclohydrolase II (**B**). GTP cyclohydrolases catalyze very complex reactions where two or three different bonds are hydrolyzed. Eubacteria, fungi and plants use GTP cyclohydrolase II (**B**) which catalyzes the release of C-8 of the purine moiety by cleavage of two different carbon-nitrogen bonds, resulting in the formation of formate, as well as the cleavage of a phosphoanhydride bond resulting in the formation of inorganic pyrophosphate [13]. On the other hands, archaea use cyclohydrolase III (**A**) and convert GTP to 2-amino-5-formylamino-6-ribosylamino-4(3*H*)-pyrimidinone monophosphate [14] [15] [16]. The enzyme product, 2,5-diamino-6-ribosylamino-4(3*H*)-pyrimidinone 5'-phosphate [17], can be converted to 5-amino-6-ribitylamino-2,4(1*H*,3*H*)-pyrimidinedione 5'-phosphate (**6**) in two enzymatic steps, including removal of the C-2 amino group of the pyrimidine ring and reduction of the ribosyl side chain. These reaction steps are significantly different for different organisms. In bacteria and plants, the reaction begins with the deamination of the position 2 amino group of the pyrimidine ring yielding the intermediate of 5-amino-6-ribosylamino-2,4(1*H*,3*H*)-pyrimidinedione 5'-phosphate (**4**) which is catalyzed by 2,5-diamino-6-ribosylamino-4(3*H*)-pyrimidinone 5'-phosphate deaminase (**D**). Subsequently, the intermediate is reduced by 5-amino-6-ribosylamino-2,4(1*H*,3*H*)-pyrimidinedione 5'-phosphate reductase (**E**) [18].

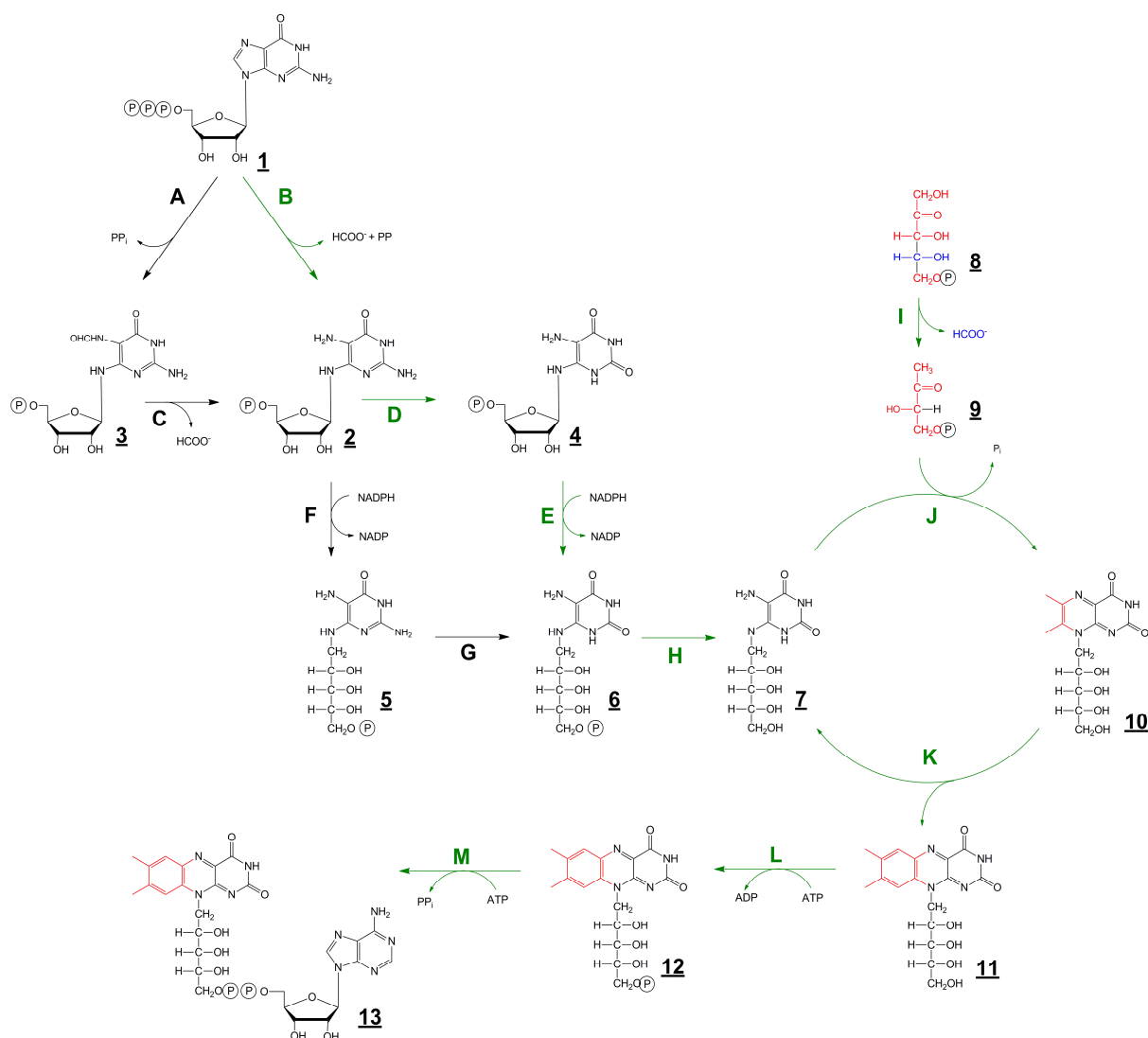


Figure 1.2 Biosynthesis of riboflavin and flavocoenzymes from Fischer, 2006 [10]. Step A, GTP cyclohydrolase III; step B, GTP cyclohydrolase II; step C, 2-amino-5-formylamino-6-ribosylamino-4(3H)-pyrimidinone 5'-phosphate hydrolase; step D, 2,5-diamino-6-ribosylamino-4(3H)-pyrimidinone 5'-phosphate deaminase; step E, 5-amino-6-ribosylamino-2,4(1H,3H)-pyrimidinedione 5'-phosphate reductase; step F, 2,5-diamino-6-ribitylamino-4(3H)-pyrimidinone 5'-phosphate reductase; step G, 2,5-diamino-6-ribitylamino-4(3H)-pyrimidinone 5'-phosphate deaminase; step H, hypothetical phosphatase; step I, 3,4-dihydroxy-2-butanone 4-phosphate synthase; step J, 6,7-dimethyl-8-ribityllumazine synthase; step K, riboflavin synthase; step L, flavokinase; step M, FAD synthetase; **1**, GTP; **2**, 2,5-diamino-6-ribosylamino-4(3H)-pyrimidinone 5'-phosphate; **3**, 2-amino-5-formylamino-6-ribosylamino-4(3H)-pyrimidinone 5'-phosphate; **4**, 5-amino-6-ribosylamino-2,4(1H,3H)-pyrimidinedione 5'-phosphate; **5**, 2,5-diamino-6-ribitylamino-4(3H)-pyrimidinone 5'-phosphate; **6**, 5-amino-6-ribitylamino-2,4(1H,3H)-pyrimidinedione 5'-phosphate, **7**; 5-amino-6-ribitylamino-2,4(1H,3H)-pyrimidinedione 5'-phosphate, **10**, 6,7-dimethyl-8-ribityllumazine; **11**, riboflavin; **12**, FMN; **13**,

FAD. Green arrows mark the plant pathway; red, fate of the four-carbon precursor **9** derived from ribulose 5-phosphate.

On the other hand, yeasts, fungi and archaea use the intermediate 2,5-diamino-6-ribitylamino-4(3*H*)-pyrimidinedione 5'-phosphate (**5**) which is formed by the catalytic action of 2,5-diamino-6-ribosylamino-4(3*H*)-pyrimidinone 5'-phosphate reductase (**F**), and is deaminated by 2,5-diamino-6-ribitylamino-4(3*H*)-pyrimidinedione 5'-phosphate deaminase (**G**) [19] [20]. The resulting 5-amino-6-ribitylamino-2,4(1*H*,3*H*)-pyrimidinedione 5'-phosphate (**6**) cannot serve as substrate for the next enzymatic reaction in the pathway, which is 6,7-dimethyl-8-ribitylluazine synthase (**J**). The enzyme can only accept 5-amino-6-ribitylamino-2,4(1*H*,3*H*)-pyrimidinedione as substrate (**7**). Therefore, **6** must be dephosphorylated in order to become a substrate for lumazine synthase. However, it is still unknown how the required dephosphorylation is brought about. The other substrate for the reaction of 6,7-dimethyl-8-ribitylluazine synthase (**J**) is 3,4-dihydroxy-2-butanone 4-phosphate (**9**). This substrate is obtained from ribulose 5-phosphate (**8**) by a skeletal rearrangement that is catalyzed by 3,4-dihydroxy-2-butanone 4-phosphate synthase (**I**), which eliminates carbon atom 4 of the substrate as formate [21] [22] [23].

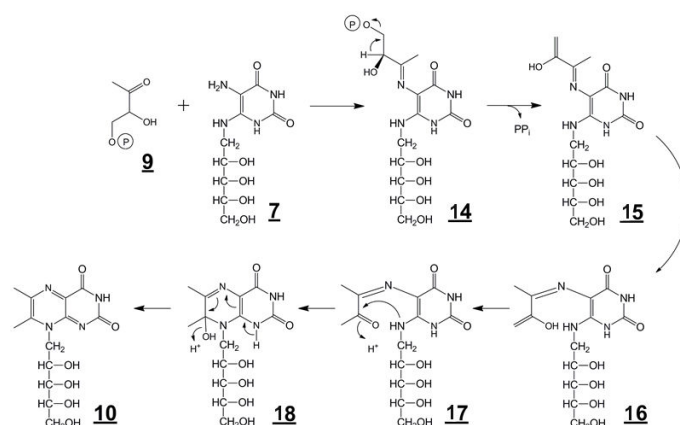


Figure 1.3 Hypothetical reaction mechanism of lumazine synthase from Kis, 1995 [24].

5-Amino-6-ribitylamino-2,4(1*H*,3*H*)-pyrimidinedione (**7**) and 3,4-dihydroxy-2-butanone 4-phosphate (**9**) are condensed by 6,7-dimethyl-8-ribitylluazine synthase (**J**) via a complex multistep reaction sequence (Figure 1.3), which starts with the formation of a Schiff base by reaction of the position 5 amino group of 5-amino-6-ribitylamino-2,4(1*H*,3*H*)-pyrimidinedione (**7**) with the carbonyl group of 3,4-dihydroxy-2-butanone 4-phosphate (**9**) [25] [24] [26]. The elimination of phosphate prepares the stage for the formation of the lumazine chromophore by ring closure under formation of 6,7-dimethyl-8-ribitylluazine (**10**). The reaction can proceed without the enzyme at room temperature in neutral aqueous solution, and the catalytic acceleration by lumazine synthase (**J**) is rather modest [27].

1.1.2 Riboflavin synthase

The final step of the riboflavin biosynthetic pathway is a most unusual dismutation catalyzed by riboflavin synthase (**K**) (for review see Fischer and Bacher, 2011 [12]). The reaction can be described as a transfer of a four-carbon unit between two identical substrate molecules, 6,7-dimethyl-8-ribityllumazine (**10**), even without any requirement for cofactors. One of the products is riboflavin (**11**) and the second product is 5-amino-6-ribitylamino-2,4(1*H*,3*H*)-pyrimidinedione (**7**), which is structurally identical with the substrate of 6,7-dimethyl-8-ribityllumazine synthase (**J**) and is recycled in the biosynthetic pathway [28] [29] [30] for review see also [11]. Interestingly, the formation of riboflavin (**11**) from 6,7-dimethyl-8-ribityllumazine (**10**) can proceed in aqueous solution in boiling water under neutral or acidic conditions without any catalyst [31] [32] [33]. The acidic protons of the position 7 methyl group of 6,7-dimethyl-8-ribityllumazine (**10**) are easily exchanged with solvent water, and this exchange is accelerated by riboflavin synthase (**K**). A series of complex reaction mechanisms have been proposed over a period of more than 4 decades.

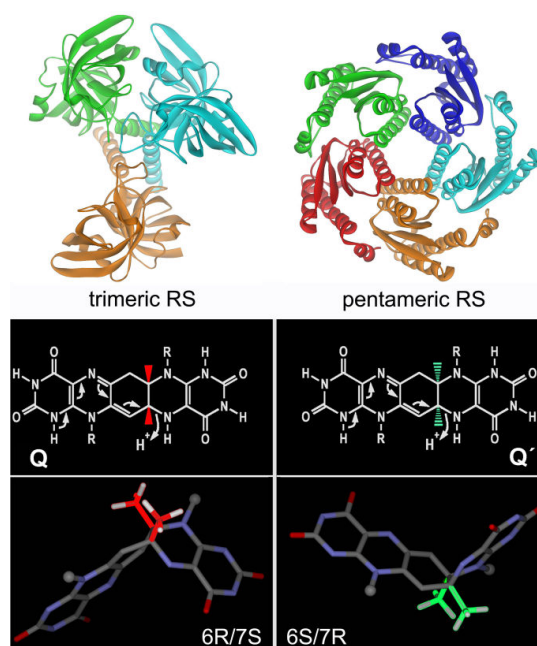


Figure 1.4 Stereochemistry of the conversion of 6,7-dimethyl-8-ribityllumazine into riboflavin catalyzed by trimeric eubacterial (left) and pentameric archaeal (right) riboflavin synthase from Fischer and Bacher, 2011 [12]. Q and Q', pentacyclic reaction intermediates. R, ribityl.

Riboflavin synthases can be categorized into two distinct groups: homotrimers and homopentamers, respectively. Riboflavin synthase from eubacteria, fungi, and plants have an extensive similarity between the DNA sequences and assemble into homotrimers [34] (see Figure 1.4, left). On the other hands, riboflavin synthase from Archaea are c_5 -symmetric homopentamers whose sequence and structure has significant similarity with lumazine synthase [35] [36] (see Figure 1.4, right). The

reaction proceeds via a pentameric adduct which differs from the intermediate of the homotrimeric enzymes with regard to the stereochemistry. More specifically, the intermediates of trimeric and pentameric riboflavin synthases are diastereomers as shown in Figure 1.4. Hence, the pentacyclic intermediate generated by archaeal riboflavin synthase cannot be processed by trimeric riboflavin synthase and vice versa (for review see Fischer and Bacher [11]).

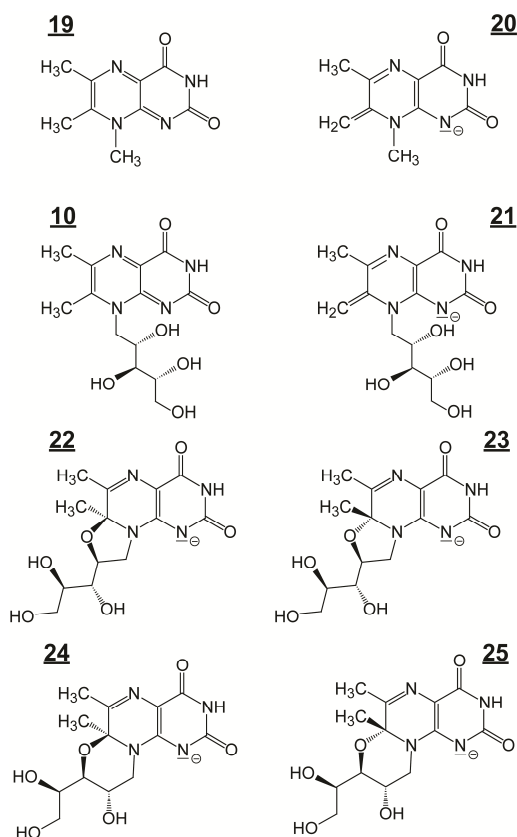


Figure 1.5 Structures of lumazine derivatives [39]. **7**, 6,7-dimethyl-8-ribityllumazine; **21**, 7-exomethylene anion of 6,7-dimethyl-8-ribityllumazine; **22 – 25**, tricyclic adduct anions of 6,7-dimethyl-8-ribityllumazine; **19**, 6,7,8-trimethyl-8-ribityllumazine; **20**, 6,7,8-trimethyl-8-ribityllumazine anion.

The riboflavin synthase substrate (6,7-dimethyl-8-ribityllumazine) and its structural analogs are characterized by unusual CH acidity of the position 7 methyl group [37] (Figure 1.5). Thus, deprotonation of 6,7,8-trimethyl-8-ribityllumazine (**19**; pKa, 8.9) affords the exomethylene anion **20**. In case of the 6,7-dimethyl-8-ribityllumazine (apparent pKa, 7.9), the exomethylene species **21** is only present in trace amounts, whereas the dominant components are two tricyclic diastereomer pairs (**22 – 25**, Figure 1.5) which arise by nucleophilic attack of the position 2' and 3' hydroxy groups, respectively, at C-7 of the pyrazine ring.

An intermediate of the riboflavin synthase-catalysed reaction was first detected spectroscopically by single-turnover experiments and was subsequently isolated and identified as the pentacyclic compound **26**, which is a covalent adduct of two molecules of 6,7-dimethyl-8-ribityllumazine (Figure 1.6) [38].

The pentacyclic compound was shown to be a catalytically competent reaction intermediate which can be cleaved by riboflavin synthase in two different ways affording either two molecules of 6,7-dimethyl-8-ribityllumazine (**10**) (reverse reaction) or one molecule each of riboflavin (**11**) and 5-amino-6-ribitylamino-2,4(1*H*,3*H*)-pyrimidinedione (**7**) (forward reaction) [38]. The forward reaction (cleavage of **26** under formation of riboflavin) is easily explained as a sequence of two elimination steps via the hypothetical intermediate **27** (Figure 1.6). On the other hand, the reversible formation of **26** from 6,7-dimethyl-8-ribityllumazine (**10**) continues to be somewhat of an enigma.

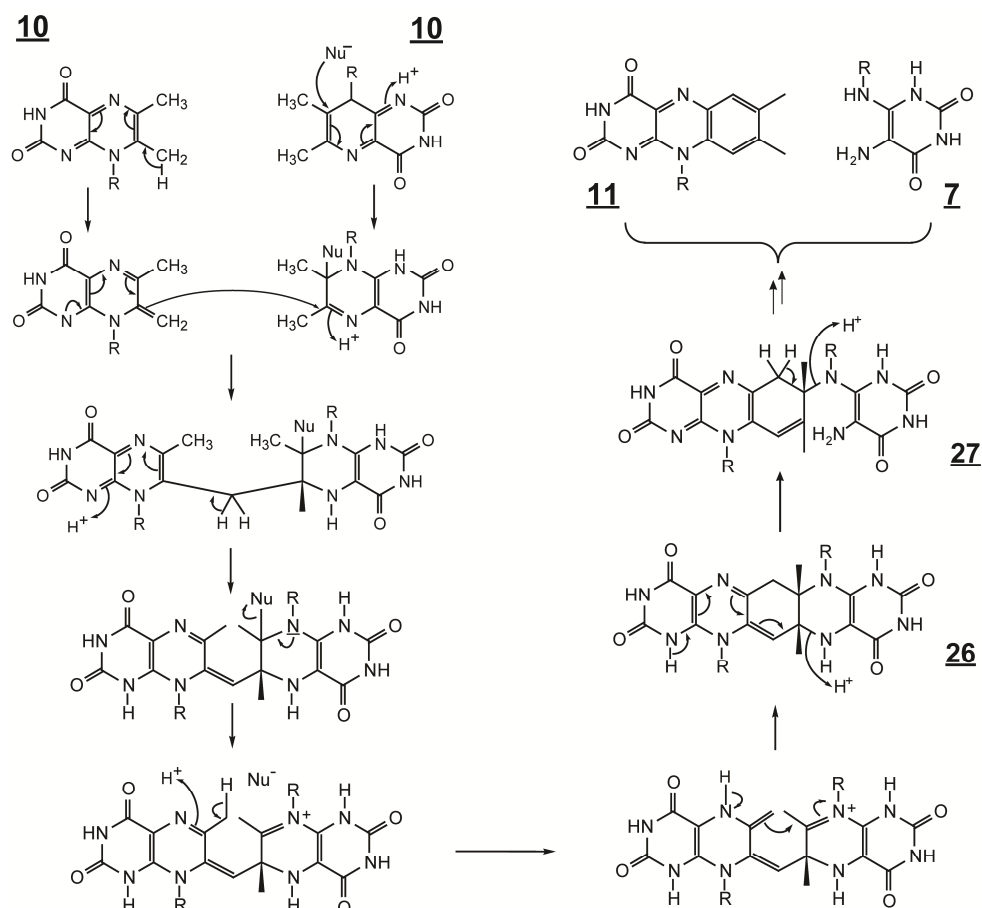


Figure 1.6 A hypothetical mechanism for the formation of riboflavin from 6,7-dimethyl-8-ribityllumazine. The pentacyclic adduct **26** has been identified as a catalytically competent intermediate of riboflavin synthase from Kim et al, 2010 [39]. R, D-ribityl.

A hypothetical reaction sequence that combines the more recently discovered intermediate **26** (Figure 1.6) with hypothetical reaction steps proposed in the 1960s by Plaut, Wood and their coworkers [40] [41] appears rather cumbersome for a reaction that can proceed under mild conditions, even without catalysis (the mechanism originally proposed by Plaut, Wood and coworkers, prior to the discovery of the pentacyclic intermediate (**26**)).

Riboflavin synthase of *Escherichia coli* is a homotrimer of 25 kDa subunits. Each subunit folds into two similar domains, in line with internal sequence similarity [42] [43] [44]. More specifically, in the

sequence alignment of N-terminal domain 1 - 97 with C-terminal domain 98 - 213 of the *E. coli* riboflavin synthase there are 25 identical amino acid residues and 22 conservative replacements (Figure 1.7).

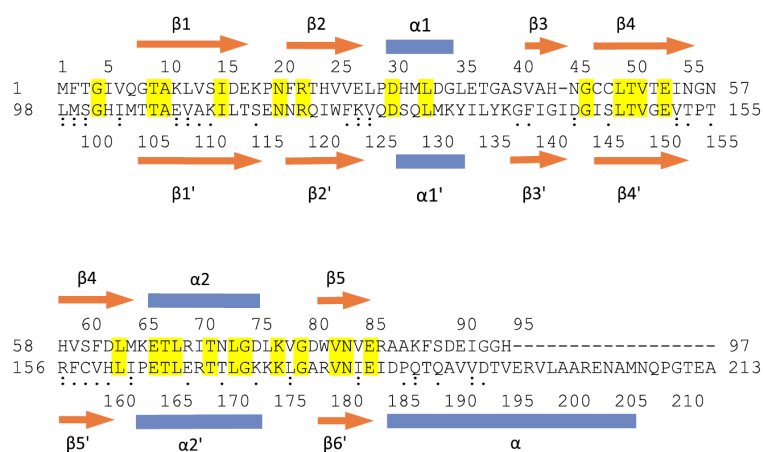


Figure 1.7 Intramolecular sequence similarity of riboflavin synthase from *Escherichia coli*. Top, N-terminal domain; bottom, C-terminal domain. Secondary structure assignment as adapted from *Liao et al*, 2001 [44].

Whereas pairs of domains are related by pseudo- c_2 symmetry, the homotrimer per se is devoid of trimeric symmetry, and spectroscopic studies of the enzyme/ligand interaction are hampered by the multiplicity of signals resulting from the topological non-equivalence of the six folding domains [45]. For this reason, the NMR studies reported in this paper were performed with a recombinant N-terminal domain of riboflavin synthase of *E. coli*, which forms a c_2 symmetric homodimer that can bind two molecules of 6,7-dimethyl-8-ribityllumazine at topologically equivalent sites [46] [47] [48].

1.1.3 Flavokinase and FAD synthetase

The final product of the riboflavin biosynthetic pathway, riboflavin (**11**), can serve as the precursor of FMN (Flavin mononucleotide) (**12**) and FAD (Flavin adenine dinucleotide) (**13**) (Figure 1.1), which are important flavoenzymes in all organisms. Therefore, the phosphorylation of riboflavin is a necessary step in all organisms. Flavokinase (riboflavin kinase, E.C. 2.7.1.26, **L**) converts riboflavin (**11**) to FMN (**12**) using ATP as phosphate donor [49] [50]. FAD synthetase (E.C. 2.7.7.2, **M**) converts FMN (**12**) to FAD (**13**) by the transfer of an adenylate unit under formation of inorganic pyrophosphate as second product [51]. Animals, fungi, plants and certain eubacteria (including *E. coli* and *B. subtilis*) have separate flavokinase and FAD synthetase enzymes. However, numerous eubacteria have bifunctional enzymes which catalyze the formation of FAD at their N-terminal domain, whereas the C-terminal domain serves as flavokinase [52].

1.2 Isotope-labeled riboflavin and 6,7-dimethyl-8-ribityllumazine

Flavins labeled with stable isotopes (deuterium, ^{13}C , ^{15}N , ^{17}O , ^{18}O) are important reagents for the study of flavoproteins using isotope-sensitive methods such as NMR, EPR, ENDOR, infrared and Raman spectroscopy that can afford information on the physical state of protein-bound ligands. This chapter will describe two methods for preparation of isotope-labeled riboflavin and 6,7-dimethyl-8-ribityllumazine.

- i.* Random isotopologue mixtures of 6,7-dimethyl-8-ribityllumazine or riboflavin can be prepared by *in vivo* biotransformation (see chapter 1.2.1).
- ii.* Enzyme-assisted synthesis of riboflavin isotopologues by *in vivo* biotransformation (see chapter 1.2.2).

Both approaches are based on the biosynthetic pathway of riboflavin (vitamin B₂). Labeled 6,7-dimethyl-8-ribityllumazine or riboflavin can be converted to FMN and FAD. These two compounds are coenzymes in a variety of flavoproteins. A wide variety of isotopologues can be produced by the same experimental approach.

1.2.1 Random isotopologue mixtures of 6,7-dimethyl-8-ribityllumazine and riboflavin by *in vivo* biotransformation

One of the methods for preparation isotopologue libraries is the biotransformation of ^{13}C -glucose isotopologues and/or $^{15}\text{NH}_4\text{Cl}$ by a recombinant *E. coli* strain engineered for expression of the *ribABGH* genes of *B. subtilis*. According to the riboflavin biosynthetic pathway, the carbon skeleton of riboflavin comes from one molecule of GTP and two molecules of ribulose-5-phosphate. These precursors arise from pentose phosphate, glycine, formate and carbon dioxide (Figure 1.8, **A**). All nitrogen atoms of riboflavin are provided by GTP. This biotransformation method affords libraries of isotopologues universally or randomly labeled with ^{13}C and/or ^{15}N [53]. Using this method, approximately 100 mg of 6,7-dimethyl-8-ribityllumazine are produced in one liter of minimal medium. Growth of the recombinant strain in medium supplemented with $[\text{U-}^{13}\text{C}_6]\text{glucose}$ and/or $^{15}\text{NH}_4\text{Cl}$ as single sources of carbon and/or nitrogen affords 6,7-dimethyl-8-ribityllumazine universally labeled with ^{13}C and/or ^{15}N . The yield of $[\text{U-}^{13}\text{C}_{13}]6,7\text{-dimethyl-8-ribityllumazine}$ was 25 mg/g $[\text{U-}^{13}\text{C}_6]\text{glucose}$. Fermentation with $[\text{U-}^{13}\text{C}_6]\text{-}$, $[\text{1-}^{13}\text{C}_1]\text{-}$, $[\text{2-}^{13}\text{C}_1]\text{-}$, or $[\text{3-}^{13}\text{C}_1]\text{glucose}$ afforded mixtures of 6,7-dimethyl-8-ribityllumazine isotopologues, predominantly with ^{13}C enrichment of single carbon atoms (Figure 1.8, **B**). The ^{13}C signal pattern of 6,7-dimethyl-8-ribityllumazine, which is isolated from the experiment with single carbon labeled glucose ($[\text{1-}^{13}\text{C}_1]\text{-}$, $[\text{2-}^{13}\text{C}_1]\text{-}$, or $[\text{3-}^{13}\text{C}_1]\text{glucose}$), is different, depending on the glucose supplement.

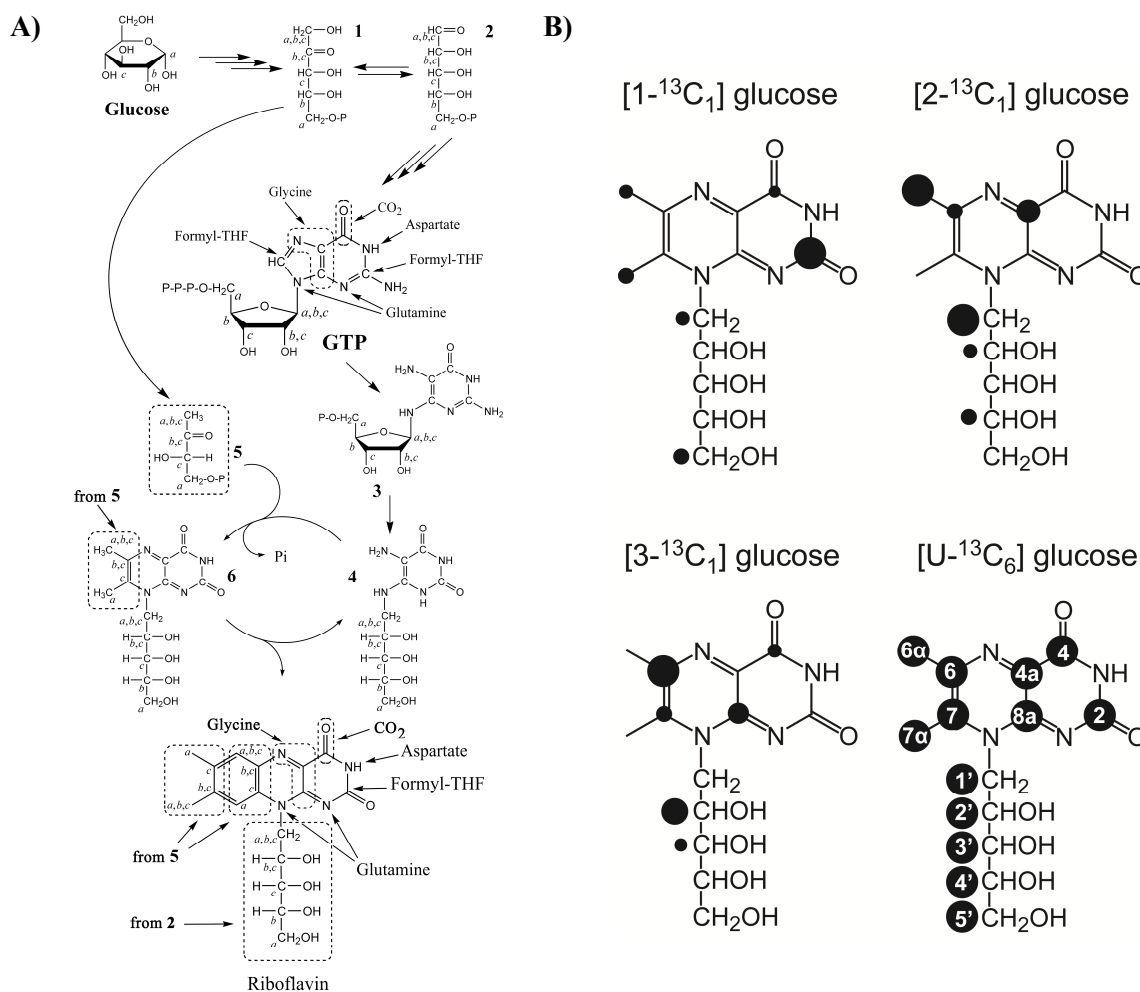


Figure 1.8 Biosynthesis of riboflavin. A) The fate of glucose carbon atoms is indicated by letters a-c. Partial scrambling in ribulose-5-phosphate (8) is due to reactions of the pentose phosphate pathway from Illarionov, 2004 [53]; B) ^{13}C -NMR spectra of 6,7-dimethyl-8-ribityllumazine (10) samples which was obtained by fermentation with $[U-^{13}\text{C}_6]$ -, $[1-^{13}\text{C}_1]$ -, $[2-^{13}\text{C}_1]$ -, or $[3-^{13}\text{C}_1]$ glucose, respectively.

1.2.2 Rapid one-pot enzyme-assisted synthesis of riboflavin

Another method for preparation of isotopologue libraries is enzyme-assisted synthesis. Figure 1.9 shows a summary of enzyme-assisted synthesis of riboflavin. The riboflavin molecule requires one molecule of 5-amino-6-ribitylamino-2,4(1*H*,3*H*)-pyrimidinedione (7) and two molecules of glucose (14) and some cofactors (ATP, PEP, NADPH, 2-ketoglutarate, and Mg^{2+}). The overall reaction comprises six enzyme-catalyzed reaction steps for the synthesis of riboflavin (11). Reaction steps are catalyzed by hexokinase (N), glucose-6-phosphatase dehydrogenase (O), 6-phosphogluconate dehydrogenase (P), 3,4-dihydroxy-2-butanone 4-phosphate synthase (I), 6,7-dimethyl-8-ribityllumazine synthase (J) and riboflavin synthase (K). Moreover, the reaction mixture contains two additional enzymes for the recycling of cofactors (pyruvate kinase, Q, and glutamate dehydrogenase, R).

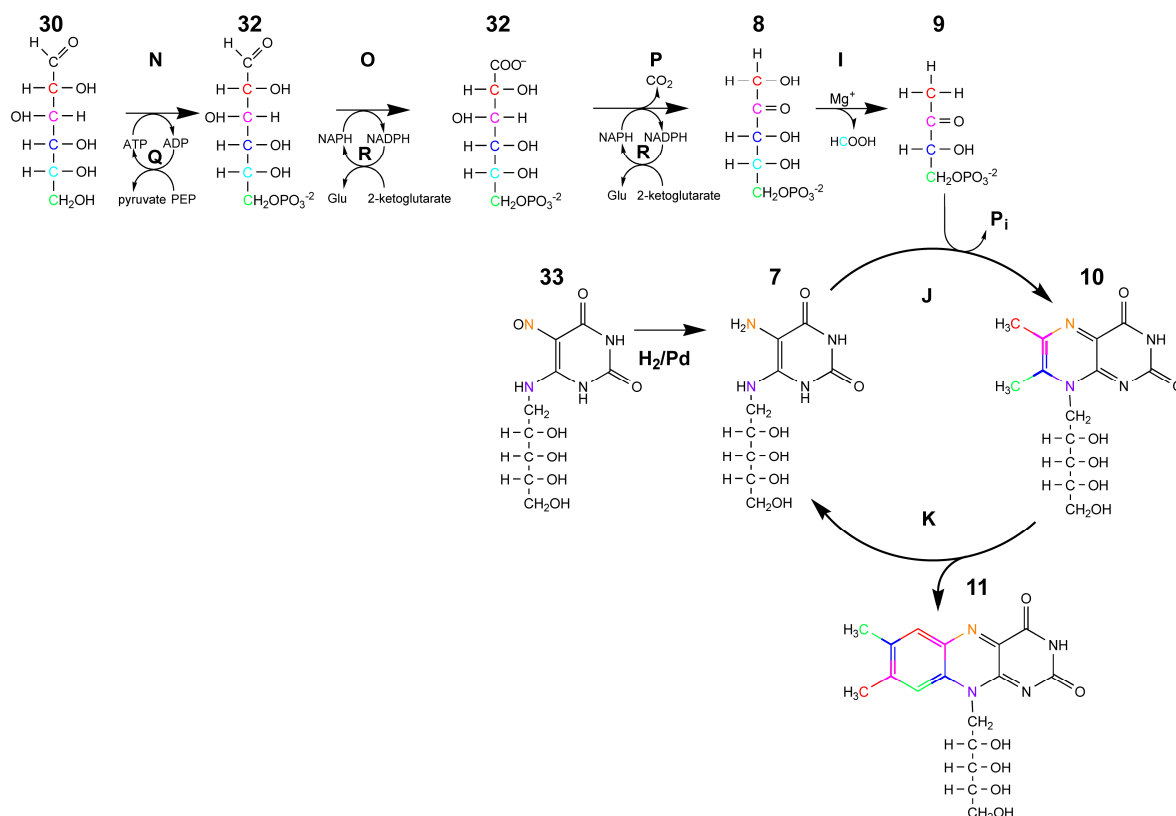


Figure 1.9 Enzymatic synthesis of riboflavin. **I**, 3,4-dihydroxy-2-butanone 4-phosphate synthase; **J**, 6,7-dimethyl-8-ribityllumazine synthase; **K**, riboflavin synthase; **N**, hexokinase; **O**, glucose-6-phosphate dehydrogenase; **P**, 6-phosphogluconate dehydrogenase; **Q**, pyruvate kinase; **R**, glutamate dehydrogenase; **7**, 5-amino-6-ribitylamino-2,4(1*H*,3*H*)-pyrimidinedione; **8**, ribulose 5-phosphate; **9**, 3,4-dihydroxy-2-butanone 4-phosphate; **10**, 6,7-dimethyl-8-ribityllumazine; **11**, riboflavin; **30**, glucose; **31**, glucose-5-phosphate; **32**, 6-phosphogluconate; **33**, 5-nitro-6-ribitylamino-2,4(1*H*, 3*H*)-pyrimidinedione.

These enzymes can be expressed in high yields in recombinant *E. coli* strain. All reaction steps are carried out as a one-pot reaction involving 8 enzymes [54]. The final product, riboflavin, is obtained as a yellow solid that is harvested by centrifugation and is then purified by chromatography or recrystallization from dilute acetic acid. The transfer of carbon atoms from glucose (**14**) into riboflavin (**11**) is shown by the different colors in Figure 1.9. Carbon atoms 1 and 5 of glucose are eliminated by the enzymatic process. The other carbons of glucose (2, 3, 4 and 6) become part of the xylol ring of riboflavin (**11**). The enzyme-assisted synthesis of riboflavin can start from a variety of ^{13}C -substituted glucose isotopologues that are commercially available. Therefore, it is possible to generate a variety of riboflavin isotopologues. The labeling pattern of final product depends on that of the starting material. For example, $[\text{U-}^{13}\text{C}_6]$ glucose affords $[\text{6},\text{6}\alpha,\text{7},\text{7}\alpha\text{-}^{13}\text{C}_4]$ 6,7-dimethyl-8-ribityllumazine which is converted into $[\text{5}\alpha,\text{6},\text{7},\text{7}\alpha,\text{8},\text{8}\alpha,\text{9},\text{9}\alpha\text{-}^{13}\text{C}_8]$ riboflavin. Similarly, $[\text{7}\alpha\text{-}^{13}\text{C}_1]$ 6,7-dimethyl-8-ribityllumazine can be prepared from $[\text{6-}^{13}\text{C}_1]$ glucose as starting material and can be converted to $[\text{7}\alpha,\text{9-}^{13}\text{C}_2]$ riboflavin.

1.3 Flavoproteins

Numerous enzymes need flavocoenzymes in order to catalyze a very wide range of redox reactions. One of the spectacular aspects of flavins is that they can adopt three different oxidation levels and that they can operate either by the transfer of single electrons or by transfer of hydride ions. The redox active isoalloxazine moiety of the flavin cofactor may undergo one or two electron transitions [55]. The oxidised form is reduced to a radical or semiquinone by one electron reduction. A second one-electron reduction converts the radical to fully reduced forms FADH₂ or FMNH₂ (Figure 1.10). Most flavoproteins bind their cofactors non-covalently, for example LOV domain, BLUF domain and DNA photolyase [56] [57] [58].

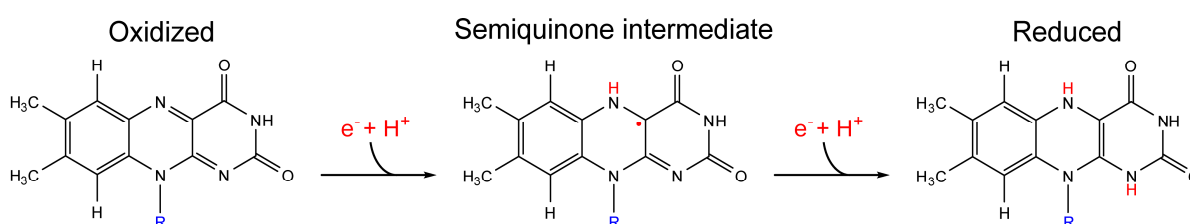


Figure 1.10 Oxidoreduction of isoalloxazine ring in flavin nucleotides via semiquinone (free radical) intermediate (center).

1.3.1 Blue-light receptors using flavin chromophores

Many light responses of microbes, plants and animals are activated by the blue and near-UV region of the sun's spectrum (320 - 500 nm). Blue-light photoreceptors are proteins that sense the light conditions and transfer this information to the organism. They come in three different types of flavoproteins: **phototropins**, **BLUF domain**, **cryptochrome**. The mechanism leading to the signaling state in each class of photoreceptor is unique and for each class there is a desire to understand how the absorption of light leads to the signaling state of the protein. **Phototropin** is most prevalent in plants and prokaryotes. Light activation of LOV domain involves the formation of a covalent adduct [59] [60]. **BLUF (Blue-light using FAD) domains** are mainly found in bacteria and algae. The BLUF proteins undergo a much more subtle change in the chromophore configuration and it is speculated that the absorption of light leads to rearrangement of a hydrogen bonding network which leads to the formation of the signaling state of the protein [61] [62]. **Cryptochromes** are found in bacteria, plants, and animals. They are involved in the entrainment by light of circadian rhythms. Light activation of cryptochromes involves reduction of the flavin cofactor to a neutral radical semiquinone intermediate [63] [64].

1.3.1.1 LOV domains

The common structural feature of the plant phototropin photoreceptor superfamily is that the proteins consist of three conserved domains. The C-terminal region contains a serine/threonine kinase domain, and the N-terminal region contains two light sensitive domains which are called “Light, Oxxygen, or Voltage” (LOV) domains [65] [66] (Figure 1.11). On the other hand, the prokaryotic phototropin contain one LOV domain and one reporter domain, which most likely is a kinase [67]. LOV1 and LOV2 domains are member of the PER/ARNT/SIM (PAS) domain superfamily [68]. Each of them consists of approximately 110 amino acids, and each LOV domain noncovalently binds a single flavin mononucleotide (FMN) as a chromophore [66]. Several crystal structures of these photoreceptors have been published [69] [70] [71]. The dark and illuminated states of LOV1 and LOV2 domains have been characterized in terms of structural differences between these two states. It has been confirmed that the reaction mechanism of LOV domain activation includes light-driven adduct formation between cofactor and protein.

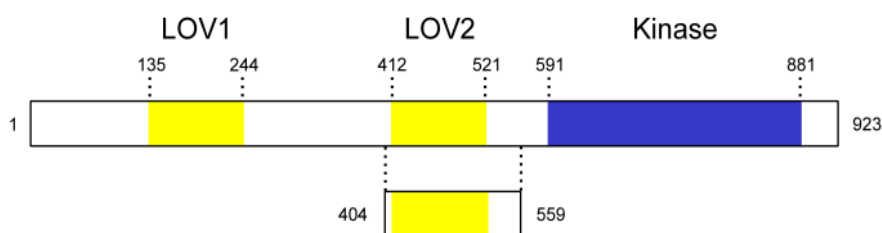


Figure 1.11 Phototropin structure of *Avena sativa*. Cloned part of the phototropin (LOV2 domain) is indicated in the bottom part of the figure.

The structures of LOV1 and LOV2 are similar and comprise five antiparallel β -strands and two α -helices [69] [70] [71]. The FMN chromophore is held tightly within a central cavity by hydrogen bonding and van der Waals forces via 11 conserved amino acids [69] [71]. Nevertheless, differences in their sequences define them as either LOV1 or LOV2 [65] [69]. The reaction mechanism has been studied in considerable detail [72] [73]. The photocycle of LOV domains can be monitored by absorbance or fluorescence spectroscopy [74] [75].

Recently, the recombinant LOV2 domain from *A. sativa* (oat) expressed and isolated from *E. coli* has been shown to undergo a simple three-state photocycle (Figure 1.12). In darkness, the FMN chromophore is noncovalently bound within the LOV domain, forming a species that has maximum optical absorption is at 447 nm (LOV 447; D-state) [66] [74] [76]. After illumination with blue light, fully oxidized FMN (LOV 447; D-state) absorbs a photon and converts to the excited triplet state with maximum optical absorptions at 660 nm (LOV 660; L-state), that in turn leads to formation of a covalent bond between the C-4a of the FMN chromophore [66] and a conserved cysteine residue within the LOV domain (LOV 390; S-state; singlet state) [77] [76] [73]. It is generally accepted that

LOV 390 represent the active signaling state that leads to photoreceptor activation. The photoreaction process is fully reversible in darkness (Figure 1.12).

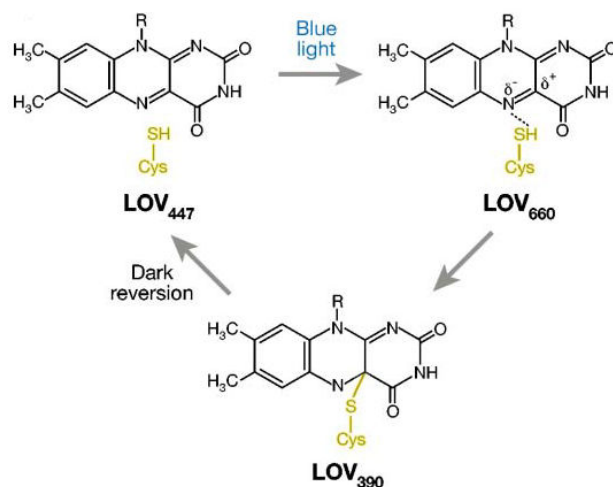


Figure 1.12 LOV domain photocycle from Christie, 2007 [78].

This hypothesis has been confirmed by NMR studies of the light induced differences in the chemical shifts of various $^{13}\text{C}/^{15}\text{N}$ and ^{31}P labeled isotopologues of FMN bound to the LOV2 domain of *A. sativa* and later-on also by X-ray crystallography and EPR spectroscopy [74] [79] [80]. In the C450A mutant of LOV2 (removal of the reactive cysteine), the flavin radical reverts to the ground state (LOV 447) at room temperature in the dark, on the time scale of minutes [75] [77] [76]. The recovery velocity depends on pH and the salt concentration of the protein solution [73] [81]. It was also shown that the adduct formation triggers the unfolding of the helical domain $J\alpha$, which serves as a linker between the LOV2 domain and the kinase domain in the phototropin [82]. This unfolding is believed to modulate the activity of the kinase domain, which is conducive to its auto-phosphorylation.

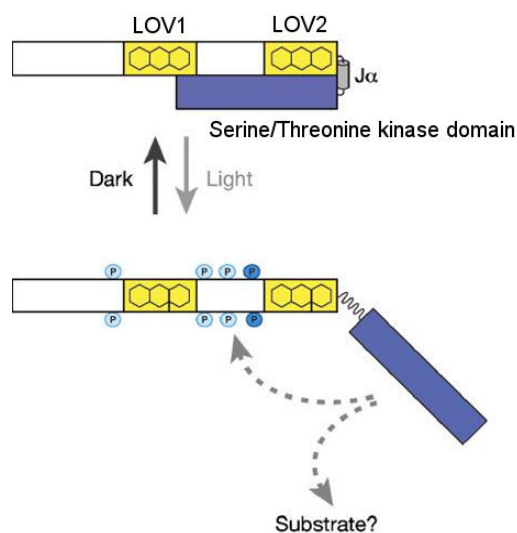


Figure 1.13 Proposed mechanism of phototropin kinase regulation from Christie, 2007 [78].

Figure 1.13 shows a schematic overview of phototropin receptor activation by light. In the dark or ground state, the phototropin receptor is un-phosphorylated and inactive. Absorption of light by the LOV2 results in a disordering of the $J\alpha$ -helix and activation of the C-terminal kinase domain, which consequently leads to auto-phosphorylation of the photoreceptor and possibly phosphorylation of an as-yet-unidentified protein substrate(s). Relative positions of known phosphorylation sites are indicated and color-coded based on their hierarchical pattern of occurrence [83].

1.3.1.2 BLUF domains

BLUF domain photosensors differ fundamentally from the rhodopsins, xanthopsins and phytochromes since the flavin chromophore cannot undergo large scale reorganization upon excitation [84]. Consequently the protein matrix must have evolved to sense subtler changes in chromophore structure resulting from light absorption. The transcriptional antirepressor AppA from the photosynthetic bacterium *Rhodobacter sphaeroides* regulates gene transcription in response to both light and oxygen [84]. AppA consists of two domains: the N-terminal BLUF domain and a C-terminal domain that is responsible for the oxygen sensitivity of the protein.

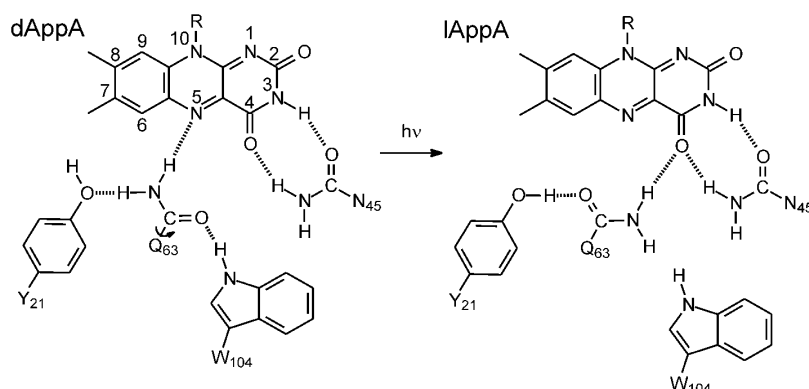


Figure 1.14 Environment of the isoalloxazine chromophore in AppA. Putative hydrogen bonding interactions are shown by dashed lines. Photoexcitation may lead to changes in the hydrogen bond network, one model for which involves a rotation of Q63 from Haigney, 2011 [85]. R is ADP-ribose.

Formation of the light-induced signaling state in AppA is characterized by a 10 nm red shift in the 445 nm electronic transition of the isoalloxazine chromophore [84] and is accompanied by a strengthening of hydrogen bond(s) to the C4=O group of the chromophore from the protein [86] [87] [88]. X-ray crystallographic studies have shown that the isoalloxazine C4=O group participates in a hydrogen bond network that also includes a conserved Q63, Y21 and W104 (Figure 1.14). This spatial structure of the protein, together with NMR spectroscopy results, supports a model for light activation that involves rotation of the Q63 side chain and an alteration in the hydrogen bonding environment of Y21

and W104 [89] [90]. As a consequence of this light-induced change in hydrogen bonding it has been proposed on structural grounds that W104 may move leading to formation of the signaling state of the protein [91]. Recent spectroscopic evidence suggests that W104 may move closer to the flavin in the signaling state [92], possibly contributing to acceleration of the ground state recovery time in the light adapted form [93].

Although the AppA signaling state has a half-life time of 15 min [84], it is formed within 1 ns of photoexcitation [94], an event thought to involve electron transfer from Y21 to the neighboring chromophore [95]. To provide further information on the early structural changes that result from light absorption, Tonge and coworkers undertook ultrafast time-resolved infrared (TRIR) studies of the AppA BLUF domain (AppA-BLUF) have been performed which led to the proposal [96] [93], now supported by computational studies [97] [98], that Q63 tautomerizes, rather than rotates, on the ultrafast time scale.

1.3.2 DNA photolyase

Cyclobutane pyrimidine dimers (CPDs; T<>T) and pyrimidine-pyrimidone (6-4) photoproducts (T[6-4]T) are the predominant structural modifications resulting from exposure of DNA to high-energy short-wavelength (< 350 nm) UV light [99] [100] (Figure 1.15).

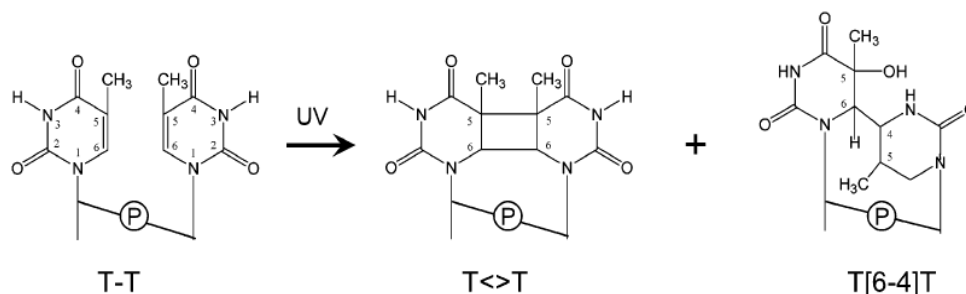


Figure 1.15 UV-induced DNA photoproducts; cyclobutane pyrimidine dimers (CPDs; T<>T) and pyrimidine-pyrimidone (6-4) (T[6-4]T) from Sancar, 2003 [101].

Both photoproducts result from $2\pi + 2\pi$ cycloadditions. Moreover, the structure of CPDs could be elucidated by Blackburn and Davies already 40 years ago [102] [103]. The potentially mutagenic or lethal modifications [104] must be repaired in order to ensure cell survival and genetic stability. This can be affected by excision repair or by photoreactivation mediated by DNA photolyases. There are two types of structurally related DNA photolyase, one called **CPD photolyase** that catalyze the light-driven cleavage of the cyclobutane ring of tricyclic pyrimidine dimers (T<>T) and the other called **6-4 photolyase** that repairs pyrimidine-pyrimidine (T[6-4]T) photoproducts [105] [106]. Both DNA photolyase types have similar sequences and most likely similar structures and reaction mechanisms [107] [108]. Generally, photolyase contains two noncovalently bound chromophoric cofactors

(catalytic cofactor and light-harvesting cofactor). The catalytic cofactors are always FAD, which directly interacts with substrate (CPD) in the photo-repair reaction. The second cofactor is either methenyltetrahydrofolate (MTHF) or 8-hydroxy-7,8-didemethyl-5-deazariboflavin (8-HDF), which acts as an antenna to harvest and transfer light energy to the catalytic cofactor.

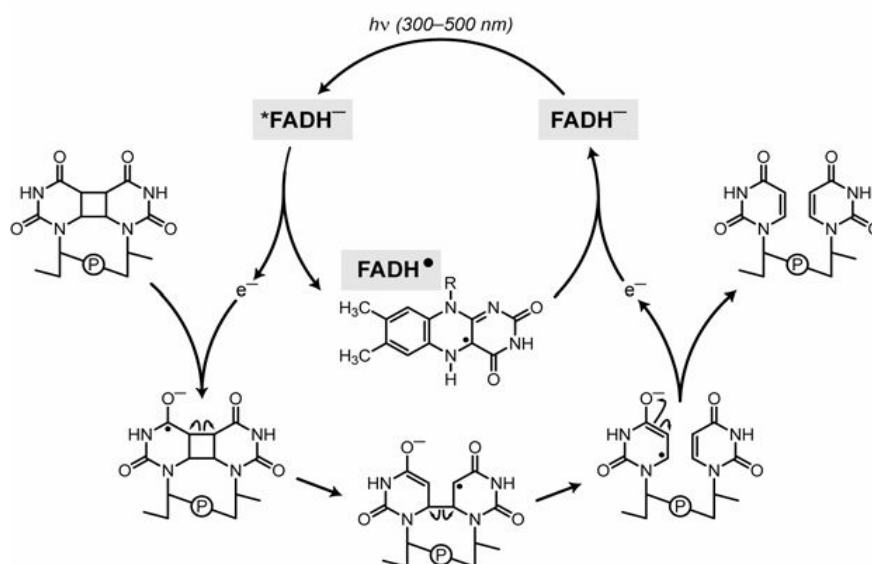


Figure 1.16 Putative reaction mechanism of DNA photolyase from Schleicher, 2005 [109].

The catalytic flavin in DNA photolyases can be found in oxidized, one-electron-reduced (neutral blue radical or anionic red radical), and two-electron reduced (neutral or anionic) forms [110] [111] [112]. The first enzymatic step in the repair of a CPD lesion is the light-dependent binding of CPD photolyase to the damaged DNA, and recognition of the CPD lesion as a substrate. The excitation energy of a photon absorbed from the light-harvesting chromophores is rapidly passed on to the active, twofold reduced, catalytic flavin cofactor (FADH^-) through a Förster-type mechanism. The excited-state FADH^- chromophore is believed to donate an electron to the pyrimidine dimer in the DNA, thus generating a substrate radical anion and a neutral FADH^\bullet radical [112] [113] [114]. The dimeric pyrimidine radical anion splits into pyrimidine monomers, and the excess electron is transferred back to the FADH^- cofactor to regenerate the initial redox state of the flavin, FADH^- (Figure 1.16).

DNA photolyase from *Thermus thermophilus* is stable up to 60 °C and in guanidine-HCl up to 2.5 M at neutral pH. The thermostable and physically stable characters are favorable for functional analysis. This enzyme contains a cavity between its two domains that is the right size to enclose an 8-HDF molecule as an antenna chromophore (Figure 1.17). However, FMN was recently biochemically shown to be an alternative candidate for the antenna chromophore in the *Thermus* photolyase [115]. Recently, the crystal structure has been solved (Protein Data Bank codes 1IQR, 2J07, 2J09) [116] [117].

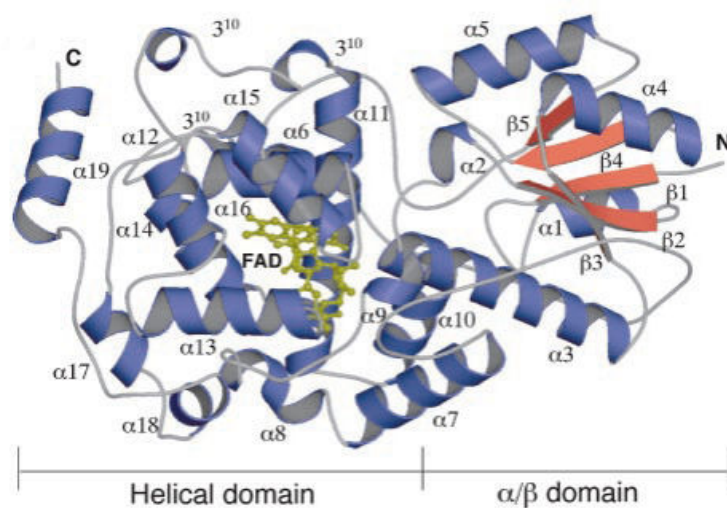


Figure 1.17 Crystal structure of *Thermus thermophilus* photolyase. FAD is shown in yellow. The N and C termini are labeled N and C, respectively from Komori, 2001 [116].

2 Materials and Methods

2.1 Materials

2.1.1 Chemicals

Table 2.1 List of chemicals used in this study.

Chemicals	Source
Acetic acid	Roth, Karlsruhe, Germany
Acetone	Roth, Karlsruhe, Germany
Acrylamide/bis-acrylamide (29 : 1), 40 %	Roth, Karlsruhe, Germany
Ammonium formate	Merck, Darmstadt, Germany
Ammonium persulfate	Sigma, Deisenhofen, Germany
Ammonium sulfate	Merck, Darmstadt, Germany
Casein hydrolysate	Roth, Karlsruhe, Germany
D ₂ O 99.9 %	ABCR, Karlsruhe, Germany
DMSO-d ₆ 99.9 %	Deutero, Kastellaun, Germany
DTT	Biomol, Hamburg, Germany
EDTA	Merck, Darmstadt, Germany
Ethanol	Merck, Darmstadt, Germany
Glucose	Merck, Darmstadt, Germany
Glycerol	Roth, Karlsruhe, Germany
Hydrochloric Acid	Merck, Darmstadt, Germany
Imidazole	Merck, Darmstadt, Germany
IPTG (Isopropyl-1-thio-β-D-galactopyranoside)	Roth, Karlsruhe, Germany
Magnesium Chloride	Merck, Darmstadt, Germany
Manganese Chloride	Sigma-Aldrich, Steinheim, Germany
Methanol	Merck, Darmstadt, Germany
Phenylmethanesulfonyl fluoride	Sigma-Aldrich, Steinheim, Germany
Potassium chloride	Merck, Darmstadt, Germany
Serva Blue G (Coomassie Brilliant Blue G-250)	Serva, Heidelberg, Germany
Sodium azide	Merck, Darmstadt, Germany
Sodium chloride	Roth, Karlsruhe, Germany
Sodium hydroxide	Merck, Darmstadt, Germany
TEMED	Roth, Karlsruhe, Germany
Tris (Hydroxymethyl) aminomethane	Merck, Darmstadt, Germany
Yeast extract	Roth, Karlsruhe, Germany
dNTP mix	New England Biolabs, Frankfurt, Germany
Agar	Roth, Karlsruhe, Germany
Agarose	Merck, Darmstadt, Germany
Ampicillin	Roth, Karlsruhe, Germany
Kanamycine	Roth, Karlsruhe, Germany
Guanidine-HCl	Sigma-Aldrich, Steinheim, Germany

Table 2.2 List of standards and Kits.

Name	Source
DNA Marker	New England Biolabs, Frankfurt, Germany
DNA sample buffer	PEQLAB, Erlangen, Germany
Gel Extract Kit	PEQLAB, Erlangen, Germany or Solgent, South Korea
PCR purification Kit or Cycle-Pure Kit	PEQLAB, Erlangen, Germany or Solgent, South Korea
Plasmid miniprep Kit	Qiagen, Hilden, Germany

2.1.2 Substrates and cofactors

FMN and phosphoenol pyruvate (PEP) were purchased from Fluka. FAD and ATP were purchased from Sigma. Riboflavin, 6,7-dimethyl-8-ribityllumazine and [4-¹⁸O₁]riboflavin were obtained from Dr. Boris Illarionov (Ikosatec, Hamburg, Germany). [1-¹³C₁]Glucose, [2-¹³C₁]glucose, [U-¹³C₆]glucose and [2-²H₁]glucose were purchased from Omicron (South Bend, Indiana, USA). [1-²H₁]Ribose was from Cambridge Isotope Laboratories (Andover, MA, USA). [7 α -¹³C₁]6,7-Dimethyl-8-ribityllumazine, [6,6 α ,7,7 α -¹³C₄]6,7-dimethyl-8-ribityllumazine, [4,10 α -¹³C₂]riboflavin and [5 α ,6,7,7 α ,8,8 α ,9,9 α -¹³C₈]riboflavin were obtained from Dr. Werner Römisch.

2.1.3 Enzymes

Name of Enzymes	Source
Ribose phosphate isomerase	Sigma, Deisenhofen, Germany
DNase I	AppliChem, Darmstadt, Germany
Pyruvate kinase	Sigma, Deisenhofen, Germany
Lysozyme	Sigma, Deisenhofen, Germany
Thrombin	Sigma, Deisenhofen, Germany
DyNAzyme-EXT	Finnzymes, Schwerte, Germany
Phusion Hot Start	Finnzymes, Schwerte, Germany
T4 DNA ligase	New England Biolabs, Frankfurt, Germany
Restriction enzyme (<i>Bam</i> HI, <i>Pst</i> I...etc)	New England Biolabs, Frankfurt, Germany
BSA	New England Biolabs, Frankfurt, Germany
Taq polymerase	Eurogentec, Koeln, Germany

2.1.4 Culture medium

The components of media were dissolved in deionized water. The medium was sterilized by autoclaving (121 °C, 1 bar, 25 min). Supplements were added as indicated.

LB (Luria Bertani) Medium	10 g/L Casein hydrolysate 5 g/L Yeast Extract 10 g/L NaCl
LB (Luria Bertani) agar plates	10 g/L Casein hydrolysate 5 g/L Yeast Extract 10 g/L NaCl 20 g/L agar
Glycerol Medium	70 % LB-Medium 30 % Glycerol
SOC-Medium for electroporation	20 g/L Casein hydrolysate 5 g/L Yeast Extract 20 mM Glucose 10 mM MgSO ₄ 10 mM NaCl 10 mM MgCl ₂ 2.5mM KCl
M9 Mineral Medium for <i>E. coli</i>	12 g/L Na ₂ HPO ₄ , pH 7.5 3 g/L KH ₂ PO ₄ 0.5 g/L NaCl 0.4 % (v/v) Vitamin-Mix 0.1 % (v/v) Trace-elements-Mix 3 g/L Glucose or 3 g/L ¹³ C-Glucose 1 g/L NH ₄ Cl or 1 g/L ¹⁵ N-NH ₄ Cl 0.138 g/L MgSO ₄ 5.5 mg/L CaCl ₂
Vitamin-Mix	20 mg/L Pyridoxamin hydrochloride 10 mg/L Thiamin hydrochloride 20 mg/L para-aminobezoic acid 20 mg/L Calcium pantothenate 5 mg/L Biotin

	10 mg/L Folic acid
	100 mg/L Cyanocobalamin
Trace-elements-Mix	16 g/L MnCl ₂ -4H ₂ O
	15 g/L CuCl ₂ -2H ₂ O
	27 g/L CoCl ₂ -6H ₂ O
	37.5 g/L FeCl ₃
	40.8 g/L sodium citrate
	84 mg/L Zn-acetate-2H ₂ O
	50 g/L Na ₂ -EDTA

2.1.5 Buffers

2.1.5.1 SDS-Polyacrylamide gel electrophoresis

All solutions were filtered and stored at room temperature.

APS solution	10 % (w/v) Ammonium peroxide sulfate
Stacking gel buffer	0.25 M Tris-HCl, pH 6.8
	0.2 % (w/v) SDS
Running gel buffer	1.5 M Tris-HCl, pH 8.8
	0.4 % (w/v) SDS
Coomassie staining solution	0.25 % (w/v) Coomassie Blue R-250
	0.2 % (w/v) Coomassie Brilliant Blue G-250
	45 % Methanol
	9 % Acetic acid
Destaining solution	20 % (v/v) Methanol
	15 % (v/v) Acetic acid
Electrophoresis buffer	25 mM Tris-HCl, pH 8.3
	192 mM Glycine
	0.1% (w/v) SDS
2X Protein sample loading buffer	60 mM Tris-HCl, pH 6.8
	5 % (w/v) SDS
	3 % (v/v) 2-Mercaptoethanol

30 % (v/v) Glycerol
10 % (w/v) Sucrose
0.02 % (w/v) Bromophenol blue

2.1.5.2 Agarose gel electrophoresis

TAE buffer	40 mM Tris-Acetate pH 8.2 1 mM EDTA
TBE buffer	98 mM Tris-Borate, pH 8.2 2 mM EDTA
EtBr staining solution	0.01 % (w/v) Ethidium Bromide

2.1.5.3 Protein determination

The mixture was adjusted to 1 L with distilled water and was stirred overnight. The solution was filtered and stored in a dark colored bottle at 4 °C.

Bradford's Reagent	0.1 g Coomassie Brilliant Blue G-250 100 ml 85 % Phosphoric acid 50 ml Ethanol
--------------------	--

2.1.5.4 Chemically competent cells

All solutions were sterile filtered and stored at room temperature.

Chemically competent cell RF1 buffer	100 mM RbCl 50 mM MnCl ₂ 30 mM Potassium acetate 10 mM CaCl ₂ 15 % Glycerol
Chemically competent cell RF2 buffer	10 mM MOPS 10 mM RbCl

75 mM CaCl₂
15 % Glycerol

2.1.5.5 Regeneration of Nickel column

All of buffers were filtrated and degassed prior to use.

Step 1 solution (3 column volumes)	50 mM EDTA, pH 8.0 500 mM NaCl
Step 2 solution (3 column volumes)	200 mM NaCl
Step 3 solution (2 column volumes)	50 mM Hepes, pH 7.0
Step 4 solution (5 column volumes)	0.02 % (w/v) Sodium azide
Step 5 solution (2 column volumes)	100 mM Nickel sulfate
Step 6 solution (5 column volumes)	0.02 % (w/v) Sodium azide

2.1.5.6 Protein purification

buffer A	50 mM Tris-HCl, pH 7.0 300 mM NaCl 20 mM imidazole 0.02 % (w/v) sodium azide
buffer B	50 mM Tris-HCl, pH 7.0 1 mM DTT 0.02 % (w/v) sodium azide
buffer C	50 mM sodium phosphate, pH 7.0 300 mM NaCl 10 mM imidazole 0.02 % (w/v) sodium azide
buffer D	50 mM Tris-HCl, pH 7.5 200 mM KCl 2.5 mM CaCl ₂
buffer E	25 mM Sodium phosphate 25 mM Potassium phosphate, pH 7.0 0.02 % sodium azide
buffer F	50 mM potassium phosphate, pH 8.0 300 mM NaCl 10 % glycerol 0.02 % (w/v) sodium azide

2.2 Instruments

Instruments	Source
Acrylamid Electrophoresis	Gel- SE 250 Mighty Small II (Hoefer Scientific Instruments, San Francisco, USA)
Agarose Electrophoresis	Gel- Chamber and gel carrier (Appligene, Heidelberg)
Autoclave	Vertical autoclaves VX-95, DX-23 (Systec, Wetztenberg)
Balance	Analysis Balance ABJ 220-4M (Kern & Sohn, Balingen-Frommern)
Bi-Destillation Apparation	Heraeus Quarzglas Destamat Bi 18E (QCS, Maintal)
Centrifuges	Sorvall super speed centrifuge RC5B Plus, RC6Plus with SS34, SH3000, SLA3000 rotors (Thermo Scientific, Osterode)
Cleanbanch	Heraeus HERAsafe (Thermo Scientific, Langenselbold)
Cuvette	Hellma-Quarzküvetten QS 1 cm (Hellma, Müllheim)
Electroporator	Electrophoresis power supply EV 231 (PEQLAB, Erlangen)
Eppendorf-Centrifuge	Jouan BR4i multifunction centrifuge (Thermo Scientific, ST Herblain, France)
Fermenter	BioFlo3000 (New Brunswick Scientific, Edison NJ, USA)
French Press	constant cell disruption system E 106 (Constant Systems, Northants, UK)
Heat block	Teche DRI-Block DB-2A (Gesellschaft für Laborgeräte mbH, Wertheim)
HPLC Instrumentation	HP Agilent 1100 HPLC (Agilent Technologies, Waldbronn)
Ice maker	LITV-IQ135 (Labcold, Basingstoke, UK)
Incubator	Heraeus Function Line Incubators B20 (Thermo Scientific, Langenselbold)
Magnetic stirrer with heating	MR-82 (Heidoph, Schwabach)
NMR-Spectrometer	Bruker AC 250, AM 360 and DRX 500 (Bruker, Karlsruhe)
PCR thermocycler	Thermocycler T3000 (Biometra, Goettingen)
Peristaltic Pump	Pharmacia LKB Pump P-1 (Amersham Bioscience, Cambridge, UK)
pH-Meter	Chem-mate pH meter (Beckman Scientific instrument division, California, USA)
Photometer	Ultraspec 4300 pro UV/Visible Spectrophotometer (Amersham Bioscience, Cambridge, UK)
Plate reader	Microplate Reader Spectra Max M2 (Molecular devices, califonia, USA), Multiskan Spectrum Microplate Spectrophotometer (Thermo Scientific, Langenselbold)
Purification system	Aektaprime plus (GE Healthcare, Uppsala, Sweden)
Rotation evaporator	Membrane pump-Vaccum pump MZ-C2 (Vaccum brand GmbH & Co, Wertheim) Rotavapor RE 111 (Büchi, Essen), Water bath (Büchi, Essen)
Shaker	Incubation shaker TH20 (edmund buehler, Hechingen), IRC-1-G CLIM-O-SHAKE (Kuhner, Birsfelden, Schweiz)
Table Vibrator	PEAX-1 (Heidoph, Schwabach)
Ultrafiltration Chamber	Ultrafiltration cell 50 ml and 10 ml (Amicon, Witten)
Ultrasonicator	Bandelin Sonopuls HD2200 (Bandelin electronic, Berlin)
Vacuum pump	Membrane pump-Vacuum pump MZ-C2 (Vaccum Brand GmbH&Co, Wertheim)
Video documentation	Biostep Bio imaging system (Biostep, Jahnsdorf)

2.3 Methods

2.3.1 Cloning and mutagenesis

2.3.1.1 PCR

PCR Mixture used in this study:

DNA Template	0.5 µl
100 pmol/µl of Forward primer	1 µl
100 pmol/µl of Reverse primer	1 µl
DNA Polymerase*	1 µl
dNTP mix**	3 µl
buffer***	10 µl or 5 µl
Distilled water	Add to 100 µl
<hr/>	
Total mixture	100 µl

-DNA Polymerase*: DyNAzyme-EXT DNA polymerase for mutagenesis and cloning, Phusion Hot Start High-Fidelity DNA polymerase for point mutagenesis.

-dNTP mix** contains (from New England Biolabs): 10 mM dATP, dCTP, dGTP and dTTP.

-10X Optimized DyNAzyme EXT Buffer*** (Finnzymes) contains: 500 mM Tris-HCl (pH 9.0 at 25 °C), 15 mM MgCl₂, 150 mM (NH₄)₂SO₄ and 1 % Triton® X-100.

-5X Phusion HF Buffer*** (Finnzymes) contains: 250 mM Tris-HCl (pH 9.0 at 25°C), 7.5 mM MgCl₂, 75 mM (NH₄)₂SO₄ and 0.1 % Triton® X-100.

PCR program used in this study:

PCR step	Temperature	Time	Cycles
Pre-denature	95 °C	5 min	1 cycle
Denature	95 °C	20 sec	20 - 30 cycles*
Annealing	50 – 60 °C**	20 sec	
Elongation	72 °C	1 min 20 sec	
Post-Elongation	72 °C	7 min	1 cycle
End	4 °C	hold	

-Cycle*: General guideline is 30 cycles. Colony PCR screening is 20 cycles. The two step mutagenesis is 25 Cycles for the 1st PCR and 20 cycles for the 2nd PCR.

-Annealing Temperature**: A guideline for determination of the annealing temperature is to use a temperature 5 °C lower than the lower T_m calculated by the nearest-neighbor method. With Phusion Hot Start DNA polymerase, primers with T_m 60 °C or higher were used. Typically the length of such primers was 20 nt or more.

2.3.1.2 DNA Restriction enzymes

Incubation of a 100 µl reaction mixture containing 1 µg of DNA and 1 unit of restriction enzyme for 1 - 2 h at 37 °C resulted in a DNA pattern free of detectable nuclease degradation as determined by agarose gel electrophoresis.

Table 2.3 Restriction enzymes used in this study (from New England Biolabs).

Name of enzyme	Restriction site	Restrictions buffer
<i>Bam</i> HI	5'...G [▼] GATCC...3' 3'...CCTAGG [▲] ...5'	NEBuffer 3**
<i>Hind</i> III	5'...A [▼] AGCTT...3' 3'...TTCGAA [▲] ...5'	NEBuffer 2*
<i>Pst</i> I	5'...CTGCA [▼] G...3' 3'...G [▲] ACGTC...5'	NEBuffer 3**
<i>Kas</i> I	5'...G [▼] GCGCC...3' 3'...CCGCGG [▲] ...5'	NEBuffer 4***
<i>Hin</i> fI	5'...G [▼] ANTC...3' 3'...CTNA [▲] G...5'	NEBuffer 4***
<i>Hph</i> I	5'...GGTGA(N) ₈ [▼] ...3' 3'...CCACT(N) ₇ [▲] ...5'	NEBuffer 4***
<i>Sna</i> BI	5'...TAC [▼] GTA...3' 3'...ATGCAT...5'	NEBuffer 4***
<i>Nde</i> I	5'...CA [▼] TATG...3' 3'...GTAT [▲] AC...5'	NEBuffer 4***

-10× NEBuffer 2* contains: 100 mM Tris-HCl, 500 mM NaCl, 100 mM MgCl₂, 10 mM dithiothreitol, pH 7.9 at 25 °C

-10× NEBuffer 3** contains: 500 mM Tris-HCl, 1 M NaCl, 100 mM MgCl₂, 10 mM dithiothreitol, pH 7.9 at 25 °C

-10× NEBuffer 4*** contains: 200 mM Tris-acetate, 500 mM potassium acetate, 100 mM magnesium acetate, 10 mM dithiothreitol, pH 7.9 at 25 °C

2.3.1.3 Isolation of PCR fragments or plasmids

PEQLAB Cycle-Pure Kit

Add 5 volumes of CP buffer to 1 volume of PCR product and mix well. If the PCR fragment is shorter than 200 bp, add 6 volumes of CP buffer to the sample. If the PCR fragment is longer than 4 kbp, add 3 volumes of CP buffer to the sample. The Mixture is applied to a HiBind-DNA column and centrifuged for 1 min. Discard flow-through and adds 750 µl of DNA Wash Buffer to the column, and then centrifuges for 1 min. Discard flow-through, centrifuge for 3 min, and then dries for 3 min. The column is then placed in a micro-centrifuge tube. Sterile water (30 µl) is added to the center of the membrane to elute DNA; let the column stand for 1min, and then centrifuge for 3 min.

PEQLAB Gel Extraction Kit

DNA was mixed with 10× DNA Sample Buffer (from PEQLAB, 5:1) and was subjected to agarose gel electrophoresis. A DNA Marker a 2-Log DNA Ladder (0.1 – 10.0 kb) from New England Biolabs was used. The gels contained 0.8 – 1 % agarose in TAE buffer. After gel electrophoresis was finished, gels were stained with 0.01 % (w/v) ethidium bromide solution and photographs were taken under UV light. For DNA isolation, DNA fragments were excised from the agarose gel with a clean, sharp scalpel. The size of the gel slices was minimized by dissection. Gel slices were weighed, an equal volume of Binding Buffer was added, and the sample was incubated for 10 min at room temperature. The mixture had normally light yellow coloration. If the color of the mixture turned to red or orange, 5 µl of 5 M sodium acetate were added. After the gel was melted, the resulting solution was applied to a PerfectBind-DNA column and centrifuged for 1 min. The flow-through was discarded, 300 µl of Binding Buffer were applied to the column, which was then centrifuged for 1 min. Flow-through was discarded, 750 µl of CG Buffer were added to the column, which was centrifuged again for 1 min. Flow-through was discarded, the column was centrifuged for 3 min and dried for 3 min. The column was then placed into a clean micro-centrifuge tube. Sterile water (30 µl) was applied to the center of the membrane. After 1 min, the column was centrifuged for 3 min.

QIAGEN QIAprep Miniprep Kit

A fresh overnight culture (10 ml) was centrifuged (4000 rpm, 15 min, RT) and the supernatant was discarded. The pellet was resuspended in 250 µl of Buffer P1 and transferred to a micro-centrifuge tube. Buffer P2 (250 µl) was added and mixed thoroughly by inverting the tube 4 - 6 times, and then 350 µl of Buffer N3 were added and mixed immediately and thoroughly by inverting the tube until the solution turned colorless. The mixture was centrifuged for 10 min at 13000 rpm, 4 °C. The supernatant was applied to a QIAprep spin column and centrifuged for 1 min. Flow through was discarded and PB Buffer (500 µl) was added to the column, which was then centrifuged for 1 min. Flow through was discarded, PE Buffer (750 µl) was added to the column, and then the latter was centrifuged for 1 min. Flow through was discarded, the column was centrifuged for 3 min, and then dried for 3 min. The

column was placed into a micro-centrifuge tube. Sterile water (30 μ l) was added to the center of the membrane. After 1 min, the column was centrifuged for 3 min.

2.3.1.4 Ligation of insert into the Vector

The ligation mixture contained vector and insert at a molar ration of 1:3. Reaction mixtures were kept at 4 °C overnight, and then purified by Cycle-Pure Kit.

Ligation Mixture used in this study:

Vector	0.1 pmol
Insert	0.3 pmol
T4 DNA Ligase	1 μ l
T4 DNA Ligase Reaction Buffer*	7.5 μ l
Distilled water	Add to 75 μ l
<hr/>	
Total mixture	75 μ l

-10X T4 DNA Ligase Reaction Buffer* (from New England Biolabs) contains: 500 mM Tris-HCl, 100 mM MgCl₂, 10 mM ATP, 100 mM dithiothreitol (pH 7.5, at 25 °C)

2.3.1.5 Transformation

Electrocompetent cells

Electrocompetent cells were prepared according to a protocol of Dower et al. (1988) [118]. A single colony of *E. coli* strain was inoculated into 700 ml of LB medium and grown at 37 °C until the optical density at 600 nm was 0.6. The suspension was incubated on ice for 30 min and centrifuged for 20 min at 3000 rpm and 4 °C. The supernatant was discarded, and the pellet was resuspended gently in 500 ml of 10 % ice-cold, sterile glycerol. The cells were centrifuged for 20 min at 3000 rpm and 4 °C. The pellet was washed with 250 ml of 10 % ice-cold, sterile glycerol and centrifuged. The pellet was washed with 20 ml of 10 % ice-cold, sterile glycerol and centrifuged. The pellet was then resuspended in 2 ml of 10 % ice-cold, sterile glycerol. Aliquots (100 μ l) were stored in liquid nitrogen.

Electrocompetent cells (50 μ l) were thawed on ice, and 1 μ l of plasmid DNA (100 ng/ μ l) or 10 μ l of ligation mixture were added. The mixture was transferred into a precooled electroporation cuvette (gap width 0.2 - 0.5 cm). The well dried cuvette was put into the electroporation chamber and an electric shock was passed through the cuvette (Parameters: capacity, 25 μ F; resistance, 200 Ω ; tension, 2.5 kV). The cells were immediately resuspended in 1 ml of SOC medium or LB medium, and the mixture was shaken for 30 min at 37 °C. The cell suspension was centrifuged at 5000 rpm for 5 min, and the pellet was spread on an LB agar plate containing selective antibiotics, and incubated at 37 °C overnight.

Chemically competent cells

A single colony of *E. coli* strain was inoculated into 10 ml of LB-medium and grown at 28 °C overnight. The overnight culture was inoculated into 500 ml of LB medium containing 5 mM MgCl₂ and 5 mM MgSO₄, and grown at 37 °C until the optical density at 600 nm was 0.4. The cell suspension was incubated on ice for 15 min and then centrifuged for 15 min at 3000 rpm and 4 °C. The supernatant was discarded, and the pellet was resuspended in 400 ml of RF1 Buffer, the suspension was incubated on ice for 15 min, and was then centrifuged for 15 min at 3000 rpm and 4 °C. The pellet was resuspended with 30 ml of RF2 Buffer. Aliquots (500 µl) were stored in liquid nitrogen.

Chemically competent cells (100 µl) were thawed on ice, and 1 µl of plasmid DNA (100 ng/µl) or 10 µl of ligation mixture were added. The mixture was incubated on ice for 10 min. The cells were heat-shocked in a 42 °C water bath for 90 seconds, and returned to ice. SOC medium or LB medium (1 ml) was added, and the mixture was shaken for 30 min at 37 °C. The medium was centrifuged at 5000 rpm for 5 min, the pellet was spread on LB agar plate containing selective antibiotics that was then incubated at 37 °C overnight.

Table 2.4 Bacterial strains used in this study.

<i>E. coli</i> strains	Relevant characteristics	Source
DNA cloning strain XL1-Blue	recA1, endA1, gyrA96, thi-1, hsdR17, supE44, relA1, lac[F', proAB, lacI ^q ZΔM15, Tn10(tet ^r)]	Bullock et al., 1987 [119]
Protein expression strain M15[pREP4]	lac, ara, gal, mtl, recA ⁺ , uvr ⁺ , [pREP4, Kan ^R , lacI]	Stueber et al., 1990 [120]
BL21[pREP4]	pREP4, lacI, kanR	Ostanin et al. 1992 [121]
BL21(DE3) pLysS	F ⁻ , ompT, hsdS _B (r _B ⁻ , m _B ⁻), dcm, gal, λ(DE3), pLysS, Cm ^r	Invitrogen

2.3.1.6 PCR screening

The original cloning primers were used for colony screening. The mixture was prepared as follows. A colony was picked up with a sterile toothpick that was then dipped into a PCR tube with an aliquot of the PCR mixture. The rest of the cells on the toothpick were streaked on an LB-agar plate supplied with appropriate antibiotics. The blank sample did not contain any cells or external DNA fragment, the positive control contained a small aliquot of the target DNA fragment. The amplified product was checked on 1 % of agarose gel. Positive clones were identified by the presence of PCR product of expected size. For isolation of the newly made plasmid construct, cells from a respective cell streak on

the LB plate were inoculated into 10 ml of LB medium supplemented with respective antibiotics. The cell culture was grown overnight at 37 °C, and cells were harvested by centrifugation. The plasmid DNA was isolated from the cell pellet by QIAprep Miniprep Kit. The isolated plasmid construct was confirmed by DNA sequencing.

Colony PCR screening Mixture used in this study:

100 pmol/μl of Forward primer	0.3 μl
100 pmol/μl of Reverse primer	0.3 μl
Taq polymerase for PCR screening	0.5 μl
dNTP mix	1 μl
Buffer*	3 μl
Distilled water	Add to 30 μl
Total mixture	30 μl

-10X Taq polymerase buffer* contains (from Eurogentec): 100 mM Tris-HCl, 500 mM KCl, 15 mM MgCl₂ (pH 8.3 at 25 °C)

2.3.1.7 Expression constructs for bifunctional flavokinase/ FAD synthetase

E. faecalis genomic DNA was amplified by PCR using the oligonucleotides EFFADS-F and EFFADS-R primers as shown in Table 2.5. The amplification was purified by Cycle-Pure Kit and served as template for a second PCR amplification using the oligonucleotides EFFADS-*Bam*HI and EFFADS-*Hind*III. The amplification was treated with the restriction enzymes *Bam*HI and *Hind*III, and purified by Cycle-Pure Kit.

Table 2.5 Oligonucleotides used in this study. Novel restriction sites are underlined.

Primer	Novel Restriction site	Nucleotide sequence
EFFADS-F		5'-GATAAATTATTGAAACCAAGTAAAGTTCT-3'
EFFADS-R		5'-TTCCTTAAACGCTTGATACGTTAAC-3'
EFFADS- <i>Bam</i> HI	<i>Bam</i> HI	5'-ATAATAGGATCCGAAAACCTGTATTTTCAGGGCCAAGTTATTCA ACTACATCATCCCTAT-3'
EFFADS- <i>Hind</i> III	<i>Hind</i> III	5'-TATTATTATAAGCTTATTTGTCCTCAGATTGTTGGAAATAGTC-3'

The purified fragments were ligated into the plasmid vector pET22-MAISPE which had been treated with the same restriction enzymes. The ligation mixture yielding the plasmid construct pET22-HCEFFADS was transformed into *E. coli* XL1-Blue cells. The colonies were screened by colony PCR screening. The selected colony was inoculated into 10 ml of LB medium supplemented with 150 mg/L

ampicillin and grown overnight at 37 °C with shaking. The cells were harvested, and plasmid DNA was isolated by QIAprep Miniprep Kit. The plasmid construct was confirmed by sequencing (GATC biotech in Germany) (Table 2.6).

Table 2.6 Plasmids used in this study.

Plasmids	Relevant characteristics	Source
pET22-MAISPE	pET22b containing the gene coding for hisactophilin from <i>D. discoideum</i> . This plasmid was used to import recombinant DNA into a host cell for cloning.	It was obtained from Dr. Victoria Illarionova.
pET22-HCEFFADS	pET22b containing the gene coding for FAD synthetase of <i>E. faecalis</i> fused to the 3'- end of the hisactophilin gene, connected by a linker segment specifying a TEV protease cleavage site.	this study (GenBank accession number HQ184465)

2.3.1.8 N-terminal domain of riboflavin synthase from *Escherichia coli*

Site directed mutagenesis was performed as described earlier [38]. The plasmid pERN was used as template. Oligonucleotides used as primers are shown in Table 2.7. PCR was performed with DyNAzyme EXT DNA polymerase (Chapter. 2.3.1.1). The mutagenesis PCR involved two rounds of amplification cycles using one mismatch and two flanking primers.

Table 2.7 Primers for site directed mutagenesis of N-terminal domain of riboflavin synthase. Codons specifying modified amino acid residues are shown in bold type. Novel restriction sites are underlined.

Primer	Amino acid replacement	Novel Restriction site	Nucleotide sequence
Forward	None	<i>Bam</i> HI	5'-GAG GAG AAA <u>GGA TCC</u> ATG TTT ACG G-3'
Reverse	None	<i>Pst</i> I	5'-GTC <u>CTG CAG</u> TTA GTG TCCGCC-3'
1	S41→C	<i>Kas</i> I	5'-GCA GCA ACC GTT ATG CGC CAC acA <u>gGC gCC</u> GGT TTC-3'
2	S41→V	<i>Kas</i> I	5'-GCA GCA ACC GTT ATG CGC CAC Gac <u>gGC gCC</u> GGT TTC-3'
3	S41→W	<i>Kas</i> I	5'-GCA GCA ACC GTT ATG CGC CAC ccA <u>gGC gCC</u> GGT TTC-3'
4	T50→A	<i>Hin</i> fI	5'-GAC ATG <u>aTT cCC</u> GTT AAT TTC CGT CAC GGe CAG GCA-3'
5	T50→W	<i>Hin</i> fI	5'-GAC ATG <u>aTT cCC</u> GTT AAT TTC CGT CAC cca CAG GCA-3'
6	T50→N	<i>Hin</i> fI	5'-GAC ATG <u>aTT cCC</u> GTT AAT TTC CGT CAC GtT CAG GCA-3'
7	C47→A	<i>Hph</i> I	5'-C CGT CAC <u>GGT gAG</u> GCA GgA ACC GTT ATG CGC C-3'
8	C47→D	<i>Hph</i> I	5'-C CGT CAC <u>GGT gAG</u> GCA Ggc ACC GTT ATG CGC C-3'
9	C47→S	<i>Hph</i> I	5'-C CGT CAC <u>GGT gAG</u> GCA Gtc ACC GTT ATG CGC C-3'
10	C48→A	<i>Hph</i> I	5'-C CGT CAC <u>GGT gAG</u> Ggc GCA ACC GTT ATG-3'
11	C48→N	<i>Hph</i> I	5'-C CGT CAC <u>GGT gAG</u> Gtt GCA ACC GTT ATG-3'
12	C48→T	<i>Hph</i> I	5'-C CGT CAC <u>GGT gAG</u> Ggt GCA ACC GTT ATG-3'
13	T67→A	<i>Sna</i> BI	5'-C GCC AAG ATT GGT AAT ACG TAA CGC TTC TTT CAT-3'

During the first round, 25 amplification cycles were carried out with the respective mismatch primer and one of two flanking primers. The amplified DNA was subjected to agarose gel electrophoresis and purified. Then, the second PCR was done using the second flanking primer and the PCR product of the first amplification as a primer for 20 additional cycles. The amplified DNA was purified by agarose gel electrophoresis and digested with *Bam*HI and *Pst*I. The digested product was purified by PCR purification Kit and ligated into the expression plasmid pQE30 (Table 2.8). This pQE30 vector was digested with the same restriction enzyme and was then subjected to agarose gel electrophoresis and purified. The ligation mixtures were purified by Cycle-Pure Kit and transformed into *E. coli* XL-1 blue cells. Positive clones were identified by colony PCR screening. The selected colony was inoculated into 10 ml of LB medium supplemented with 150 mg/L ampicillin and grown overnight at 37 °C with shaking. The cells were harvested and plasmid DNA was isolated by QIAprep Miniprep Kit. All plasmid constructs were confirmed by sequencing (Genotech Co. Ltd in Dae-Jeon, Korea).

Table 2.8 Plasmids used in this study.

Plasmid	Relevant characteristics	Source
pQE30	Expression vector	QIAGEN
pERN	pNCO113 containing the gene for the wild type N-terminal domain of <i>E. coli</i> riboflavin synthase	Eberhardt et al., 2001 [46]
pERN-C48S	pNCO113 containing the gene for the C48S mutant N-terminal domain of <i>E. coli</i> riboflavin synthase	Eberhardt et al., 2001 [46]
pQE30-NRS-WT	pQE30 containing the gene for the wild type N-terminal domain of <i>E. coli</i> riboflavin synthase	Kim et al., 2010 [39]
pQE30-NRS-mutant variants	pQE30 containing the gene for the mutant variants N-terminal domain of <i>E. coli</i> riboflavin synthase	Kim et al., 2010 [39]

2.3.1.9 DNA photolyase from *Thermus thermophilus*

The plasmid pNCO-TTCPD was treated with the restriction enzymes *Nde*I and *Bam*HI. The resulting restriction fragments were separated by agarose gel electrophoresis. The purified fragment ligated into the hyperexpression vector pET22b⁺ that had been digested with the same enzymes. The ligation mixture was purified by Cycle-Pure Kit and transformed into *E. coli* XL-1 blue cells. Positive clones were identified by colony PCR screening. The selected colony was inoculated into 10 ml of LB medium supplemented with 150 mg/L ampicillin and grown overnight at 37 °C with shaking. The cells were harvested and plasmid DNA was isolated by QIAprep Miniprep Kit. The sequence of the construct was confirmed by sequencing (GATC biotech in Germany) (Table 2.9).

Table 2.9 Plasmids used in this study.

Plasmid	Relevant characteristics	Source
pET22b+	Expression vector	
pNCO-TTCPD	pNCO113 containing the gene for the DNA photolyase from <i>Thermus thermophilus</i>	It was obtained from Prof. Markus Fischer (Universität Hamburg, Hamburg, Germany).
pET22b-TTCPD	pET22b+ containing the gene for the DNA photolyase from <i>Thermus thermophilus</i>	This study

2.3.2 Transformation and expression

2.3.2.1 Riboflavin and flavocoenzyme biosynthesis enzymes

Most of the enzymes were expressed from recombinant plasmid (Table 2.10); some of enzymes were purchased from Sigma.

Table 2.10 Enzymes used for riboflavin synthesis.

Enzyme name	EC-Nr	Strain	Reference	Plasmid	Monomer (Da)
Ribose kinase	2.7.1.15	<i>E. coli</i>		BL21-pET22b-EcRKc11	33898
Ribose phosphate isomerase	5.3.1.6	<i>S. oleracea</i>	Sigma		53000
3,4-Dihydroxy-2-butanon 4-phosphate synthase	4.1.99.12	<i>E. coli</i>	Römisch et al., 2002 [54]	M15[pRep4]-pQE30-ribB#2	24752
Lumazin synthase	2.5.1.78	<i>B. subtilis</i>	Fischer et. al., 2001 [122]	M15[pRep4]-pNCO-RibH-WT	17109
Riboflavin synthase	2.5.1.9	<i>E. coli</i>	Illarionov et. al., 2001 [38]	M15[pRep4]-pNCO-rosy	23444
Flavokinase	2.7.1.26	<i>S. pombe</i>	It was obtained from Dr. Monika Joshi.	M15[pREP4]-pNCO-FkSSP	18913
Bifunctional Flavokinase/FAD synthetase		<i>E. faecalis</i>	This study	BL21- pET22-HCEFFADS	36067

Ribose kinase of *Escherichia coli*

The recombinant plasmid of BL21-pET22b-EcRKc11 was transformed into *E. coli* strain BL21[pREP4]. The recombinant strain was inoculated into 50 ml of LB medium supplemented with 150 mg/L ampicillin and 25 mg/L kanamycin, and grown at 37 °C overnight. 10 ml from the overnight culture

was inoculated into 2 L flasks containing 800 ml of LB medium supplemented with 150 mg/L ampicillin and 25 mg/L kanamycin, and grown at 37 °C with shaking for 4 h. IPTG was added to a final concentration of 1 mM, and shaking was continued at 30 °C overnight. The cells were harvested by centrifugation (5000 rpm, 4 °C, 40 min), washed with 50 ml of 0.9 % NaCl, and then stored at -80 °C.

3,4-Dihydroxy-2-butanone 4-phosphate synthase of *Escherichia coli*

The recombinant plasmid of pQE30-ribB#2 was transformed into *E. coli* strain BL21[pREP4]. The recombinant strain was inoculated into 50 ml of LB medium supplemented with 150 mg/L ampicillin and 25 mg/L kanamycin, and grown at 37 °C overnight. 10 ml from the overnight culture was inoculated into 2 L flasks containing 800 ml of LB medium supplemented with 150 mg/L ampicillin and 25 mg/L kanamycin, and grown at 37 °C with shaking for 4 h. IPTG was added to a final concentration of 1 mM, and shaking was continued at 30 °C overnight. The cells were harvested by centrifugation (5000 rpm, 4 °C, 40 min), washed with 50 ml of 0.9 % NaCl, and then stored at -80 °C.

Lumazine synthase of *Bacillus subtilis*

The recombinant plasmid pNCO-RibH-WT was transformed into *E. coli* strain BL21[pREP4]. The recombinant strain was inoculated into 50 ml of LB medium supplemented with 15 mg/L erythromycin, 20 mg/L kanamycin, and grown at 32 °C overnight. 10 ml from the overnight culture were transferred into 2 L flasks containing 800 ml of LB medium supplemented with 15 mg/L erythromycin, 20 mg/L kanamycin, and grown at 32 °C with shaking for 4 h. IPTG was added to a final concentration of 1 mM, and shaking was continued at 32 °C overnight. The cells were harvested by centrifugation (5000 rpm, 4 °C, 40 min), washed with 50 ml of 0.9 % NaCl, and then stored at -80 °C.

Riboflavin synthase of *Escherichia coli*

The recombinant plasmid pNCO-rosy was transformed into the *E. coli* strain M15[pREP4]. The recombinant strain was inoculated into 50 ml of LB medium supplemented with 150 mg/L ampicillin and 25 mg/L kanamycin, and grown at 37 °C overnight. 10 ml from the overnight culture were transferred into 2 L flasks containing 800 ml of LB medium supplemented with 150 mg/L ampicillin and 25 mg/L kanamycin, and grown at 37 °C with shaking for 4h. IPTG was added to a final concentration of 1 mM, and shaking was continued at 30 °C overnight. The cells were harvested by centrifugation (5000 rpm, 4 °C, 40 min), washed with 50 ml of 0.9 % NaCl, and then stored at -80 °C.

Flavokinase of *Schizosaccharomyces pombe*

The recombinant plasmid pNCO-FkSSP was transformed into the *E. coli* strain M15[pREP4]. The recombinant strain was inoculated into 50 ml of LB medium supplemented with 150 mg/L ampicillin

and 25 mg/L kanamycin, and grown at 37 °C overnight. 10 ml from the overnight culture was inoculated into 2 L flasks containing 800 ml of LB medium supplemented with 150 mg/L ampicillin and 25 mg/L kanamycin, and grown at 37 °C with shaking for 4 h. IPTG was added to a final concentration of 1 mM, and shaking was continued at 30 °C overnight. The cells were harvested by centrifugation (5000 rpm, 4 °C, 40 min), washed with 50 ml of 0.9 % NaCl, and then stored at -80 °C.

Bifunctional Flavokinase/FAD synthetase of *Enterococcus faecalis*

The recombinant plasmid pET22-HCEFFADS was transformed into the *E. coli* strain BL21(DE3). The recombinant strain was inoculated into 50 ml of LB medium supplemented with 150 mg/L ampicillin and grown at 37 °C overnight. 10 ml from the overnight culture were transferred into 2 L flasks containing 800 ml of LB medium supplemented with 150 mg/L ampicillin and grown at 37 °C with shaking for 4 h. IPTG was added to a final concentration of 1 mM, and shaking was continued at 30 °C overnight. The cells were harvested by centrifugation (5000 rpm, 4 °C, 40 min), washed in 50 ml of 0.9 % NaCl, and then stored at -80 °C.

2.3.2.2 N-terminal domain of riboflavin synthase of *Escherichia coli*

The recombinant plasmids pQE30-NRS-WT and pQE30-NRS-mutants were transformed into the *E. coli* strain M15[pREP4]. The recombinant strain was inoculated into 50 ml of LB medium supplemented with 150 mg/L ampicillin and 25 mg/L kanamycin, and grown at 37 °C overnight. 10 ml from the overnight culture were inoculated into 2 flasks containing 800 ml of LB medium supplemented with 150 mg/L ampicillin and 25 mg/L kanamycin, and grown at 37 °C with shaking for 4 h. IPTG was added to a final concentration of 1 mM, and shaking was continued at 30 °C overnight. The cells were harvested by centrifugation (5000 rpm, 4 °C, 40 min), washed in 50 ml of 0.9 % NaCl, and then stored at -80 °C.

2.3.2.3 LOV2 domain of *Avena sativa* phototropin

The recombinant plasmids pNCO-HISACT-ASLOV2-WT-LC and pNCO-HISACT-ASLOV2C450A-LC were transformed into the *E. coli* strain M15[pREP4]. The recombinant strain was inoculated into 50 ml of LB medium supplemented with 150 mg/L ampicillin and 25 mg/L kanamycin, and grown at 37 °C for 8 h. 10 ml of culture were transferred into 2 L flasks containing 800 ml of LB medium supplemented with 150 mg/L ampicillin and 25 mg/L kanamycin, and grown at 37 °C with shaking for 3 h. IPTG was added to a final concentration of 1 mM, and shaking was continued at 30 °C overnight. The cells were harvested by centrifugation (5000 rpm, 4 °C, 40 min), washed in 50 ml of 0.9 % NaCl, and then stored at -80 °C.

2.3.2.4 BLUF domain of AppA protein of *Rhodobacter sphaeroides*

The recombinant plasmid pET15b-WTAppA was transformed into the *E. coli* strain BL21(DE3). The recombinant strain was inoculated into 50 ml of LB medium supplemented with 100 mg/L ampicillin and grown at 30 °C for 8 h. 10 ml of culture were inoculated into 2 L flasks containing 800 ml of TB medium supplemented with 100 mg/L ampicillin and grown at 30 °C with shaking for 4 h. IPTG was added to a final concentration of 1 mM, and shaking was continued at 18 °C overnight. The cells were harvested by centrifugation (5000 rpm, 4 °C, 40 min), washed with 50 ml of 0.9 % NaCl, and then stored at -80 °C.

2.3.2.5 DNA photolyase of *Thermus thermophilus*

The plasmid specifying the sub-cloned DNA photolyase of *Thermus thermophilus* (pET22b-TTCPD) was transformed into the *E. coli* strain BL21 [pREP4]. The recombinant strain was inoculated into 50 ml of LB medium supplemented with 150 mg/L ampicillin and grown at 30 °C for overnight. 10 ml from the overnight culture were inoculated into 2 L flasks containing 800 ml of TB medium supplemented with 150 mg/L ampicillin and grown at 30 °C with shaking for 6 h. IPTG was added to a final concentration of 1 mM, and shaking was continued at 18 °C for 48 h. The cells were harvested by centrifugation (5000 rpm, 4 °C, 40 min), washed in 50 ml of 0.9 % NaCl, and then stored at -80 °C.

2.3.3 SDS polyacrylamide gel electrophoresis

Protein fractions were monitored using discontinuous sodium dodecyl sulfate polyacrylamide gel electrophoresis (SDS-PAGE) according to Laemmli, 1970 [123]. Gels were prepared using the SDS-PAGE discontinuous buffer system with vertical slab gels. The components of the separating gel solution were mixed together, and then loaded into the slab deposited between two glass plates on the gel caster. The top of the gel was overlaid with isopropanol.

Table 2.11 SDS-PAGE discontinuous buffer system using this study.

	Stacking Gel (4 %)	Running Gel (15 %)	Running Gel (17 %)
Acrylamide	0.5 ml	3.5 ml	4.3 ml
Stacking Gel buffer	2.5 ml		
Running Gel buffer		2.5 ml	2.5 ml
D.W	2 ml	3.75 ml	3 ml
10 % (w/v) APS	75 µl	100 µl	100 µl
TEMED	5 µl	5 µl	5 µl

The polymerisation of acrylamide was completed after 1 h. After removing the isopropanol, the stacking gel solution was prepared and loaded on top of the separating gel (air bubbles avoided) in the presence of a 10 wells comb. The polymerisation of stacking gel was completed after 20 min. The slab gel was placed on the SE 250 Mighty Small II electrophoresis system (Hoefer Scientific, San Francisco, USA). Protein samples were mixed with Protein sample loading buffer at a ratio of 1:1. The mixtures were heated at 95 °C for 10 min and 7 µl of protein samples were loaded into the wells. Standard proteins were used as molecular weight markers (Table 2.12). The electrophoresis system was powered from a power supply with 20 mA per gel. After running for 2 h, the gel was removed carefully and stained in the coomassie staining solution (0.25 % coomassie blue R-250, 0.2 % coomassie brilliant blue G-250, 45 % methanol and 9 % acetic acid) for 30 min. The gel was then destained with the destaining solution (20 % methanol and 15 % acetic acid) for 1 h (see Methods 2.1.5.2).

Table 2.12 5 Standard proteins were used as protein marker.

Protein	Approximate Molecular Weight in kDa
Albumin, Bovine	66.0
Albumin, Egg	45.0
Glycerolaldehyde-3-phosphate-dehydrogenase	36.0
Carbonic anhydrase, Bovine	29.0
Trypsin-Inhibitor, Soyabean	20.0
α-lactalbumin, Bovinemilk	13.7

2.3.4 Protein purification

2.3.4.1 Purification of enzymes for riboflavin biosynthesis

2.3.4.1.1 Ribose kinase of *Escherichia coli*

Frozen cell mass (20 g) was resuspended in 50 ml of buffer A (50 mM Tris-HCl pH 7, 300 mM NaCl, 20 mM imidazole and 0.02 % sodium azide). Lysozyme (5 mg), DNase I (5 mg), and phenylmethanesulfonyl (0.5 mM) were added. The mixture was incubated at room temperature for 30 min with stirring and then passed through a French Press. Cell debris was removed by centrifugation (15000 rpm, 60 min, 4 °C) and the supernatant was placed on the top of a Ni⁺-column (2 × 15 cm) that had been equilibrated with buffer A. The flow rate was 2 ml/min. The column was washed with 5 column volumes of buffer A and was then developed with 300 ml of buffer A with a linear gradient of imidazole (20 mM – 1 M). Fractions were analyzed by SDS-PAGE and selected fractions were combined and dialyzed against 50 mM Tris-HCl (pH 7) containing 1 mM DTT and 0.02 % sodium

azide. The solution was concentrated to a volume of 15 ml by ultrafiltration. Aliquots (1 ml/tube) were stored at -80 °C.

2.3.4.1.2 3,4-Dihydroxy-2-butanone 4-phosphate synthase of *Escherichia coli*

Frozen cell mass (20 g) was resuspended in 50 ml of buffer A (50 mM Tris-HCl pH 7, 300 mM NaCl, 20 mM imidazole and 0.02 % sodium azide). Lysozyme (5 mg), DNase I (5 mg), and phenylmethanesulfonyl fluoride (0.5 mM) were added. The mixture was incubated at room temperature for 30 min with stirring and then passed through a French Press. Cell debris was removed by centrifugation (15000 rpm, 60 min, 4 °C) and the supernatant was placed on the top of a Ni⁺-column (2 × 15 cm) that had been equilibrated with buffer A. The flow rate was 2 ml/min. The column was washed with 5 column volumes of buffer A and was then developed with 300 ml of buffer A with a linear gradient of imidazole (20 mM – 1 M). Fractions were analyzed by SDS-PAGE and selected fractions were combined and dialyzed against 50 mM Tris-HCl (pH 7) containing 1 mM DTT and 0.02 % sodium azide. The solution was concentrated to a volume of 15 ml by ultrafiltration. Aliquots (1 ml/tube) were stored at -80 °C.

2.3.4.1.3 Lumazine synthase of *Bacillus subtilis*

Frozen cell mass (20 g) was resuspended in 50 ml of buffer B (50 mM Tris-HCl pH 7, 1 mM DTT, 0.02 % sodium azide). Lysozyme (5 mg), DNase I (5 mg), and phenylmethanesulfonyl fluoride (0.5 ml) were added. The mixture was incubated at room temperature for 30 min with stirring and then passed through a French Press. Cell debris was removed by centrifugation (15000 rpm, 60 min, 4 °C) and the supernatant was placed on the top of a Q-Sepharose column (2 × 20 cm) that had been equilibrated with buffer B. The flow rate was 2 ml/min. The column was washed with 5 column volumes of buffer B and was then developed with 300 ml of buffer B with a linear gradient of potassium chloride (0 – 1 M). Fractions were analyzed by SDS-PAGE and by enzyme assay, and selected fractions were combined and dialyzed against buffer B. The protein was applied to a prepacked HiLoad 26/10 Q-Sepharose column that had been equilibrated with buffer B. The column was washed with 3 column volumes of buffer B and was then developed with 500 ml of buffer B with a linear gradient of potassium chloride (0 – 1 M). Fractions were analyzed by SDS-PAGE and by enzyme assay, and selected fractions were combined and dialyzed against 50 mM Tris-HCl (pH 7) containing 1 mM DTT and 0.02 % sodium azide. The solution was concentrated to a volume of 15 ml by ultrafiltration. Aliquots (1 ml/tube) were stored at -80 °C.

2.3.4.1.4 Riboflavin synthase of *Escherichia coli*

Frozen cell mass (20 g) was resuspended in 50 ml of buffer C (50 mM sodium phosphate, pH 7, containing 300 mM sodium chloride, 10 mM imidazole and 0.02 % sodium azide). Lysozyme (5 mg), DNase I (5 mg), and phenylmethanesulfonyl fluoride (0.5 mM) were added. The mixture was incubated at room temperature for 30 min with stirring and was then passed through a French Press. Cell debris was removed by centrifugation (15000 rpm, 60 min, 4 °C) and the supernatant was placed on the top of a Ni⁺-column (2 × 15 cm) that had been equilibrated with buffer C. The flow rate was 2 ml/min. The column was washed with 5 column volumes of buffer A and was then developed with 300 ml of buffer C with a linear gradient of imidazole (20 – 500 mM). After analysis by SDS-PAGE, fractions were combined and concentrated to a volume of 15 ml by ultrafiltration. Aliquots (1 ml/tube) were stored at -80 °C.

2.3.4.1.5 Flavokinase of *Schizosaccharomyces pombe*

Frozen cell mass (20 g) was suspended in 50 ml of buffer B (50 mM Tris-HCl pH 7, 1 mM DTT, 0.02 % sodium azide). Lysozyme (5 mg), DNase I (5 mg) and phenylmethanesulfonyl fluoride (0.5 mM) were added. The mixture was incubated at room temperature for 30 min with stirring and was then passed through a French Press. Cell debris was removed by centrifugation (15000 rpm, 60 min, 4 °C) and the supernatant was placed on the top of a Q-Sepharose column (2 × 20 cm) that had been equilibrated with buffer B. The flow rate was 2 ml/min. The column was washed with 5 column volumes of buffer B and was then developed with 300 ml of buffer B with a linear gradient of potassium chloride (0 – 1 M). Fractions were analyzed by SDS-PAGE and by enzyme assay, and selected fractions were combined and dialyzed against buffer B. The protein was applied on a prepacked HiLoad 26/10 Q-Sepharose column that had been equilibrated with buffer B. The column was washed with 3 column volumes of buffer B and was then developed with 500 ml of buffer B with a linear gradient of potassium chloride (0 – 1 M). Fractions were analyzed by SDS-PAGE and by enzyme assay, and selected fractions were combined and dialyzed against 50 mM Tris-HCl (pH 7) containing 1 mM DTT and 0.02 % sodium azide. The solution was concentrated to a volume of 15 ml by ultrafiltration. Aliquots (1 ml/tube) were stored at -80 °C.

2.3.4.2 Bifunctional flavokinase/FAD synthetase of *Enterococcus faecalis*

Frozen cell mass (20 g) was suspended in 50 ml of buffer A (50 mM Tris-HCl pH 7, 300 mM NaCl, 20 mM imidazole, 0.02 % sodium azide). Lysozyme (5 mg), DNase I (5 mg) and phenylmethanesulfonyl fluoride (0.5 mM) were added. The mixture was incubated at room temperature for 30 min with stirring and was then passed through a French Press. Cell debris was removed by centrifugation (15000 rpm, 60 min, 4 °C) and the supernatant was placed on the top of a

Ni⁺-column (2 × 15 cm) that had been equilibrated with buffer A. The flow rate was 2 ml/min. The column was washed with 5 column volumes of buffer A and was then developed with 300 ml of buffer A with a linear gradient of imidazole (20 mM – 1 M). Fractions were analyzed by SDS-PAGE and selected fractions were combined and dialyzed against 50 mM Tris-HCl (pH 7) containing 1 mM DTT and 0.02 % sodium azide. The protein was concentrated to a volume of 15 ml by ultrafiltration. Aliquots (1 ml/tube) were stored at -80 °C.

2.3.4.3 N-terminal domain of riboflavin synthase of *Escherichia coli*

Frozen cell mass (10 g) was suspended in 50 ml of buffer C (50 mM sodium phosphate, pH 7, containing 300 mM sodium chloride, 10 mM imidazole and 0.02 % sodium azide). Lysozyme (5 mg), DNase I (5 mg) and phenylmethanesulfonyl fluoride (0.5 mM) were added. The mixture was incubated at room temperature for 30 min with stirring and was then passed through a French Press. Cell debris was removed by centrifugation and the supernatant was placed on the top of a Ni⁺-column (2 × 15 cm) that had been equilibrated with buffer C. The flow rate was 2 ml/min. The column was washed with 5 column volumes of buffer C and was then developed with 200 ml of buffer C with a linear gradient of imidazole (10 - 500 mM). After analysis by SDS-PAGE, fractions were combined and dialyzed against buffer C, and then stored at -80 °C.

2.3.4.4 LOV2 domain of *Avena sativa* phototropin

Frozen cell mass (6 g) was suspended in 50 ml of buffer A (50 mM Tris-HCl pH 7, 300 mM NaCl, 20 mM imidazole, 0.02 % sodium azide). Lysozyme (5 mg), DNase I (5 mg) and phenylmethanesulfonyl fluoride (0.5 mM) were added. The mixture was incubated at room temperature for 30 min with stirring and was then passed through a French Press. Cell debris was removed by centrifugation and the supernatant was placed on the top of a Ni⁺-column (2 × 15 cm) that had been equilibrated with buffer A. The flow rate was 2 ml/min. The column was washed with 5 column volumes of buffer A and was then developed with 200 ml of buffer A with a linear gradient of imidazole (20 mM - 1M). After analysis by SDS-PAGE, fractions were combined and concentrated to a volume of 10 ml by ultrafiltration.

Removal of Hisactophilin domain from the LOV2 fusion protein

Purified protein (50 mg) was applied to a prepacked HiPrep 26/10 Desalting column that had been equilibrated with buffer D (50 mM Tris-HCl pH 7.5, 200 mM KCl, 2.5 mM CaCl₂). The column was developed with 100 ml of buffer D. The protein was monitored by UV spectrometry and by SDS-PAGE. Selected fractions were combined and 5 units of thrombin were added per mg of protein. The mixture was incubated overnight at room temperature with gentle shaking. The solution was applied to a Ni⁺-column (2 × 5 cm) that had been equilibrated with buffer A. The flow rate was 2 ml/min. The

column was developed with 100 ml of buffer A. The flow-through was concentrated to a volume of 5 ml by ultrafiltration, and was then applied to a prepacked HiPrep 26/10 Desalting column that had been equilibrated with buffer E (25 mM Na/K phosphate pH 7 containing 0.02 % sodium azide). The column was developed with 100 ml of buffer E. The fractions were monitored by UV photometry and by SDS-PAGE. Selected fractions were combined and concentrated to a volume of 0.7 ml by ultrafiltration, and then stored at -80 °C.

2.3.4.5 BLUF domain of AppA of *Rhodobacter sphaeroides*

Frozen cell mass (20 g) was suspended in 50 ml of buffer C (50 mM sodium phosphate, pH 7, containing 300 mM sodium chloride, 10 mM imidazole and 0.02 % sodium azide). Lysozyme (5 mg), DNase I (5 mg) and phenylmethanesulfonyl fluoride (0.5 mM) were added. The mixture was incubated at room temperature for 30 min with stirring and was then passed through a French Press. Cell debris was removed by centrifugation (15000 rpm, 60 min, 4 °C) and the supernatant was placed on the top of a Ni⁺-column (2 × 15 cm) that had been equilibrated with buffer C. The flow rate was 2 ml/min. The column was washed with 5 column volumes of buffer C and was then developed with 300 ml of buffer C with a linear gradient of imidazole (20 – 500 mM). After analysis by SDS-PAGE, fractions were combined and concentrated to a volume of 15 ml by ultrafiltration. Aliquots (1 ml/tube) were stored at -80 °C.

2.3.4.6 DNA photolyase of *Thermus thermophilus*

Frozen cell mass (30 g) was suspended in 50 ml of anaerobic buffer F (50 mM potassium phosphate, pH 8, containing 300 mM sodium chloride, 10 % glycerol and 0.02 % sodium azide). Lysozyme (5 mg), DNase I (5 mg) and phenylmethanesulfonyl fluoride (0.5 mM) were added. The mixture was incubated at room temperature for 30 min with stirring and was then passed through a French Press under argon gas. Cell debris was removed by centrifugation at 15000 rpm, 4 °C for 40 min, using stainless steel centrifuge tubes. The supernatant was transferred into a glove box containing an inert atmosphere (pO₂ < 1ppm). All subsequent purification procedures were performed inside the glove box and buffers used were prepared under anaerobic conditions. The supernatant was placed on the top of a Ni⁺-column (2 × 5 cm) that had been equilibrated with buffer F under anaerobic condition. The flow rate was 2 ml/min. The column was washed with 5 column volumes of buffer F and was then developed with 100 ml of buffer F with a linear gradient of imidazole (0 - 500 mM). After analysis by SDS-PAGE, fractions were combined and dialyzed against 50 mM potassium phosphate (pH 8) containing 1mM DTT and 0.02 % sodium azide under anaerobic conditions and were then concentrated to a volume of 0.5 ml by ultrafiltration and stored at -80 °C.

2.3.5 Enzyme-assisted synthesis of riboflavin isotopologues

2.3.5.1 Preparation of a random isotopologue mixture of 6,7-dimethyl-8-ribityllumazine by *in vivo* biotransformation

Isotopologues of 6,7-dimethyl-8-ribityllumazine and riboflavin were prepared by published procedures [53]. Recombinant *E. coli* strain M15[pREP4, pRFN4] was grown overnight at 37 °C in shaking flasks containing 100 ml of LB medium supplemented with 50 mg/L of ampicillin and 20 mg/L of kanamycin. Cells were collected by centrifugation (5000 rpm, 4 °C, 10 min) and were resuspended in 700 ml of M9 medium supplemented with 50 mg/L ampicillin, as well as ¹³C-labeled glucose (4 g/L) or ¹⁵NH₄Cl (2 g/L). The suspension was incubated at 30 °C with shaking overnight. It was then centrifuged, and the supernatant was passed through a Florisil column (2 × 10 cm) and washed with 2 column volumes of water. The column was developed with 50 % acetone. Fractions were monitored photometrically.

Earlier fractions (containing 6,7-dimethyl-8-ribityllumazine) were combined and evaporated to a small volume under reduced pressure and applied to a Dowex 50 WX 8 column (1.5 × 20 cm, H⁺ form) that had been equilibrated with water. The column was developed with water overnight and effluent fractions were monitored photometrically. Selected fractions were combined, evaporated to dryness under reduced pressure and stored at -80 °C. Alternatively, 6,7-dimethyl-8-ribityllumazine was applied to a preparative RP-18 HPLC column (25 × 300 mm) and developed with 90 mM formic acid containing 10 % methanol. Later fractions (containing riboflavin) were combined and evaporated to a small volume under reduced pressure, and stored at -80 °C.

2.3.5.2 Preparation of deuterium-labeled riboflavin by enzyme-assisted synthesis

Most of the enzymes were expressed from recombinant plasmid (Table 2.10); some of enzymes were purchased from Sigma.

5-Amino-6-ribitylamino-2,4(1*H*,3*H*)-pyrimidinedione

5-Nitro-6-ribitylamino-2,4(1*H*,3*H*)-pyrimidinedione (1.5 g) and 180 mg of palladium/charcoal (10 %) were suspended in 50 ml of D₂O in a 250 ml round-bottom flask. The mixture was hydrogenated for 48 h at room temperature and atmospheric pressure. DTT was added to a final concentration of 100 mM and aliquots (2 ml) were stored at -80 °C. All of the enzymes (Table 2.10) of this study were transferred into D₂O buffer before use.

2.3.5.2.1 [6,8 α -²H₂]riboflavin

A reaction mixture was prepared in 5 ml of H₂O containing 100 mM sodium phosphate (pH 7), 1 mM magnesium sulfate, 0.02 % sodium azide, 5 mM DTT, 3 mM [1-¹H₂]ribose, 1.5 mM 5-amino-6-ribitylamino-2,4(1*H*,3*H*)-pyrimidinedione, 6 units of ribose phosphate isomerase (Sigma), 10 mg of 3,4-dihydroxy-2-butanone 4-phosphate-synthase, 1.8 mg of lumazine synthase and 0.4 mg of riboflavin synthase. The mixture was incubated at room temperature for 48 h inert an inert atmosphere in a glove box. The progress of the reaction was monitored by thin layer chromatography (microcrystalline cellulose plates, Macherey-Nagel; eluent, 350 mM phosphate, pH 7.0). The mixture was centrifuged (4000 rpm, 20 min, 4 °C). The pellet was dried in a desiccator overnight. Solid riboflavin was checked by mass spectrometry (FAB methods), dissolved in 0.7 ml of DMSO-d₆, and analyzed by ¹H-NMR.

2.3.5.2.2 [6,7 α ,8 α ,9-²H₈]riboflavin

A reaction mixture was prepared in 5 ml of D₂O containing 100 mM sodium phosphate (pH 7), 1 mM magnesium sulfate, 0.02 % sodium azide, 5 mM DTT, 3 mM ribose-5-phosphate, 1.5 mM 5-amino-6-ribitylamino-2,4(1*H*,3*H*)-pyrimidinedione, 6 units of ribose phosphate isomerase (Sigma), 10 mg of 3,4-dihydroxy-2-butanone 4-phosphate-synthase, 1.8 mg of lumazine synthase and 0.4 mg of riboflavin synthase. All enzymes had been dialyzed against D₂O buffer. The mixture was incubated at room temperature for 48 h under inert atmosphere in a glove box. The progress of the reaction was monitored by thin layer chromatography (microcrystalline cellulose plates, Macherey-Nagel; eluent, 350 mM phosphate, pH 7.0). The mixture was centrifuged (4000 rpm, 20 min, 4 °C). The pellet was dried in a desiccator overnight. Solid riboflavin was checked by mass spectrometry (FAB methods) and dissolved in 0.7 ml of DMSO-d₆, and then analyzed by ¹H-NMR.

2.3.5.2.3 [7 α ,9-²H₄]riboflavin

A saturated solution of 6,7-dimethyl-8-ribityllumazine (25 °C) in 2 ml of D₂O was incubated overnight at room temperature. 100 mM of sodium phosphate (pH 7) containing 1 mM DTT and 0.3 mg of riboflavin synthase was added, and the mixture was incubated at room temperature for 48 h. The riboflavin synthase had been equilibrated with D₂O. The progress of the reaction was monitored by thin layer chromatography (microcrystalline cellulose plates, Macherey-Nagel; eluent, 350 mM phosphate, pH 7.0). After 48 h, the mixture was centrifuged (4000 rpm, 20 min, 4 °C). The pellet was dried in a desiccator overnight. Solid riboflavin was checked by mass spectrometry (FAB method) and dissolved in 0.7 ml of DMSO-d₆, and then analyzed by ¹H-NMR.

2.3.5.2.4 [6,8 α -²H₄]riboflavin

A reaction mixture was prepared in 50 ml of D₂O containing 100 mM sodium phosphate (pH 7) containing 1 mM magnesium sulfate, 0.02 % sodium azide, 5 mM DTT, 6 mM ribose-5-phosphate, 6 mM 5-amino-6-ribitylamino-2,4(1*H*,3*H*)-pyrimidinedione, 120 units of ribose phosphate isomerase (Sigma), 40 mg of 3,4-dihydroxy-2-butanone-4-phosphat synthase and 12 mg of lumazine synthase. The mixture was incubated at room temperature for 48 h under an inert atmosphere in a glove box. The progress of the reaction was monitored by thin layer chromatography (microcrystalline cellulose plates, Macherey-Nagel; eluent, 350 mM phosphate, pH 7.0). The reaction mixture was centrifuged (4000 rpm, 20 min, 4 °C). The supernatant was collected and filtered through a 0.2 μ m pore size syringe filter (cellulose acetate, Macherey-Nagel). The filtrated solution was concentrated to a volume of 5 ml. The concentrated sample was applied to a Dowex 50 WX8 column (1 \times 30 cm, H⁺ form) that was developed with water. The effluent was monitored photometrically and by thin layer chromatography. Fractions were combined and evaporated to a small volume under reduced pressure. The residue was dissolved in 5 ml of 100 mM sodium phosphate (pH 7) containing 1 mM DTT and 12 mg of riboflavin synthase. The mixture was incubated at room temperature for 48 h and was then centrifuged (4000 rpm, 20 min, 4 °C). The pellet was dried in a desiccator overnight. Solid riboflavin was checked by mass spectrometry (FAB method) and dissolved in 0.7 ml of DMSO-d₆, and then analyzed by ¹H-NMR.

2.3.5.3 Enzyme-assisted synthesis of FMN

A reaction mixture (total volume, 20 ml) containing 100 mM Tris-HCl, pH 8.0, 10 mM magnesium chloride, 0.02 % sodium azide, 5 mM DTT, 0.5 mM ATP, 6 mM phosphoenol pyruvate, 0.5 mM riboflavin or isotope-labeled riboflavin, 5 units of pyruvate kinase from rabbit muscle (Sigma) and 2 mg of flavokinase was incubated at 37 °C overnight. The progress of the reaction was monitored by thin layer chromatography (microcrystalline cellulose plates, Macherey-Nagel; eluent, 350 mM phosphate, pH 7.0). When the riboflavin had mostly disappeared (typically after about 12 h), the reaction mixture was evaporated to dryness under reduced pressure and stored at -80 °C.

2.3.5.4 Enzyme-assisted synthesis of FAD

A reaction mixture (total volume, 20 ml) containing 100 mM Tris-HCl, pH 8.0, 10 mM magnesium chloride, 0.02 % sodium azide, 5 mM DTT, 7 mM ATP, 20 mM phosphoenol pyruvate, 0.5 mM isotope-labeled riboflavin, 5 units of inorganic pyrophosphatase from baker's yeast (Sigma), 5 units of pyruvate kinase from rabbit muscle (Sigma) and 1 mg of recombinant flavokinase/FAD-synthetase of *Enterococcus faecium* were incubated at 37 °C overnight. The progress of the reaction was monitored by thin layer chromatography (microcrystalline cellulose plates, Macherey-Nagel;

eluent, 350 mM phosphate, pH 7.0). When riboflavin and FMN had mostly disappeared (typically after about 12 h), the reaction mixture was evaporated to dryness under reduced pressure. The remained solid was dissolved in 3 ml of water, and the solution was passed through a 0.2 μm pore size syringe filter (cellulose acetate, Macherey-Nagel). Aliquots (1 ml) of the filtrate were loaded on top of a RP18 reverse phase HPLC column (25 \times 300 mm) that was developed with a 40 % of aqueous methanol. Fractions (elution volume, 10 – 15 ml) were combined and concentrated by evaporation under reduced pressure.

2.3.6 Determination of protein and flavin cofactor concentration

The amount of protein was determined by the Coomassie Brilliant Blue Dye (Bradford) method modified by Read and Northcote [124]. 1 μl of protein sample was diluted in 49 μl of buffer, and then added to 950 μl of Bradford reagent in a 1 ml cuvette. As a reference, 50 μl of buffer without protein was mixed with 950 μl of Bradford reagent. The absorbance was measured at 595 nm after 2 minutes incubation at room temperature. The amount of protein was estimated from a standard curve using bovine serum albumin as standard protein. The concentration of the free substrates and reconstituted protein in this study was determined photometrically using the extinction coefficient value of each respective ligand. The extinction coefficient values are shown in the Table 2.13.

Table 2.13 Spectroscopic properties of enzymes.

Name	λ [nm]	ϵ [$\text{M}^{-1}\text{cm}^{-1}$]	Reference
5-amino-6-ribitylamino-2,4(1 <i>H</i> ,3 <i>H</i>)-pyrimidindion	268	24500	Plaut et al.,1971 [125]
6,7-demityl-8-ribityllumazine	410	10300	Plaut et al.,1971 [125]
Riboflavin	470	9600	Plaut et al.,1971 [125]
FMN	446	12200	Koziol 1971 [126]
FAD	450	11300	Hinkson 1968 [127]
FMN with LOV2 of <i>A. sativa</i>	447	13800	Salomon et al., 2000 [77]
Neutral radical form of FADH [•] with DNA photolyase	580	4800	Jorns et al., 1990 [128]

2.3.7 Reconstitution of proteins with cofactors

2.3.7.1 N-terminal domain of riboflavin synthase of *Escherichia coli*

A solution of purified N-terminal domain of riboflavin synthase (30 mg) in 50 ml of buffer A was placed on the top of a Ni⁺-column (2 × 5 cm) that was then washed with 10 column volumes of buffer A (mutant protein with replacement of C47 and C48 required washing the column with 5 column volumes of 8 M urea followed by 10 column volumes of buffer A). Buffer A (20 ml) containing 1.5 - 2 mg of isotopically labeled 6,7-dimethyl-8-ribityl-lumazine or riboflavin was circulated through the column overnight. The column was then washed with 200 ml of buffer A and developed with 100 ml of buffer A with a linear gradient of imidazole (10 - 500 mM). Fractions were analyzed by SDS-PAGE and UV spectrometry. Selected fractions were combined and dialyzed against 50 mM sodium phosphate (pH 6.9, 8.5, 9.2 or 11.0) containing 1 mM DTT and 0.02 % sodium azide, and then concentrated to a column of 0.5 ml by ultrafiltration.

2.3.7.2 LOV2 domain of *Avena sativa* phototropin

Frozen cell mass (6 g) was suspended in 50 ml of buffer D (50 mM Tris-HCl pH 7, 300 mM NaCl, 20 mM imidazole, 0.02 % sodium azide). Lysozyme (5 mg), DNase I (5 mg) and phenylmethanesulfonyl fluoride (0.5 mM) were added. The mixture was incubated at room temperature for 30 min with stirring and then passed through a French Press. Cell debris was removed by centrifugation and the supernatant was placed on the top of a Ni⁺-column (2 × 5 cm) that had been equilibrated with buffer D. The column was washed with 5 column volumes of buffer D containing 6 M guanidine-HCl until the effluent had become colorless, and then buffer D containing 4 mg of FMN or isotopically labeled FMN was circulated through the column overnight under protection from light. The column was washed with buffer D and was then developed with 100 ml of buffer D with a linear gradient of imidazole (20 mM - 1 M). After analysis by SDS-PAGE, fractions were combined and concentrated to a volume of 5 ml by ultrafiltration. The hisactophilin domain was removed by thrombin cleavage and LOV2 domain was equilibrated with buffer F (chapter 2.3.4.3). The protein was concentrated to a volume of 0.7 ml by ultrafiltration, and then stored at -80 °C.

2.3.7.3 DNA photolyase of *Thermus thermophilus*

A solution of purified DNA photolyase (20 mg) in 50 ml of buffer C (50 mM potassium phosphate, pH 8, 300 mM sodium chloride and 0.02 % sodium azide) was placed on the top of a Ni⁺-column (2 × 5 cm), which had been equilibrated with buffer C. The column was washed with buffer C containing 6 M guanidine-HCl until the effluent had become colorless. Buffer C containing 4 mg of FMN or isotopically labeled FMN was circulated through the column overnight. The column was then washed

with 200 ml of buffer C and developed with 100 ml of buffer C with a linear gradient of imidazole (0 – 1 M). Effluent was monitored photometrically and SDS-PAGE. Selected fractions were combined and dialyzed against 50 mM potassium phosphate (pH 8) containing 1 mM DTT and 0.02 % sodium azide. The solution was concentrated by ultrafiltration and stored at -80 °C.

2.3.8 Spectroscopic methods

2.3.8.1 Optical spectroscopy

Optical spectra were recorded using an Ultraspec 4300 pro UV/Visible Spectrophotometer (Amersham Bioscience, Cambridge, UK) using the software program SWIFT II. Spectra were taken in quartz cuvettes with a path length of 10 mm from 250 nm to 550 nm, with a scanning speed of 4626 nm/min and a band width of 0.1 nm. Enzyme assays were monitored by a Microplate Reader Spectra Max M2 (Molecular Devices, California, USA) or Multiscan Spectrum Microplate Spectrophotometer (Thermo Scientific, Langenselbold).

2.3.8.2 CD spectroscopy

Circular dichroism (CD) spectra were recorded using a Jasco J-715 spectropolarimeter with temperature controller PFD-350S using the software program J-700 for Windows. The spectra were taken at 20 °C in quartz cuvettes with a path length of 0.1 cm. The spectra were collected between 185 and 250 nm, with 50 nm/min scanning speed, a response time setting of 1 sec, a band width of 1.0 nm. The average of 10 scans was recorded.

2.3.8.3 NMR spectrometry

Samples contained 50 mM sodium phosphate (pH 6.9, 8.5, 9.2, or 11.0), 10 % D₂O, 20 μM [1-¹³C₁]glucose (as internal standard) and 1.5 to 2 mM protein loaded with isotopically labeled 6,7-dimethyl-8-ribityllumazine as indicated. NMR spectra were recorded at 290 K using a DRX 500 spectrometer (Bruker Instruments, Karlsruhe, Germany). Composite pulse decoupling was used for ¹³C, ¹⁵N-NMR measurements.

2.3.8.4 Mass spectrometry

FAB (Fast atom bombardment) mass spectra were recorded on a VG70-250F Magnetic Sector Mass Spectrometer (VG Analytical, UK). It was equipped with Xenon-FAB ionization. FAB ionization requires that the sample is mixed with a suitable matrix of m-NBA (3-nitrobenzyl alcohol) and introduced into the ion source on a target probe.

3 Results and Discussion

Studies on the reaction mechanism of riboflavin synthase

3.1 Preparation and reconstitution of N-terminal riboflavin synthase domain

The *ribC* gene of *E. coli* (X69109) codes for a riboflavin synthase of 213 amino acid residues. A striking feature of the amino acid sequence is the similarity between the N-terminal (sequence residues 1 – 97 amino acid) and the C-terminal (98 – 213 amino acid) part. X-Ray crystallography has confirmed that the two homologous segments fold into two similar domains. The N-terminal domain can be expressed as an artificial, homodimeric protein [46]. The artificial homodimer has been shown earlier to bind one riboflavin molecule per subunit. Whereas the artificial protein is devoid of enzyme activity, it is well suited for NMR experiments since it has a relatively low molecular weight of 12 kDa. Moreover, the NMR signals of the two subunits are degenerate as a consequence of the strict c_2 symmetry of the homodimer; this is conducive to a favorable reduction of signal complexity.

Table 3.1 Plasmids used for optimized gene expression.

Plasmid	Relevant characteristics	Source
p4 ₁	pBluescriptIISK containing the 6 kb of fragment from the digested cDNA of <i>E. coli</i> RR28 with <i>Sau3AI</i> restriction enzyme	Eberhardt et al.,1996 [129]
pERS	pNCO113 containing the <i>ribC</i> gene	Eberhardt et al.,1996 [129]
pERN	pNCO113 containing the gene for the wild type of the N-terminal riboflavin synthase domain	Eberhardt et al.,2001 [46]

The plasmid pERN was obtained from Dr. Sabine Eberhardt (Table 3.1) and amplified by PCR using the oligonucleotide of NRS-F and NRS-R as primers (see Methods 2.3.1.8). The PCR product was digested with *BamHI* and *PstI*, and the resulting fragment was cloned into the vector pQE30 where the open reading frame is preceded by a poly-histidine-tag sequence. The recombinant N-terminal riboflavin synthase domain is expressed efficiently in a recombinant *E. coli* strain and can be easily purified by Ni⁺-column chromatography due to the 6-histidine tag present at the N-terminus (see Methods 2.3.4.3). The resulting protein appeared approximately 90% pure as judged by SDS-PAGE (Figure 3.1). The molecular weight of N-terminal riboflavin synthase domain (black box in Figure 3.1) is around 12 kDa as estimated by SDS-PAGE.

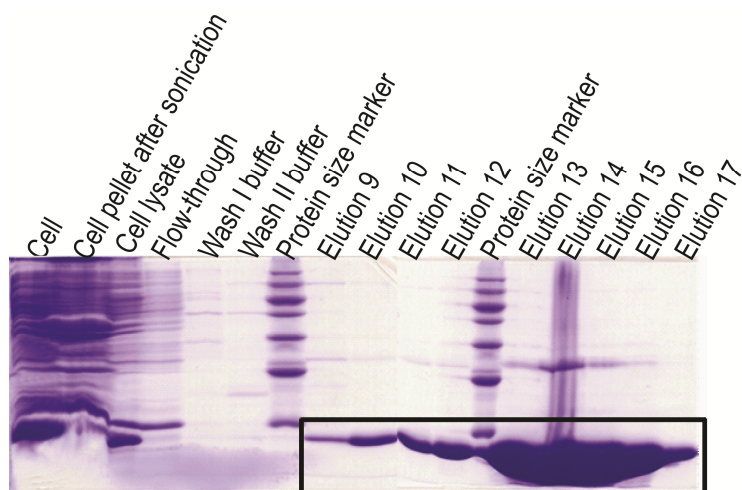


Figure 3.1 SDS-PAGE of riboflavin synthase domain. Black box indicates N-terminal riboflavin synthase domain. Protein size markers; 66 kDa, 45 kDa, 36 kDa, 30 kDa, 20 kDa, 13 kDa.

As shown by crystallographic analysis (Figure 3.2), riboflavin is surrounded with helix α_2 , strands β_4 and β_5 of one of subunits and the short loop from the N-terminus of the other subunit. Residues of this first shell are very close to the bound riboflavin, and several of those form hydrogen bonds with riboflavin, most notably Thr50, Asp62, Met64 and Thr67. Ser41 is not directly hydrogen-bonded to riboflavin. Nevertheless, when the residue is mutated to Ala, the enzyme had strikingly low rates as compared to wild type enzyme [130]. In addition, Cys47 and 48 were highly conserved in the riboflavin synthases from different microorganisms.

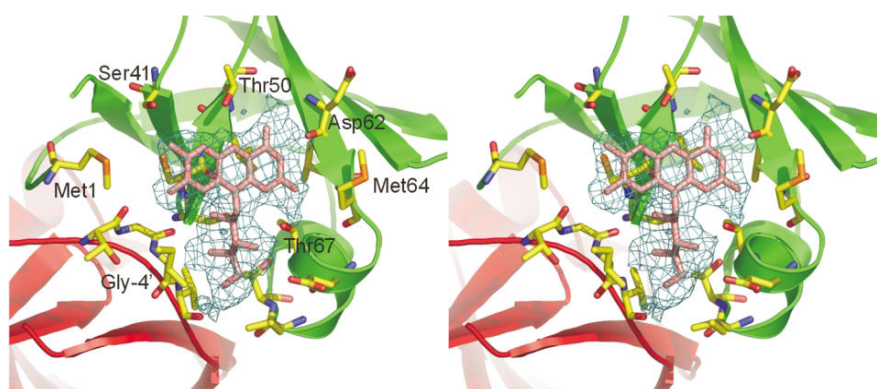


Figure 3.2 Riboflavin binding site of the N-terminal domain of riboflavin synthase (stereo pair), Subunits A and B of the homodimer are shown in green and red, respectively from Meining, 2003 [48].

In this study, we exchanged the following amino acids in the N-terminal domain of riboflavin synthase: Ser41, Ala43, Cys47, Cys48, Thr50, Glu66, Thr67 (Table 2.7). The mutagenic PCR involved two rounds of amplification cycles using one mismatch and two flanking primers (NRS-F and

NRS-R) (see Methods **2.3.1.8**). The pQE30-NRS-WT was used as a template plasmid. After two rounds of PCR, the product fragments were isolated, digested with *Bam*HI and *Pst*I, and the resulting fragments were cloned into the Vector pQE30, which had been treated with the same restriction enzymes. The recombinant plasmids (pQE30-NRS-mutants) are expressed efficiently in a recombinant *E. coli* strain and the recombinant proteins can be easily purified by Ni⁺-column chromatography due to the 6-histidine tag present at the N-terminus (see Methods **2.3.4.3**). The purity of isolated proteins was estimated to be higher 90 % (Figure 3.3).

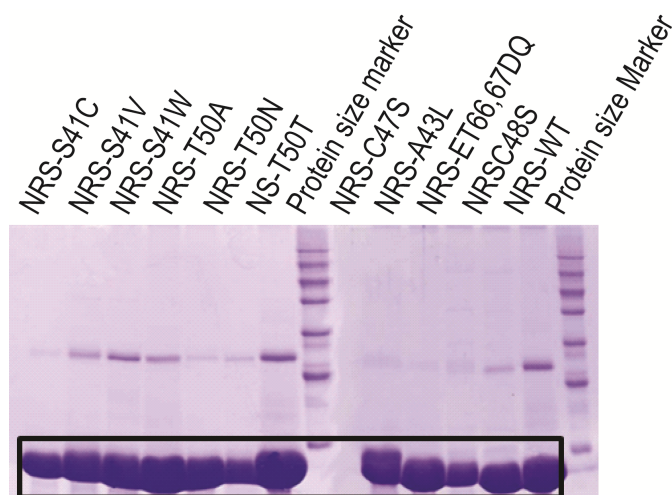


Figure 3.3 SDS-PAGE of isolated of N-terminal riboflavin synthase domain (wild type and mutant proteins, black box). NRS is N-terminal riboflavin synthase domain. Protein size markers; 66 kDa, 45 kDa, 36 kDa, 30 kDa, 20 kDa, 13 kDa.

3.1.1 Optical spectroscopy of the N-terminal riboflavin synthase domain

3.1.1.1 Characterization of the recombinant N-terminal riboflavin synthase domain by UV-VIS spectroscopy

The supernatants obtained after heat treatment of crude extracts containing the recombinant N-terminal riboflavin synthase domain had been shown earlier to contain riboflavin and 6,7-dimethyl-8-ribityllumazine at molar ratios varying from 0.9 to 3.3 [46]. In line with that, optical spectra of freshly prepared N-terminal riboflavin synthase domain indicated that the isolated protein contained a mixture of 6,7-dimethyl-8-ribityllumazine and riboflavin, but the proteins did not appear to be saturated with these ligands. The proteins, as isolated, were therefore reconstituted after removal of the bound ligands. Specifically, bound ligands were removed by treatment with urea, and the resulting apoprotein were reconstituted with 6,7-dimethyl-8-ribityllumazine (see Methods **2.3.7.1**). The reconstituted proteins showed a protein-ligand ratio of 1:1. The concentration of reconstituted protein samples can therefore be estimated via the absorption of the 6,7-dimethyl-8-ribityllumazine chromophore (Figure 3.4, A). Wild type N-terminal riboflavin synthase domain reconstituted with 6,7-dimethyl-8-ribityllumazine

has an absorbance maximum at 413 nm, slightly red-shifted as compared to free 6,7-dimethyl-8-ribityllumazine (407 nm). Notably, the absorbance maximum of the bound ligand can be shifted by several nm by certain mutations of riboflavin synthase N-terminal domain (Figure 3.4, **B**).

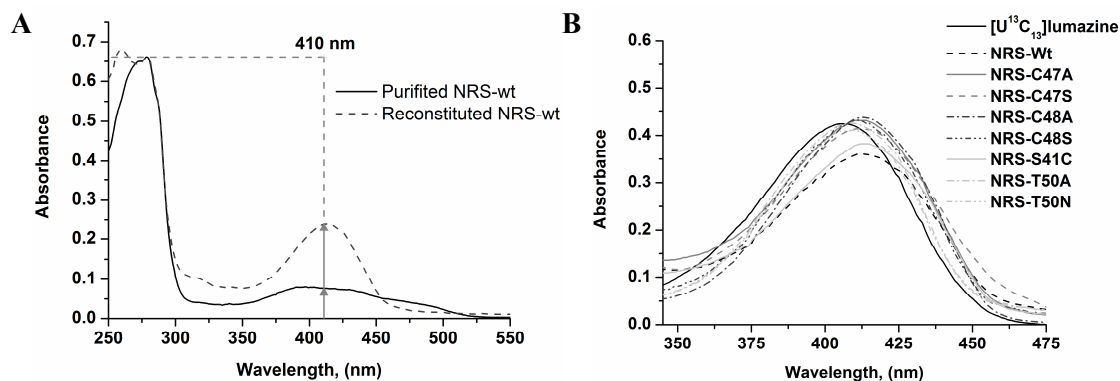


Figure 3.4 Absorption spectra of N-terminal riboflavin synthase domain. N-terminal riboflavin synthase domain before and after reconstitution with 6,7-dimethyl-8-ribityllumazine (**A**) and 6,7-dimethyl-8-ribityllumazine in complex with N-terminal riboflavin synthase domains; the free ligand is also shown for comparison. The concentration of protein bound ligand varied from 36 μM to 42 μM (**B**).

3.1.1.2 Photometric titration of recombinant N-terminal riboflavin synthase domain

Spectrophotometric titrations were conducted by monitoring the absorption change at 407 nm (neutral 6,7-dimethyl-8-ribityllumazine) and at 312 nm (anionic 6,7-dimethyl-8-ribityllumazine) (Figure 3.5). The pK_a values for 6,7-dimethyl-8-ribityllumazine and 6,7,8-trimethylumazine measurements in aqueous solution and of 6,7-dimethyl-8-ribityllumazine in complex with the N-terminal riboflavin synthase domain are listed in the Table 3.2. The spectra at pH 6.9 are all similar. However, when the pH is changed to alkaline, substantial differences become apparent.

The difference in the absorption spectra of 6,7-dimethyl-8-ribityllumazine and 6,7,8-trimethylumazine in alkaline aqueous solution is well understood. Whereas deprotonation of 6,7,8-trimethylumazine affords the exo-methylene anion, the deprotonation of 6,7-dimethyl-8-ribityllumazine affords a complex mixture of anions that is dominated by several tricyclic anion species and where the exo-methylene anion is only present in small amounts. Under mildly alkaline conditions the 6,7-dimethyl-8-ribityllumazine in complex with the protein has absorbance maxima at 311 nm and 370 nm, similar to 6,7,8-trimethylumazine. It is suggested that the N-terminal riboflavin synthase domain can bind only the exo-methylene anion, but none of the tricyclic anions.

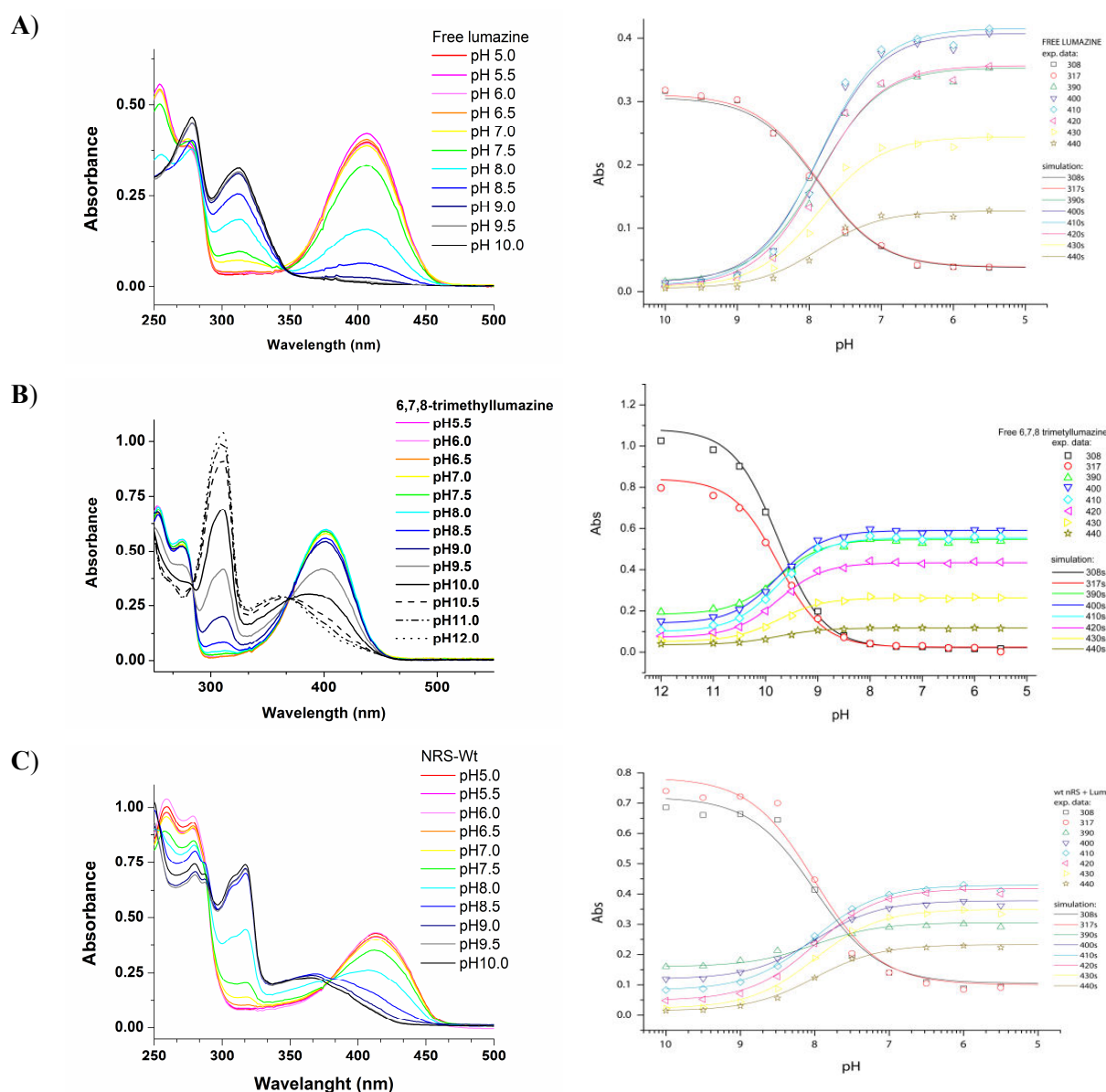


Figure 3.5 Photometric titration of 6,7-dimethyl-8-ribityllumazine derivatives. **A)** Free 6,7-dimethyl-8-ribityllumazine; **B)** Free 6,7,8-trimethylllumazine; **C)** 6,7-dimethyl-8-ribityllumazine in complex with wild type N-terminal riboflavin synthase domain.

Table 3.2 Optical properties of 6,7-dimethylllumazine derivatives.

Sample	pK _a	Absorbance maxima (nm)		Isosbestic points (nm)
		pH 6.9	pH 11	
A. Free 6,7-dimethyl-8-ribityllumazine	7.85	407	312	284, 346
B. 6,7,8-trimethylllumazine	9.76	401	311, 360	284, 369
C. 6,7-dimethyl-8-ribityllumazine in complex with wild type N-terminal riboflavin synthase domain	8.00	413	318, 370	289, 378

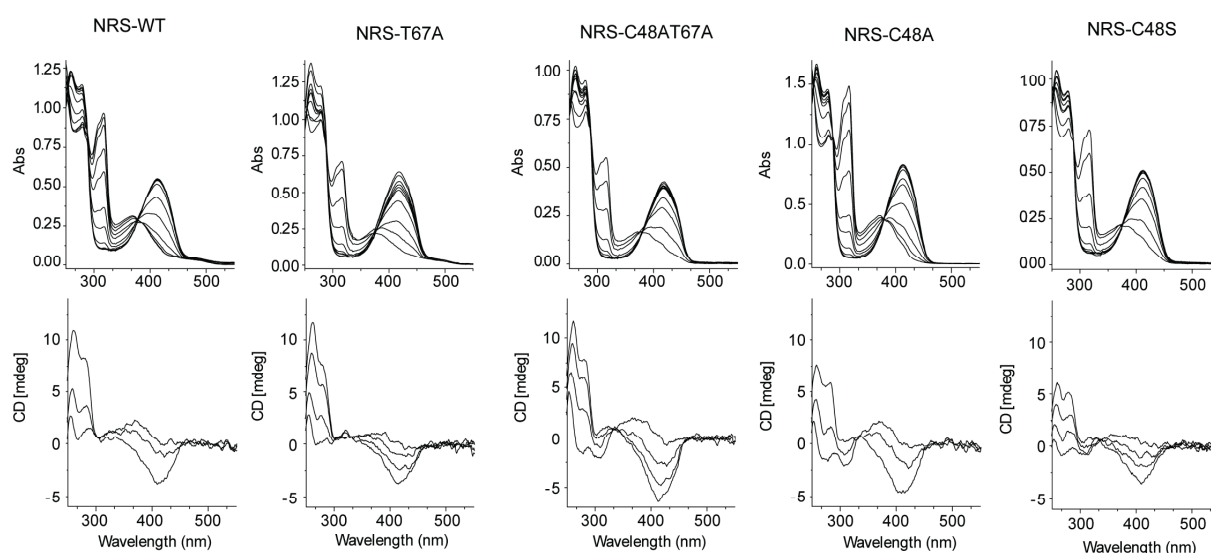


Figure 3.6 pH titration of 6,7-dimethyl-8-ribityllumazine in complex with wild type or mutant variants of N-terminal riboflavin synthase domain. Titrations were monitored photometrically (top) and circular dichroism (CD) (bottom) (50 mM of sodium phosphate buffer at pH 6.9, 8.5, 9.2 and 10.5).

Figure 3.6 shows the photometric titration spectra and CD spectra of 6,7-dimethyl-8-ribityllumazine in complex with wild type or mutant N-terminal riboflavin synthase domain. Spectrophotometric titrations were conducted by monitoring the absorption change at 407 nm (neutral 6,7-dimethyl-8-ribityllumazine) and at 312 nm (anionic 6,7-dimethyl-8-ribityllumazine). Qualitatively, the spectra appear similar. Well-defined isosbestic points around 378 nm are observed throughout (Figure 3.6).

Table 3.3 Optical properties of 6,7-dimethyl-8-ribityllumazine in complex with mutant variants of the N-terminal riboflavin synthase domain.

	pK _a	Absorbance maxima (nm)		Isosbestic points (nm)
		pH 6.9	pH 10	
Complex with NRS-wild type	8.00	413	318, 370	289, 378
Complex with NRS-C47A	8.23	413	317, 371	377
Complex with NRS-C48A	8.49	413	317, 371	379
Complex with NRS-C48AT67A	9.12	420	315, 372	380
Complex with NRS-C48S	9.15	413	316, 371	375
Complex with NRS-C48ST67A	9.18	418	315, 389	375
Complex with NRS-C48T	8.66	414	315, 371	377
Complex with NRS-T50A	10.10	409	317, 376	369
Complex with NRS-T50N	> 9.0	408	315, 394	363
Complex with NRS-T67A	8.91	418	315, 375	375

The pK_a values are shown in Table 3.3. Generally, higher values were observed in the experiments with mutant proteins as compared to wild type protein. Specifically, the T50A mutant has the highest pK_a (10.1). The pK_a of T50N could not be measured under these experimental conditions. T50N mutant has an isosbestic point at 363 nm, the shortest wavelength as compared with the other mutants. X-ray crystallography has suggested earlier that Thr50 forms a hydrogen bond with N-5 of the bound ligand. This hydrogen bond is abolished by replacement of Thr50. The data suggest that the hydrogen bond present in the wild type contributes to the stabilization of the exomethylene anionic species.

3.1.2 NMR spectroscopy of recombinant N-terminal riboflavin synthase domain

3.1.2.1 Preparation of isotopologue libraries by biotransformation of ^{13}C -Glucose

Isotopologues of 6,7-dimethyl-8-ribityllumazine and riboflavin, respectively, were prepared by fermentation of a recombinant *E. coli* strain with [$\text{U-}^{13}\text{C}_6$]glucose, [$1\text{-}^{13}\text{C}_1$]glucose or [$2\text{-}^{13}\text{C}_1$]glucose as the carbon source (see Method 2.3.5.1). To produce isotopologues of 6,7-dimethyl-8-ribityllumazine, the recombinant strain was grown in minimal medium (1 L) supplied with 4 g of ^{13}C -labeled glucose. Fermentation products were harvested using a Florisil column and were purified by ion exchange chromatography. Typical yields were in the range of 100 mg labelled of 6,7-dimethyl-8-ribityllumazine per 1 L of medium. The resulting samples have been reported earlier to represent mixture of various isotopologues present at different abundance (Figure 3.7; C, D and E) [53]. [$7\alpha\text{-}^{13}\text{C}_1$]- and [$6,6\alpha,7,7\alpha\text{-}^{13}\text{C}_4$]-6,7-Dimethyl-8-ribityllumazines (Figure 3.7; A and B) were produced by one-pot enzyme-assisted synthesis [54]. The reaction mixture contained [$\text{U-}^{13}\text{C}_6$]glucose or [$6\text{-}^{13}\text{C}_1$]glucose. The overall yields of 6,7-dimethyl-8-ribityllumazine based on isotope-labeled glucose were about 90 %.

3.1.2.2 ^{13}C -NMR spectroscopy of isotopologues of 6,7-dimethyl-8-ribityllumazine and riboflavin in complex with recombinant N-terminal riboflavin synthase domain

The purified protein was reconstituted with selectively isotope-labeled 6,7-dimethyl-8-ribityllumazine, which had been prepared according to 3.2.3.1 (see also Methods 2.3.7.1). Ligands were added to apoprotein. The mixtures were dialyzed against 50 mM sodium phosphate (pH 6.9) containing 1 mM DTT and 0.02 % sodium azide, and were then concentrated by ultrafiltration. NMR samples contained 1.5 to 2 mM protein loaded with isotopically labeled 6,7-dimethyl-8-ribityllumazine as indicated, 10 % of D_2O and 20 μM of [$1\text{-}^{13}\text{C}_1$]glucose (as internal standard) (see Methods 2.3.8.3. NMR spectra were accumulated for about 14 h at 290 K.

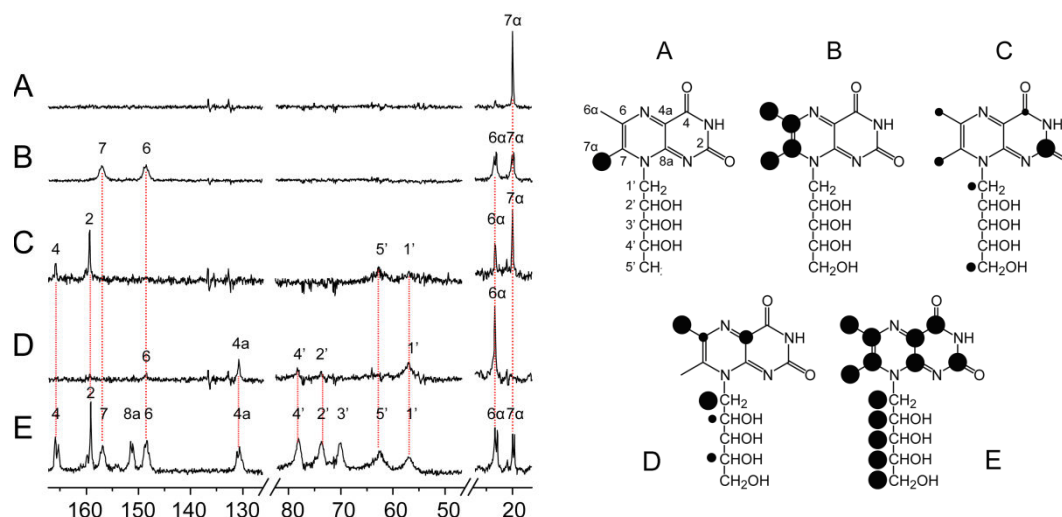


Figure 3.7 Left, ^{13}C -NMR spectra of isotopologues of 6,7-dimethyl-8-ribityllumazine in complex with the N-terminal domain of riboflavin synthase (wild type) at pH 6.9. Right, labeling patterns of 6,7-dimethyl-8-ribityllumazine isotopologues. A; $[7\alpha\text{-}^{13}\text{C}_1]$ 6,7-dimethyl-8-ribityllumazine, B; $[6\alpha,6,7,7\alpha\text{-}^{13}\text{C}_4]$ 6,7-dimethyl-8-ribityllumazine, C; 6,7-dimethyl-8-ribityllumazine biosynthesized from $[1\text{-}^{13}\text{C}_1]$ glucose, D; 6,7-dimethyl-8-ribityllumazine biosynthesized from $[2\text{-}^{13}\text{C}_1]$ glucose, E; $[U\text{-}^{13}\text{C}_{13}]$ 6,7-dimethyl-8-ribityllumazine, the size of the dots indicates ^{13}C enrichment.

The ^{13}C -NMR spectrum of $[U\text{-}^{13}\text{C}_{13}]$ 6,7-dimethyl-8-ribityllumazine (Figure 3.7, E) in complex with N-terminal riboflavin synthase domain are shown in Figure 3.7. It shows that the carbon signals of bound $[U\text{-}^{13}\text{C}_{13}]$ 6,7-dimethyl-8-ribityllumazine do not overlap; the number of signals is the same as in the spectrum of the free $[U\text{-}^{13}\text{C}_{13}]$ 6,7-dimethyl-8-ribityllumazine. Thus, each signal in the spectra of the protein-ligand complexes reflects a single carbon of the bound ligand. Specifically, the two doublet signals at 23.3 and 19.9 ppm reflect the methyl carbons 6α and 7α , the signals between 50 and 80 ppm are due to the ribityl carbons, the downfield-shifted signals between 130 and 170 ppm are due to carbons of the xylene ring. The signal at 159.4 ppm can be assigned unequivocally to C-2 due to its singlet signature.

On the basis of the known isotopologue composition of 6,7-dimethyl-8-ribityllumazine labeled at the four different carbon atoms, all signals can be assigned unequivocally. For example, the ^{13}C -NMR spectrum of $[7\alpha\text{-}^{13}\text{C}_1]$ 6,7-dimethyl-8-ribityllumazine in complex with N-terminal riboflavin synthase domain (Figure 3.7, A) shows a singlet at 19.9 ppm which can be assigned to C- 7α . On the other hand, the protein reconstituted with $[U\text{-}^{13}\text{C}_{13}]$ 6,7-dimethyl-8-ribityllumazine shows two doublet signals for C- 6α and C- 7α . Therefore, the signal (23.3 ppm) can be assigned as C- 6α . The spectrum of $[6\alpha,6,7,7\alpha\text{-}^{13}\text{C}_4]$ 6,7-dimethyl-8-ribityllumazine in complex with protein (Figure 3.7, B) shows doublet signals for C- 6α and C- 7α , and two signals at 148.6 and 157.1 ppm. Only the C-6 atom of lumazine acquires ^{13}C -labeling from $[2\text{-}^{13}\text{C}_1]$ glucose, and therefore, the signal detected at 148.6 ppm in the

spectrum can be clearly assigned to C-6. Therefore the signal at 157.1 ppm can be assigned to C-7. For the xylene ring, C-4 is observed when $[1-^{13}\text{C}_1]$ glucose was used as carbon source and C-4a is observed when $[2-^{13}\text{C}_1]$ glucose was used as carbon source. Furthermore Figure 3.7. **C** and **D** show that the signal at 165.9 ppm can be assigned to C-4 and the signal at 130.8 ppm can be assigned to C-4a. For carbon atoms of the ribityl side chain the signals of C-1' and C-5' are detected in the isotopologue mixture obtained from $[1-^{13}\text{C}_1]$ glucose and signal of C-1', C-2', C-4' are detected in the isotopologue mixture obtained from $[2-^{13}\text{C}_1]$ glucose. On this basis, the signal at 57.1 ppm is present both in the spectra **C** and **D** and can be assigned to C-1'. Moreover, the signal at 62.6 ppm in the spectrum **C** can be assigned to C-5', and the signals at 78.2 and 73.9 ppm in the spectrum **D** can be assigned to C-4' and C-2', respectively. Except of the signals for C-8a and C-3', all other signals can be detected by the use of random isotopologue libraries from $[1-^{13}\text{C}_1]$ glucose and $[2-^{13}\text{C}_1]$ glucose or selectively labeled $[7\alpha-^{13}\text{C}_1]$ 6,7-dimethyl-8-ribityllumazine and $[6\alpha,6,7,7\alpha-^{13}\text{C}_4]$ 6,7-dimethyl-8-ribityllumazine. The signal at 151.5 ppm can be assigned to C-8a. The signal at 70.2 ppm which is located in the ribityl region can be assigned to C-3'. The assignments in the present experiment agree with the assignments reported earlier [53].

The mutants of the N-terminal riboflavin synthase domain were reconstituted with $[\text{U}-^{13}\text{C}_{13}]$ 6,7-dimethyl-8-ribityllumazine using the same procedure as for the wild type protein (Figure 3.7. **E**) (see Methods **2.3.7.1**). ^{13}C -NMR spectra of the mutant variants of N-terminal riboflavin synthase domain in complex with $[\text{U}-^{13}\text{C}_{13}]$ 6,7-dimethyl-8-ribityllumazine at pH 6.9 are shown in Figure 3.8. The assignment for all carbon atoms signals of the bound ligand was based on the previously made assignment for the ligand in complex with the wild type protein. Chemical shift values are summarized in Table 3.4.

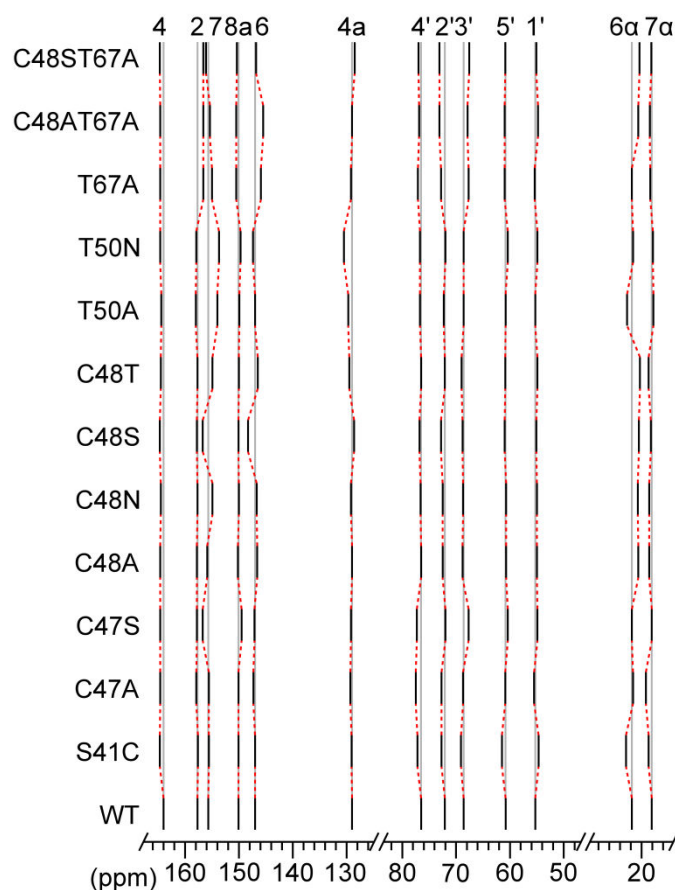


Figure 3.8 Correlation of ^{13}C -NMR chemical shifts of $[\text{U-}^{13}\text{C}_{13}]6,7\text{-dimethyl-8-ribityllumazine}$ in complex with wild type of the N-terminal riboflavin synthase domain or mutant variants.

C-4 chemical shifts of all mutants were about 0.6 ppm downfield from the wild type. The T67 mutants show a 1.1 ppm upfield shift at the C-2 position. The C-7 signal is shifted upfield more than 2 ppm in the T50N and T50A mutants. On the other hand, the C47S, C48S mutants afforded a 1 ppm downfield shift of that carbon signal. The C-6 signal is shifted upfield for the T67A mutant (1.1 ppm), but downfield shifted (1.3 ppm) for the C48S mutant. NMR spectra were also measured for two double mutants C48AT67A and C48ST67A. For C48AT67A mutant, the C-6 signal shifted a 1.6 ppm upfield (it appears that the shifts observed for the C48A mutant (0.4 ppm) and the T67A mutant (1.1 ppm) are roughly additive). The C48ST67A mutant shows a 0.2 ppm upfield shift at the C-6 signal (approximately the sum of the 1.3 ppm downfield shift of the C48S mutant and the 1.1 ppm upfield shift of the T67 mutant). The C-4a signal has a relatively large downfield shift (1.5 ppm) in case of the T50N mutant. The C-6 α signal is upfield shifted by about 1.3 ppm in all C48 mutants and downfield shifted around 1 ppm in C41C and T50N mutants. For the C-7 α signal chemical shift values are similar for wild type mutant except of C47A mutant, where it was 1.1 ppm downfield shifted.

Table 3.4 ^{13}C -NMR chemical shifts of $[\text{U-}^{13}\text{C}_{13}]6,7\text{-dimethyl-8-ribityllumazine}$ in complex with the N-terminal domain of riboflavin synthase (wild type or mutants). The chemical shift of the internal standard ($[\text{1-}^{13}\text{C}_1]\text{glucose}$) is 97.4 ppm.

Carbon Position		4	2	7	8a	6	4a	4'	2'	3'	5'	1'	6a	7a
NRS-WT	$\delta^{13}\text{C}$	165.9	159.4	157.1	151.5	148.6	130.8	78.2	73.9	70.2	62.6	57.1	23.3	19.9
	J_{cc}	73	-	Nd	55	53	68	Nd	Nd	nd	nd	nd	47	44
NRS-S41C	$\delta^{13}\text{C}$	166	159.2	157.2	151.5	148.6	130.7	78.8	74.3	70.7	63.1	56.3	24.7	20.5
	J_{cc}	80	-	49	61	56	67	Nd						
NRS-C47A	$\delta^{13}\text{C}$	165.9	159.5	157.2	151.5	148.9	130.9	79.1	73.6	70.3	62.5	57.1	23.4	20.0
	J_{cc}	74	-	38	52	nd	nd	Nd	Nd	nd	Nd	nd	51	43
NRS-C47S	$\delta^{13}\text{C}$	165.9	159.4	158.3	150.9	148.7	130.8	78.9	73.6	69.3	62.0	56.5	23.6	19.9
	J_{cc}	77	-	Nd	62,1	nd	nd	Nd	Nd	nd	nd	nd	nd	Nd
NRS-C48A	$\delta^{13}\text{C}$	165.9	159.4	157.5	151.5	148.2	130.6	78.1	74.1	70.4	62.3	56.6	22.5	20.4
	J_{cc}	75	-	45	59	51	71	Nd	Nd	nd	nd	nd	54	46
NRS-C48N	$\delta^{13}\text{C}$	165.9	159.4	156.5	151.4	148.3	130.9	78.2	74.1	70.3	62.4	57.0	22.1	20.0
	J_{cc}	75	-	46	62	55	66	Nd	Nd	nd	nd	nd	50	44
NRS-C48S	$\delta^{13}\text{C}$	166.0	159.4	158.3	151.4	149.5	130.2	78.1	74.1	70.4	62.2	56.7	22.3	20.1
	J_{cc}	76	-	28	50	47	67	Nd	Nd	nd	nd	nd	50	40
NRS-C48T	$\delta^{13}\text{C}$	165.9	159.3	156.5	151.4	148.1	131.1	78.1	73.8	70.6	62.5	57.1	22.7	20.5
	J_{cc}	76	-	45	62	53	74	Nd	Nd	nd	nd	nd	52	49
NRS-T50A	$\delta^{13}\text{C}$	165.7	159.7	155.7	151.3	148.6	131.4	78.3	73.9	70.2	62.4	56.9	24.1	19.7
	J_{cc}	78	-	Nd	54	nd	nd	Nd	Nd	nd	nd	nd	55	46
NRS-T50N	$\delta^{13}\text{C}$	166.0	159.6	155.3	151.2	149.5	132.1	78.3	73.8	70.3	62.0	56.5	23.5	19.7
	J_{cc}	74	-	Nd	51	nd	nd	Nd	Nd	nd	nd	nd	42	44
NRS-T67A	$\delta^{13}\text{C}$	165.9	158.2	156.6	151.9	147.5	130.8	78.7	74.4	69.2	62.6	57.0	23.2	19.8
	J_{cc}	75	-	49	62	54	71	Nd	Nd	nd	nd	nd	51	46
NRS-C48AT67A	$\delta^{13}\text{C}$	165.9	158.2	157.0	151.9	147.1	130.6	78.5	74.7	69.4	62.6	56.4	22.4	20.3
	J_{cc}	76	-	48	61	54	67	Nd	Nd	nd	nd	nd	55	46
NRS-C48ST67A	$\delta^{13}\text{C}$	166.0	158.3	157.7	151.8	148.4	130.2	78.6	74.7	69.3	62.6	56.7	22.2	20.0
	J_{cc}	73	-	47	59	56	70	Nd	Nd	nd	nd	nd	52	47

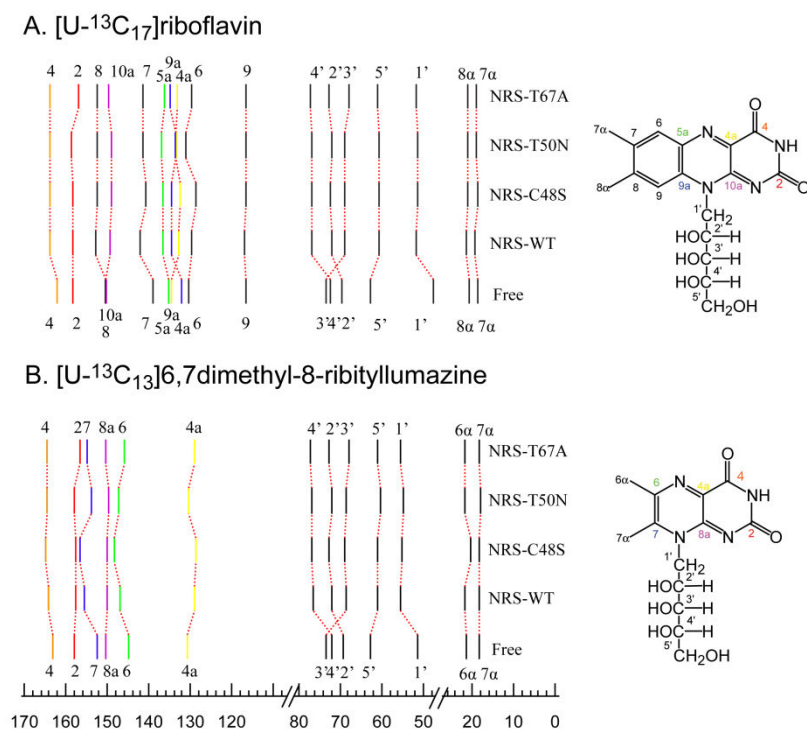


Figure 3.9 ^{13}C chemical shift values of $[\text{U}-^{13}\text{C}_{17}]$ riboflavin (A) and $[\text{U}-^{13}\text{C}_{13}]$ 6,7-dimethyl-8-ribityllumazine (B) bound to wild type or mutant N-terminal domains of riboflavin synthase.

Figure 3.9 shows chemical shifts of $[\text{U}-^{13}\text{C}_{17}]$ riboflavin (A) and $[\text{U}-^{13}\text{C}_{13}]$ 6,7-dimethyl-8-ribityllumazine (B) in complex with the N-terminal riboflavin synthase domain (wild type and mutant proteins) at 6.9. As expected, the NMR spectrum of $[\text{U}-^{13}\text{C}_{17}]$ riboflavin in complex with N-terminal domain of riboflavin synthase has 4 signals more than $[\text{U}-^{13}\text{C}_{13}]$ 6,7-dimethyl-8-ribityllumazine. ^{13}C chemical shift values of the spectra have similar general patterns. Specifically, at the ribityl chain part, almost the same pattern of ^{13}C chemical shifts was observed. Cognate carbon atoms from riboflavin and 6,7-dimethyl-8-ribityllumazine are emphasized by colored line.

3.1.2.3 Characterization of recombinant N-terminal riboflavin synthase domain under neutral and alkaline conditions by ^{13}C , ^{15}N -NMR spectroscopy

The ^{13}C -NMR spectra of 6,7-dimethyl-8-ribityllumazine measured at alkaline pH had been previously unequivocally assigned [131] [53]. Notably, the spectra are far more complex than under neutral conditions (Figure 3.11; B, C, D and E). At least five molecular species have been reported to be in equilibrium in alkaline solution [131] (two 5-membered ring anions, two 6-membered ring anions and the 7α exo-methylene anion) (Figure 3.10).

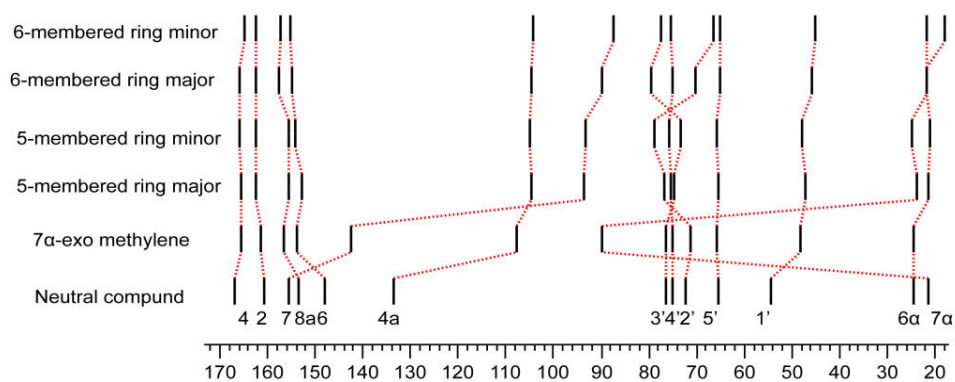


Figure 3.10 ^{13}C chemical shifts of 6,7-dimethyl-8-ribityllumazine derivatives (from Bown, 1986 [131]).

The analysis of the 6,7-dimethyl-8-ribityllumazine enriched primarily at C 7 α position (Figure 3.11, **B**) allowed one to assign the peak at 88.9 ppm to C 7 α position of the exomethylene anion. This exomethylene anion of 6,7-dimethyl-8-ribityllumazine was present around 17 % in the equilibrium mixture.

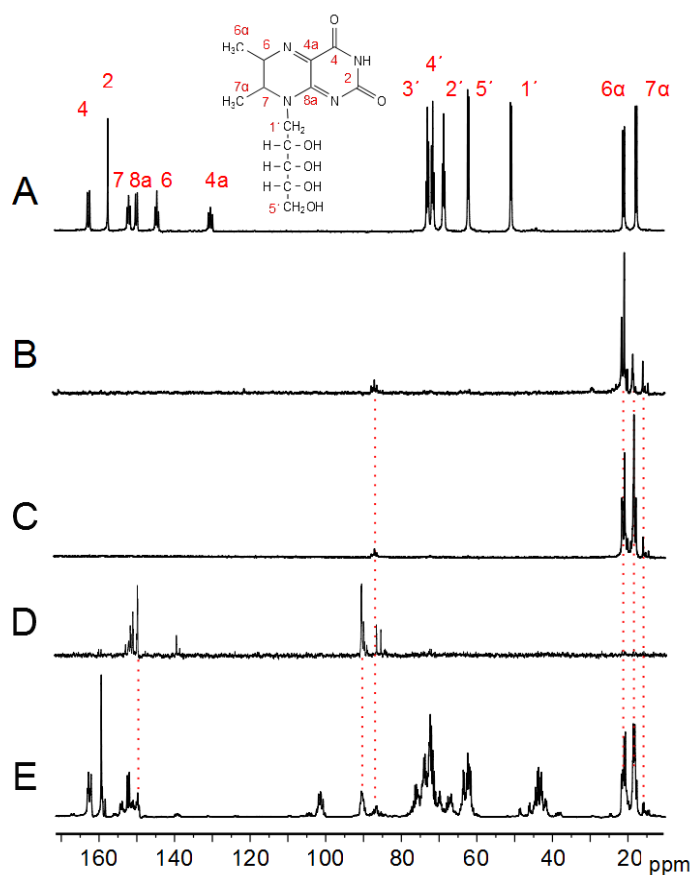


Figure 3.11 ^{13}C -NMR spectra of free 6,7-dimethyl-8-ribityllumazine in 50 mM Tris-HCl at pH 6.9 (A) and pH 9.5 (B, C, D, E). (A, E: $[\text{U-}^{13}\text{C}_{13}]$ 6,7-dimethyl-8-ribityllumazine, B: $[\text{7}\alpha\text{-}^{13}\text{C}_1]$ 6,7-dimethyl-8-ribityllumazine, C: $[\text{6}\alpha, \text{7}\alpha\text{-}^{13}\text{C}_2]$ 6,7-dimethyl-8-ribityllumazine, D: $[\text{6,7-}^{13}\text{C}_2]$ 6,7-dimethyl-8-ribityllumazine).

The ^{13}C -NMR spectrum of $[\text{U-}^{13}\text{C}_{13}]6,7\text{-dimethyl-8-ribityllumazine}$ in complex with N-terminal riboflavin synthase domain at pH 11 is shown in Figure 3.12. It is immediately obvious that this spectrum is less complex than that of the lumazine in solution. This is surprising since one might expect that the complexity is enhanced by binding to the protein. Figure 3.12 shows that each carbon of bound $[\text{U-}^{13}\text{C}_{13}]6,7\text{-dimethyl-8-ribityllumazine}$ is represented by a single signal (with evidence of ^{13}C ^{13}C coupling); at least in that respect, the spectrum is similar to that of the protein-bound ligand at neutral pH. Based on the neutral assignments, the signal assignments were obtained by the use of random isotopologue libraries from $[1\text{-}^{13}\text{C}_1]\text{glucose}$ and $[2\text{-}^{13}\text{C}_1]\text{glucose}$ and selectively ^{13}C -labeled $[7\alpha\text{-}^{13}\text{C}_1]6,7\text{-dimethyl-8-ribityllumazine}$ and $[6\alpha,6,7,7\alpha\text{-}^{13}\text{C}_4]6,7\text{-dimethyl-8-ribityllumazine}$. For example, the signal at 160.2 ppm can be assigned unequivocally to C-2 due to its singlet signature. The downfield-shifted signals between 130 and 170 ppm are due to carbons of the xylene ring. The signals between 50 and 80 ppm are due to the ribityl carbons. The doublet at 22.8 ppm reflects the methyl carbon 6α and the signal at 88.9 ppm is assigned as C- 7α .

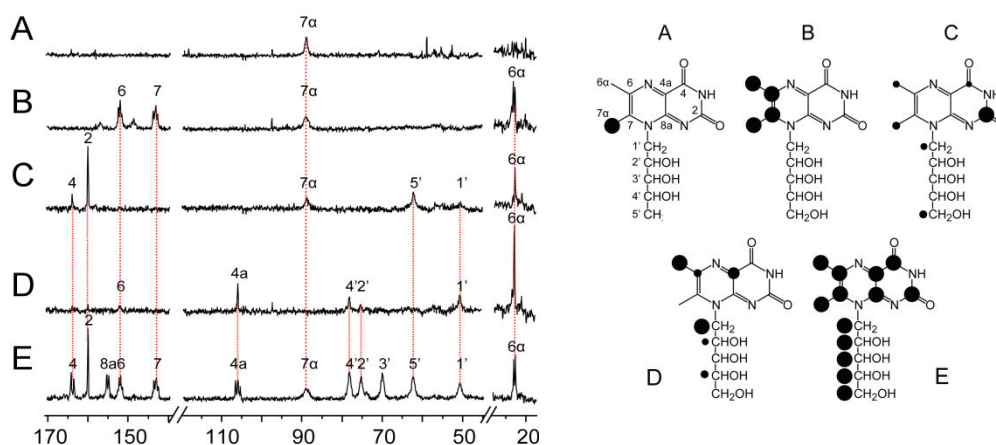


Figure 3.12 Left, ^{13}C -NMR spectra of isotopologues of 6,7-dimethyl-8-ribityllumazine in complex with the N-terminal domain of riboflavin synthase (wild type) at pH 11.0 (alkaline). Right, labeling patterns of 6,7-dimethyl-8-ribityllumazine isotopologues. A; $[7\alpha\text{-}^{13}\text{C}_1]6,7\text{-dimethyl-8-ribityllumazine}$, B; $[6\alpha,6,7,7\alpha\text{-}^{13}\text{C}_4]6,7\text{-dimethyl-8-ribityllumazine}$, C; 6,7-dimethyl-8-ribityllumazine biosynthesized from $[1\text{-}^{13}\text{C}_1]\text{glucose}$, D; 6,7-dimethyl-8-ribityllumazine biosynthesized from $[2\text{-}^{13}\text{C}_1]\text{glucose}$, E; $[\text{U-}^{13}\text{C}_{13}]6,7\text{-dimethyl-8-ribityllumazine}$, the size of the dots indicates ^{13}C enrichment.

Figure 3.13 shows ^{13}C -NMR spectra of the N-terminal riboflavin synthase domain (wild type) in complex with $[\text{U-}^{13}\text{C}_{13}]6,7\text{-dimethyl-8-ribityllumazine}$ at different pH values (pH 6.9, 8.5 and 9.0). Different ^{13}C signal sets (each comprising 13 signals and obviously representing all carbon atoms of the bound ligand) were observed at pH 6.9 and 9.0. The spectrum at pH 8.5 shows a mixture of these respective components. Hence, the neutral and the alkaline species observed are not in rapid exchange (Figure 3.13 and Table 3.5). Each ^{13}C signals of bound ligand was assigned in this study. Major pH-

associated chemical shift changes are observed for C-7 α (shifted downfield by about 69 ppm), C-4a (shifted upfield by about 25 ppm), C-7 (shifted upfield by about 14 ppm) and C-1' (shifted upfield by about 6 ppm) (Figure 3.13 and Table 3.5).

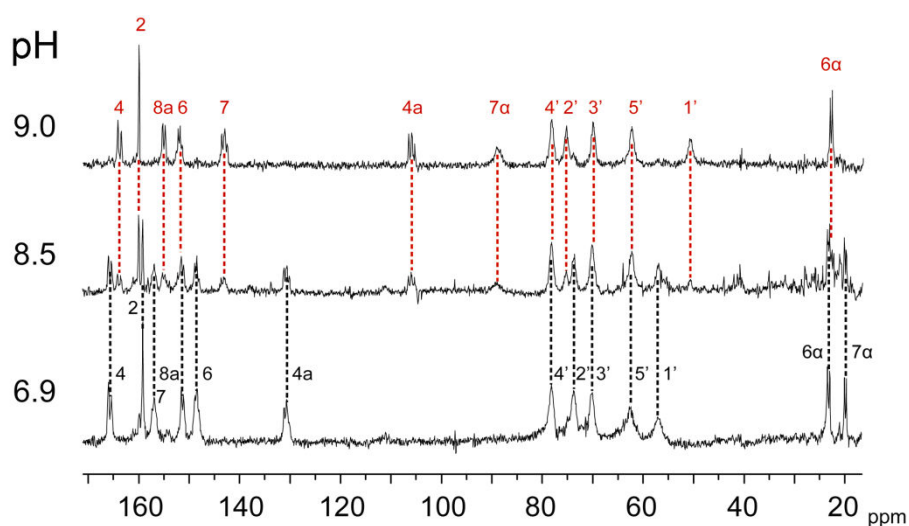


Figure 3.13 ^{13}C -NMR chemical shifts of $[\text{U-}^{13}\text{C}_{13}]6,7\text{-dimethyl-8-ribityllumazine}$ in complex with N-terminal domain of riboflavin synthase (wild type). (pH 9.0, pH 8.5, pH 6.9) Internal standard is $[1\text{-}^{13}\text{C}_1]\text{glucose}$ (97.4 ppm).

Table 3.5 NMR data of selectively $[\text{U-}^{13}\text{C}_{13}]6,7\text{-dimethyl-8-ribityllumazine}$ in complex with the wild type N-terminal riboflavin synthase domain (NRS-WT).

^{13}C position	Chemical shifts (ppm)	
	pH 6.9	pH 9.0
4	165.9	164.0
2	159.4	160.2
7	157.1	143.2
8a	151.5	155.2
6	148.6	152.0
4a	130.8	106.0
4'	78.2	78.3
2'	73.9	75.3
3'	70.2	70.0
5'	62.6	62.5
1'	57.1	50.6
6 α	23.3	22.8
7 α	19.9	88.9

We have also obtained ^{15}N -NMR spectra of the recombinant riboflavin synthase domain in complex with various ^{15}N -labeled samples of 6,7-dimethyl-8-ribityllumazine at neutral (pH 6.9) and alkaline conditions (pH 11). These data are also summarized in Table 3.6. Single-labelled $[5-^{15}\text{N}_1]$ - and $[8-^{15}\text{N}_1]$ -6,7-dimethyl-8-ribityllumazine were used for chemical shift assignments.

Table 3.6 NMR data of selectively ^{15}N -labeled 6,7-dimethyl-8-ribityllumazine bound to the wild type N-terminal domain of riboflavin synthase.

pH	^{15}N position	$[1,3,5,8-^{15}\text{N}_4]$ 6,7-dimethyl-8-ribityllumazine	$[8-^{15}\text{N}_1]$ 6,7-dimethyl-8-ribityllumazine with WT	$[5-^{15}\text{N}_1]$ 6,7-dimethyl-8-ribityllumazine with WT	$[1,3,5,8-^{15}\text{N}_4]$ 6,7-dimethyl-8-ribityllumazine with WT
6.9	1N	182.15			183.85
	3N	160.06			162.36
	5N	331.62		327.57	327.53
	8N	196.11	197.86		197.71
11.0	1N				183.24
	3N				150.29
	5N			274.00	273.76
	8N		118.53		118.52

Major upfield shifts were noted for the signals of N-5 (53.57 ppm) and N-8 (79.33 ppm) upon transition from neutral to alkaline pH, and these can be safely assumed to reflect the transition from the neutral molecule to the exomethylene anion of the bound ligand. Notably, ^{15}N assignments had not been previously reported for the exomethylene anion of 6,7-dimethyl-8-ribityllumazine (in fact, they would not be easily obtained for the free ligand in solution because of sensitivity limitations, since the exomethylene form is a minor species under these conditions) (Table 3.6).

NMR experiments were performed using ^{13}C - and ^{15}N -labelled isotopologues of 6,7-dimethyl-8-ribityllumazine in complex with the wild type and mutant proteins under neutral and acidic conditions. Chemical shifts modulation caused by the amino acid replacements are summarized in Figure 3.14. The replacement of threonine 50 by alanine shifts the ^{15}N -NMR signal of N-5 to downfield. The neutral 6,7-dimethyl-8-ribityllumazine and the exo-methylene anion of 6,7-dimethyl-8-ribityllumazine in complex with the protein are similarly affected. This is well in line with the presence of a hydrogen bond between the side chain hydroxy group of threonine 50 and N-5 of the ligand (Figure 3.14). The chemical shift changes accompanying the replacement of threonine 67 by alanine are smaller, both at neutral and alkaline pH. Notably, that amino acid substitution causes a slight downfield shift of C-3' carrying a hydroxy group that has been proposed to be involved in hydrogen bond interaction with the side chain hydroxy group of threonine 67 [48]. A similar pattern of ^{13}C chemical shifts is also observed when riboflavin was used as ligand.

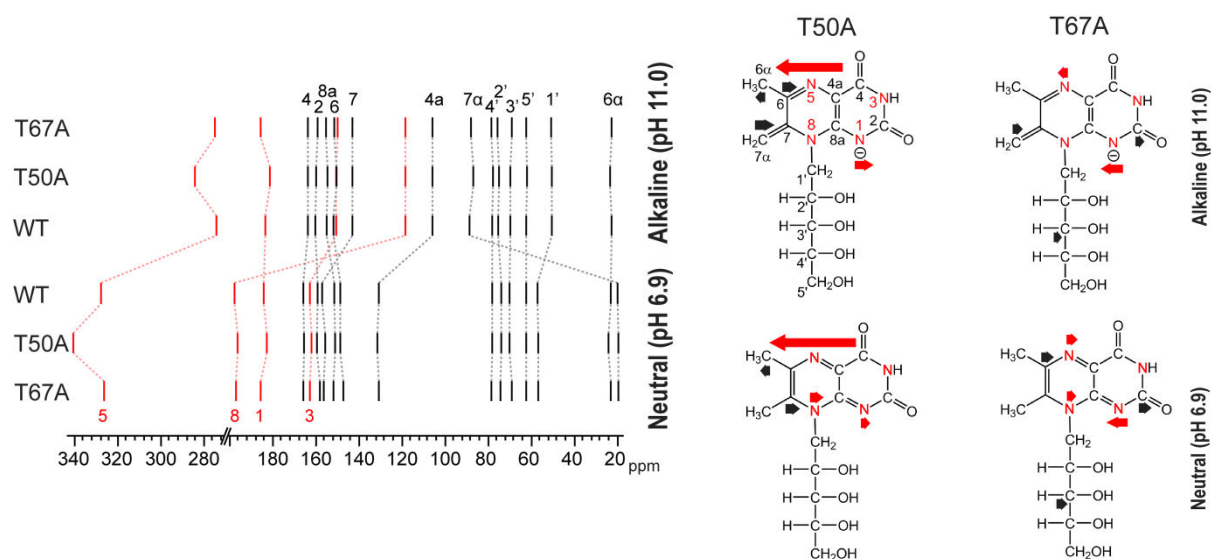


Figure 3.14 Left, ^{13}C chemical shifts (black) and ^{15}N chemical shifts (red) of 6,7-dimethyl-8-ribityllumazine in complex with the N-terminal domain of riboflavin synthase (wild type (WT) or mutant as indicated). Right, impact of point mutations on the chemical shifts of 6,7-dimethyl-8-ribityllumazine and its exo-methylene anion (8) is shown by arrows (^{13}C shift effects are shown in black, ^{15}N shift effects are shown in red).

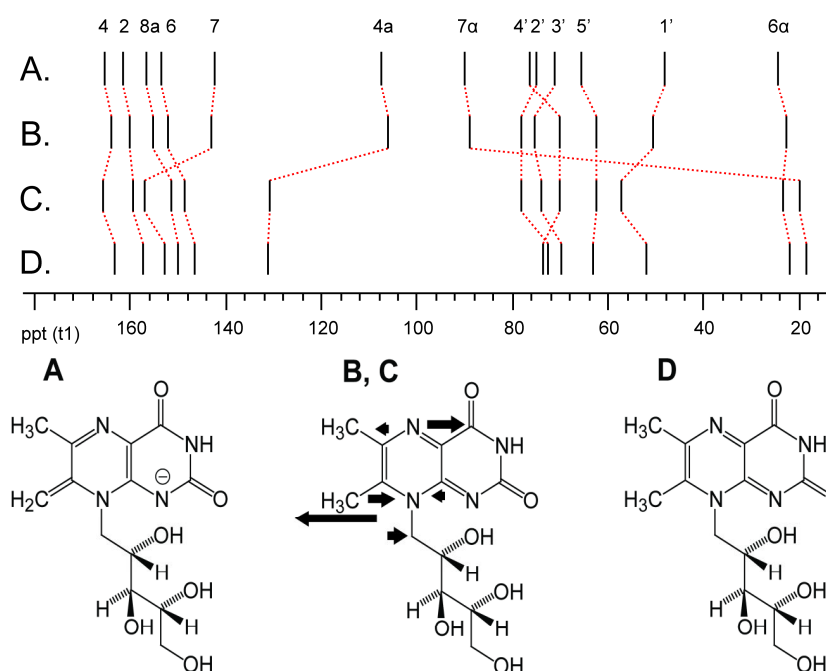


Figure 3.15 ^{13}C -NMR chemical shift correlation of 6,7-dimethyl-8-ribityllumazine. (A, Free 7 α -exomethylene anion; B, 6,7-dimethyl-8-ribityllumazine in complex with wild type N-terminal riboflavin synthase domain at pH 9.2; C, 6,7-dimethyl-8-ribityllumazine in complex with wild type N-terminal riboflavin synthase domain at pH 7.0; D, free 6,7-dimethyl-8-ribityllumazine at pH 7.0)

In summary, the transition from neutral 6,7-dimethyl-8-ribityllumazine to the exo-methylene anion causes major chemical shift changes. These changes are tentatively interpreted as an increase in electron density at these respective positions and suggest that the negative charge is delocalized predominantly to the pyrazine ring of the bicyclic lumazine system.

As shown by X-ray crystallography, the N-terminal riboflavin synthase domain binds the 6,7-dimethyl-8-ribityllumazine in a shallow surface depression (Figure 3.16) [42] [47] [48]. One side of the heterocyclic molecule is solvent-exposed. The protein contacts the heterocyclic moiety predominantly via backbone elements that are believed to engage in hydrogen bonding. The γ hydroxy group of threonine 50 has been proposed to serve as a hydrogen bond donor for N-5, and the γ hydroxy group of threonine 67 is believed to serve as a hydrogen bond donor for N-1 of bound ligand. Moreover, that hydroxy function is also a candidate for an acceptor-type hydrogen bond interaction with the position 3' hydroxy group of the ribityl side chain.

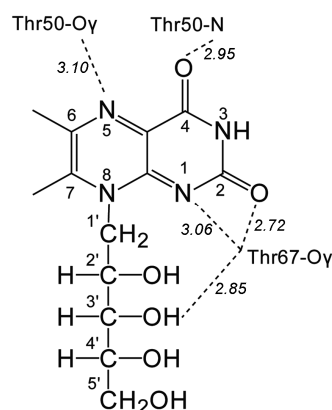


Figure 3.16 Hydrogen bond contacts of 6,7-dimethyl-8-ribityl in complex with the N-terminal riboflavin synthase domain (based on the structure of riboflavin in complex with the N-terminal riboflavin synthase domain; PDB code 1PKV (from Meining, 2003 [48]). Hydrogen-bonding distances (\AA) are shown in italics.

In order to analyze the proposed hydrogen bonding network in more detail, we replaced the threonine residues 50 and 67 with alanine residues in the N-terminal riboflavin synthase domain of *E. coli*. pK_a values for 6,7-dimethyl-8-ribityllumazine in complex with the various mutant proteins were obtained by photometric titration (Table 3.3). The replacement of threonine residues 50 or 67 with alanine decreased the acidity of protein-bound 6,7-dimethyl-8-ribityllumazine by one to two orders of magnitude.

In alkaline aqueous solutions of 6,7-dimethyl-8-ribityllumazine, the exomethylene anion **21** (Figure 1.5) is only present as a trace component (less than 1 % as estimated by optical absorbance spectroscopy) in the complex equilibrium mixture comprising at least five anionic species (Figure 1.5). On the other hand, the exomethylene form is the only anionic species detectably binding to the N-

terminal domain dimer of riboflavin synthase. The pKa of 6,7,8-trimethylumazine (**19**) is 9.8, as compared to the apparent pKa of 7.9 for 6,7-dimethyl-8-ribityllumazine (Table 3.2). However, since the exomethylene anion (**21**) accounts for 100 % of anions in case of 6,7,8-trimethylumazine (**19**) and less than 1 % in case of 6,7-dimethyl-8-ribityllumazine (**10**), the values signify that the CH acidity of the position 7 methyl group is about the same in both compounds. The higher apparent acidity of 6,7-dimethyl-8-ribityllumazine is not caused by a change in CH acidity but by the higher stability of the tricyclic anions. The data obtained with mutant proteins support the notion that the exomethylene anion (**21**) is specifically stabilized by hydrogen bonding with the side chain hydroxy groups of threonine residues 50 and 67. Mutations that abolish the hydrogen-bonding capacity of these amino acids increase the pKa of the ligand (equivalent to reduced CH acidity of the position 7 methyl group). The data suggest that the free enthalpy of the exomethylene anion is lowered to a larger degree by binding to the wild type protein as compared to that of the neutral molecule. The N-terminal domain of riboflavin synthase has been shown to serve as the acceptor site for C-4 transfer between the two substrate molecules [42]. The stabilization of the exomethylene anion (**21**) by the N-terminal domain is well in line with the requirements of the hypothetical reaction mechanism shown in Figure 1.6. However, as pointed out earlier, the previously published mechanistic hypotheses, including the specific variation on that theme that is shown in Figure 1.6, require the obligatory participation of a nucleophile (designated Nu in Figure 1.6), but protein structure analysis in conjunction with mutagenesis studies has failed to identify an amino acid residue that would qualify for that function [42] [47] [48]. Although a water molecule could be implicated, as a last-ditch defense, to serve as the elusive nucleophile (Nu in Figure 1.6), it appears timely to explore alternative mechanistic concepts. Such an alternative, centered on the concept of hydride transfer between the exomethylene anion and a second substrate molecule followed by 4 + 2 cycloaddition, is presented in the Figure 3.17. Specifically, we propose that the exomethylene anion **21** bound at the N-terminal domain of riboflavin synthase donates a hydride ion to C-7 of a neutral **10** that is bound at the C-terminal domain of an adjacent subunit, thus affording (1*H*,7*H*)-dihydro-6,7-dimethyl-8-ribityllumazine (**29a**) and the dehydrolumazine derivative **28**. Tautomerization of **29a** may yield (1*H*,5*H*)-dihydro-6,7-dimethyl-8-ribityllumazine (**29b**), which could then undergo a 4 + 2 cycloaddition, affording the pentacyclic intermediate **26a**. These proposed reaction steps are discussed in more detail below.

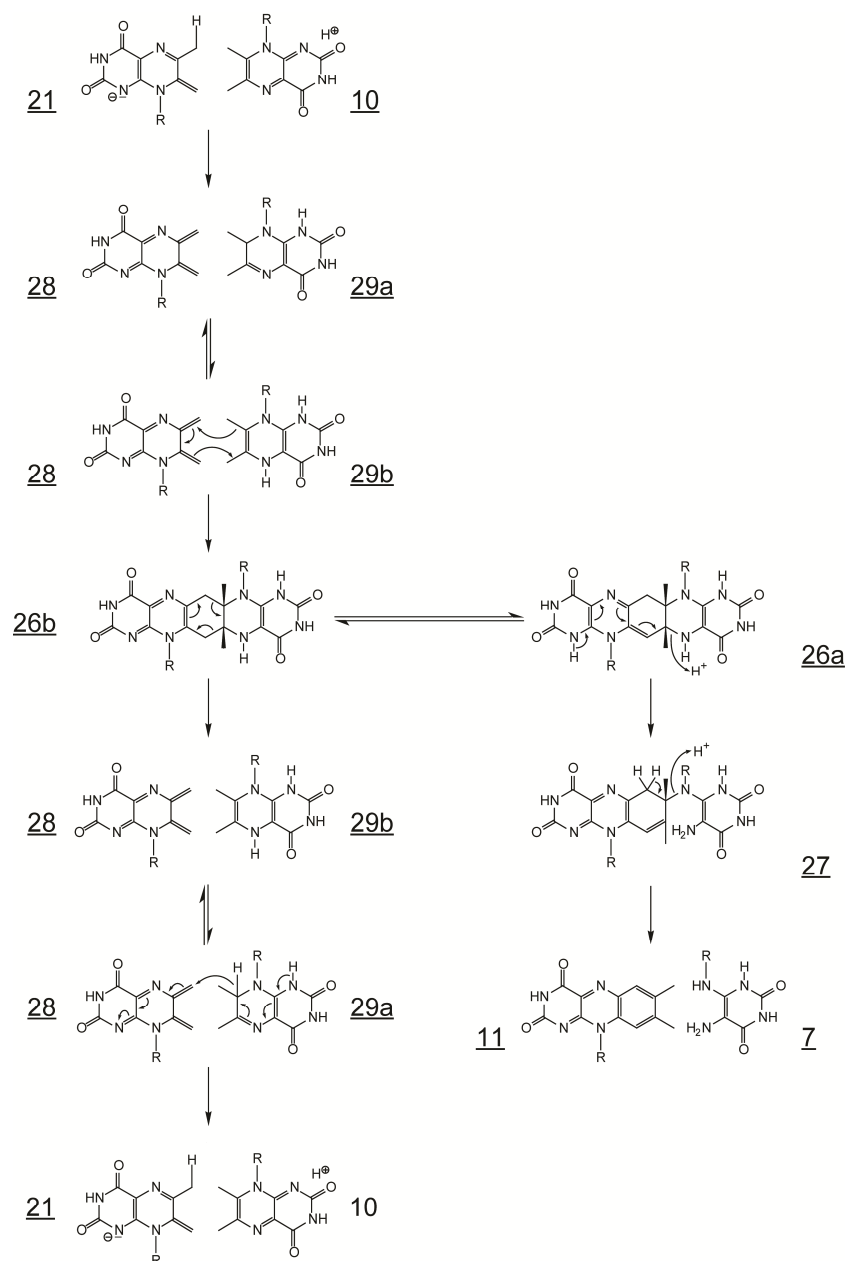


Figure 3.17 Proposed mechanism for riboflavin synthase reaction via hydride transfer and fragmentation of the experimentally documented pentacyclic intermediate [39].

(i) The proposed hydride transfer between anionic **21** and neutral **10** resembles the Cannizzaro reaction, affording an alcohol and a carboxylate anion by dismutation of an aromatic aldehyde, where an anionic species resulting from the addition of a hydroxy group of one aldehyde molecule donates a hydride ion to a neutral aldehyde molecule. Notably, the Cannizzaro reaction proceeds extremely fast in aqueous solution at room temperature. It should also be noted that hydride transfer, in general, is one of the most common elementary processes in enzyme catalysis [132]. In parallel with riboflavin, **10** can undergo two-electron reduction, affording a dihydro derivative. The pyrazine moiety of **21** is electron-rich, as shown by its ^{13}C and ^{15}N chemical shifts (cf. Figure 3.14). At the active site of *E. coli* riboflavin synthase, the two bound substrate molecules are ideally placed to enable the transfer of

hydride from the position 6 methyl group of the exomethylene anion **21** (bound at the N-terminal domain) to C-7 carbon of **1** (bound at the C-terminal domain) [42]. The distance to be traversed is quite short, and vanishing and emerging π orbitals have favorable orientations.

(ii) The two-electron reduction product of **1** exists as an equilibrium mixture of the tautomers **29a** and **29b** [132].

(iii) The electronics favor an inverse-electron-demand 4 + 2 cycloaddition involving overlap of the HOMO of the dienophile **29b** with the LUMO of the diene **28**. This scenario for the reaction is favored by the electron-donating groups on the dienophile and the electron-withdrawing groups on the diene. The diene is electron-poor due to conjugative interactions involving the two electronegative carbonyl groups, as well as the two N-1 and N-5 imine nitrogens. On the other hand, the dienophile **29b** is electron-rich through donation of electrons by the N-5 enamine nitrogen atom. Electron donation from the N-8 ribitylamino nitrogen toward the dienophile is less important, because it is part of a vinylogous amide system.

(iv) The mechanism proposed in Figure 1.6 and 3.17 are both very well in line with the large isotope effects that were observed already in 1970 with 6 α deuterium and tritium isotopologs of **10** as substrates of riboflavin synthase [133]. Specifically, the hypothetical mechanism in Figure 1.6 requires the abstraction of a proton from the 6 α -methyl group of the lumazine molecule destined to serve as four-carbon acceptor, and the novel hypothesis proposed in Figure 3.17 requires the transfer of a hydride anion. In both hypothetical pathways, the heterolytic cleavage of the carbon-hydrogen could qualify as a rate determining step; hence, hydrogen isotope effects fail to decide between the two hypotheses under discussion.

(v) With the hypothesis in Figure 3.17, the reverse and forward reactions affording two molecules of **10** or one respective molecule of each **11** and **7** are both catalyzed with similar velocity by riboflavin synthase [38, 134]. It should be mentioned that the two fragmentation pathways affording either **10** or a mixture of **11** and **7**, respectively, are believed to depart from different tautomers of the pentacyclic intermediate (Figure 3.17). Notably, the tautomers **26a** and **26b** are endowed with different sets of predetermined fracture points (Figure 3.17).

(vi) In contrast to the mechanism in Figure 1.6, and related concepts, the novel hypothetical mechanism (Figure 3.17) has no requirement for an amino acid side chain to act as a nucleophile (or for any nonprotein nucleophile). This is advantageous since X-ray crystallography and mutation screening have failed to identify an amino acid residue that could serve as the elusive nucleophile in Figure 1.6 [42, 130].

(vii) By comparison with the reaction sequence shown in Figure 1.6, the novel hypothesis is parsimonious with regard to the number of reaction steps conducive to the pentacyclic intermediate.

Hyperfine mapping of FMN bound to the LOV photoreceptor domain of phototropin

3.2 Enzyme-assisted synthesis of riboflavin isotopologues and flavincoenzymes

A one-pot method for the preparation of riboflavin isotopologues labeled with ^{13}C in every desired position of the xylene moiety has been published [54]. The starting materials are commercially available ^{13}C labeled glucose isotopologues, which are converted into riboflavin using enzymes of the oxidative pentose phosphate pathway in combination with recombinant enzymes of the riboflavin biosynthetic pathway [54]. In this study, isotope-labeled ribose was explored as an alternative synthon. The reaction steps for enzymatic conversion of ribose to riboflavin are summarized in Figure 3.18 and the transfer of carbon atoms from D-ribose (**34**) into riboflavin is indicated by different colors.

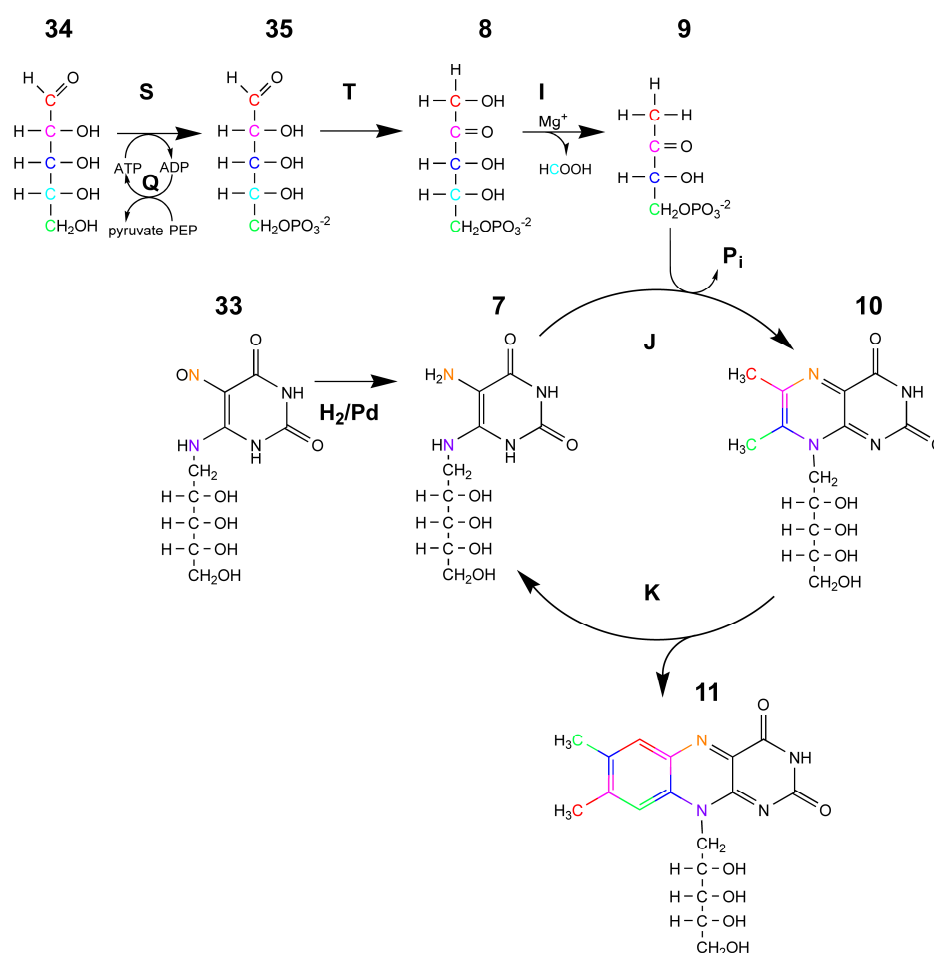


Figure 3.18 Enzyme-assisted synthesis of riboflavin from D-ribose (**34**). **S**, Ribose kinase; **T**, ribose-5-phosphate isomerase; **I**, 3,4-dihydroxy-2-butanone-4-phosphate synthase; **J**, 6,7-dimethyl-8-ribityllumazine synthase; **K**, riboflavin synthase; **Q**, flavokinase.

One mol of D-ribose (**34**) is converted to 1 mole of ribulose-5-phosphate (**8**) using 1 mol of ATP. ATP can be regenerated in situ by pyruvate kinase (**Q**) using phosphoenolpyruvate (PEP) as phosphate

donor. C-1, 2, 3 and C-5 of ribulose-5-phosphate (**8**) are incorporated into 3,4-dihydroxy-2-butanone-4-phosphate (**9**), and C-4 is removed as formic acid by the enzyme-catalyzed conversion and this step is thermodynamically irreversible. One mol of 5-amino-6-ribitylamino-2,4(1*H*,3*H*)-pyrimidinedione (**7**) is condensed with 3,4-dihydroxy-2-butanone 4-phosphate (**9**), affording 6,7-dimethyl-8-ribityllumazine (**10**) under the catalytic action of 6,7-dimethyl-8-ribityllumazine synthase (**J**). Riboflavin synthase (**K**) catalyzes the transfer of a four carbon fragment between 2 molecules of 6,7-dimethyl-8-ribityllumazine (**10**), resulting in the formation of 1 mol of riboflavin (**11**) and 1 mol of 5-amino-6-ribitylamino-2,4(1*H*,3*H*)-pyrimidinedione (**7**), which can be recycled by 6,7-dimethyl-8-ribityllumazine synthase (**J**).

All reaction steps can be performed as a one-pot reaction. The one-pot mixture was incubated at room temperature for 48 hours under an inert atmosphere in a glove box. The final product, riboflavin (**11**), was obtained in yields of 45 % based on D-ribose (**34**). Riboflavin crystallizes spontaneously from the one-pot reaction mixture and can be harvested by centrifugation and purified by recrystallization. The produced riboflavin can be converted into the flavocoenzymes FMN and FAD. The following paragraphs describe the preparation of the riboflavin biosynthesis enzymes that are required for the enzyme-assisted method for the preparation of riboflavin isotopologues. The preparation of individual isotopologues is then reported in more detail.

3.2.1 Preparation of enzymes for enzyme-assisted flavin biosynthesis

3.2.1.1 Ribose kinase of *Escherichia coli*

The *rbsK* gene of *E. coli* specifies a ribose kinase comprises 214 amino acid residues. The recombinant plasmid (BL21-pET22b-EcRKc11) was obtained from Dr. Boris Illarionov (Ikosatec, Hamburg, Germany). The recombinant ribose kinase is expressed efficiently in a recombinant *E. coli* strain and can be easily purified by Ni⁺-column chromatography due to the 6-histidine tag present at the N-terminus (see Methods 2.3.4.1.1).

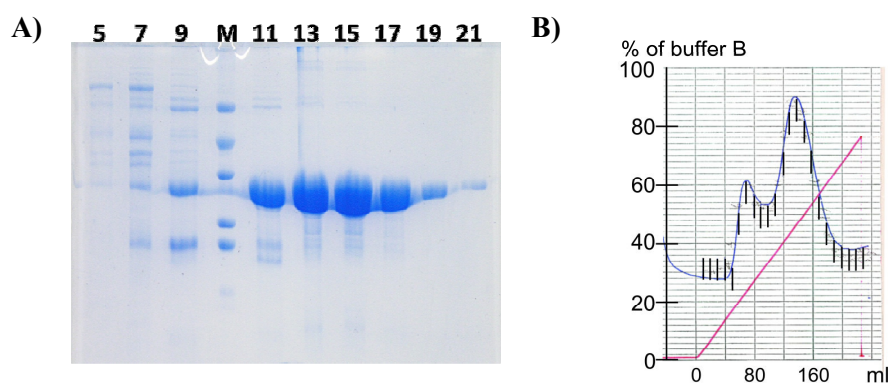


Figure 3.19 Analysis of the recombinant ribose kinase. **A)** SDS-PAGE (M; protein size marker, fraction 12 to 21 were combined), **B)** Chromatography on Ni⁺-column.

The recombinant ribose kinase was eluted with around 300 mM imidazole and the resulting protein appeared approximately 90 % pure. The molecular weight was about 34 kDa as judged by SDS-PAGE (Figure 3.19).

3.2.1.2 3,4-Dihydroxy-2-butanone 4-phosphate synthase of *Escherichia coli*

The *ribB* gene of *E. coli* specifies 3,4-dihydroxy-2-butanone 4-phosphate synthase (**I**) comprising 217 amino acid residues. The recombinant plasmid (pQE30-ribB#2) was obtained from Prof. Markus Fischer (Universität Hamburg, Hamburg, Germany). The recombinant DHBP synthase is expressed efficiently in a recombinant *E. coli* strain and can be easily purified by Ni⁺-column chromatography due to the 6-histidine tag present at the N-terminus (see Methods 2.3.4.1.2). The recombinant DHBP synthase was eluted with 300 mM of imidazole and the resulting protein appeared approximately 90 % pure as judged by SDS-PAGE (Figure 3.20). DHBP synthase is a homodimeric protein comprising two identical 23 kDa subunits. SDS-PAGE of the recombinant protein afforded an approximate molecular weight of 23 kDa in line with the calculated value [135].

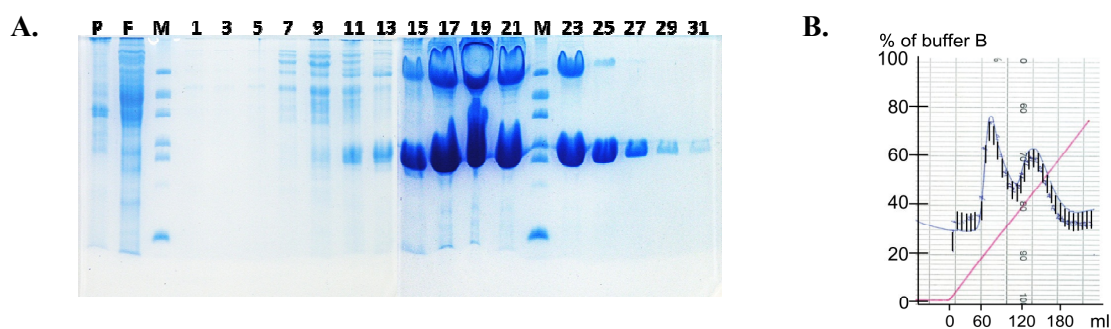


Figure 3.20 Analysis of recombinant 3,4-dihydroxy-2-butanone 4-phosphate synthase of *E. coli*. **A**, SDS-PAGE (P, pellet; F, flow through; M; protein size markers; lane from 1 to 31 are elution fractions); **B**, a photometric profile (280 nm) of chromatography on Ni⁺-column.

3.2.1.3 6,7-Dimethyl-8-ribityllumazine synthase of *Bacillus subtilis*

The *ribH* gene of *B. subtilis* specifies a 6,7-dimethyl-8-ribityllumazine synthase (**J**) comprising 154 amino acid residues. The gene fragment was cloned into the vector pNCO113. The recombinant plasmid (pNCO-RibH-WT) was obtained from Dr. Ilka Haase (Universität Hamburg, Hamburg, Germany). The recombinant 6,7-dimethyl-8-ribityllumazine synthase is expressed efficiently in a recombinant *E. coli* strain and can be purified by Q-Sepharose chromatography (see Methods 2.3.4.1.3). The purified enzyme cannot be recognized easily on SDS-PAGE (Figure 3.21, **A**). As shown in the Figure 3.21 **A**, almost every elution fraction contained proteins in with molecular weight around 17 kDa. Therefore, fractions were assayed for 6,7-dimethyl-8-ribityllumazine synthase (**J**)

activity. The reaction mixture (0.1 ml) contained 100 mM Tris-HCl (pH 7), 100 mM NaCl, 1 mM DTT, 0.02% NaN₃, 0.3 mM 3,4-dihydroxy-2-butanone 4-phosphate, 0.3 mM 5-amino-6-ribitylamino-2,4(1*H*,3*H*)-pyrimidinedione and 30 μ l of respective chromatography fraction. The mixture was incubated at 37 °C for 20 min and 6,7-dimethyl-8-ribityllumazine was monitored by fluorescence (Figure 3.21, C).

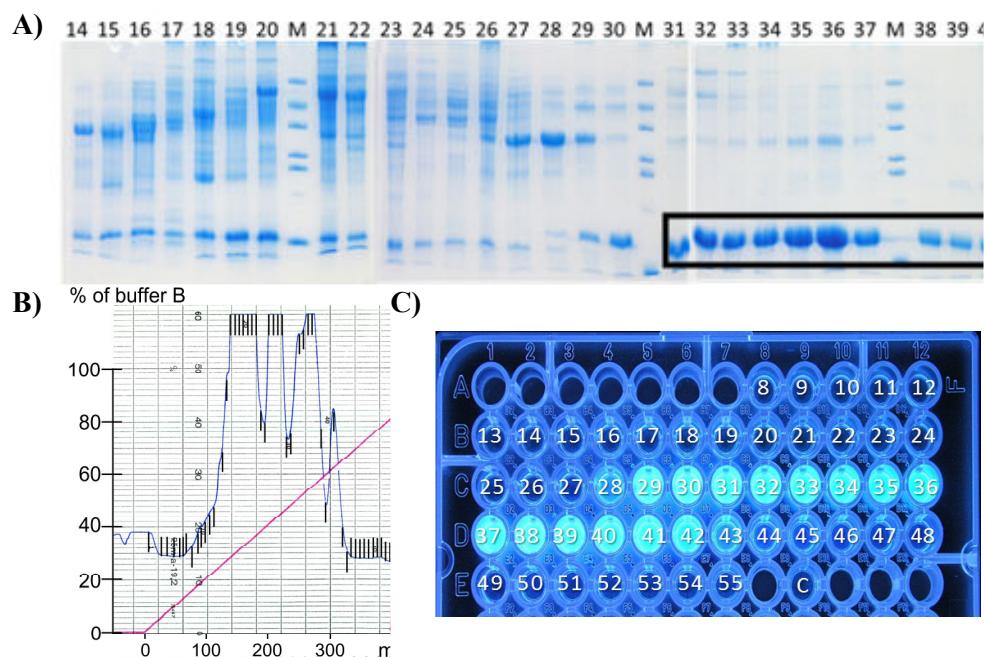


Figure 3.21 Analysis of the recombinant 6,7-dimethyl-8-ribityllumazine synthase. **A)** Analysis by SDS-PAGE (M is protein size marker. Lanes 14 to 40 are elution fractions. The target protein is indicated with black box, **B)** chromatography by Q-Sepharose column, **C)** analysis of fractions by enzyme activity test.

As is clear from Figure 3.21 C, the recombinant 6,7-dimethyl-8-ribityllumazine synthase was eluted from the Q-Sepharose column at about 420 mM KCl (Figure 3.21, B). The protein itself is a homopentamer comprising five identical 17 kDa subunit. SDS-PAGE afforded a molecular weight estimate that is well in line with the expected value. The resulting protein appeared approximately 90 % pure (Figure 3.21 in black box).

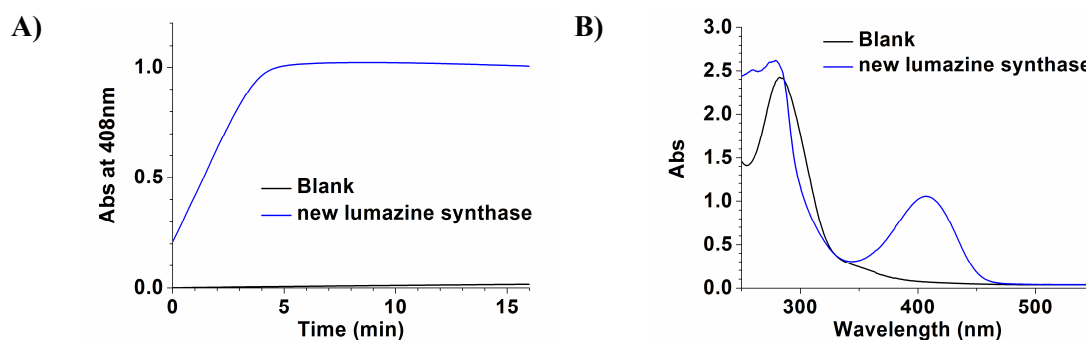


Figure 3.22 Enzyme activity analysis of 6,7-dimethyl-8-ribityllumazine synthase.

The activity of 6,7-dimethyl-8-ribityllumazine synthase (**J**) was confirmed in a separate experiment (Figure 3.22). Formation of 6,7-dimethyl-8-ribityllumazine (**10**) from 5-amino-6-ribitylamino-2,4(1*H*,3*H*)-pyrimidinedione (**7**) and 3,4-dihydroxy-2-butanone 4-phosphate (**9**). The assay mixtures (0.5 ml) contained 0.15 mM of substrates **7** and **9**, 100 mM Tris-HCl (pH 7), 0.02 % NaN₃ and 5 μl of 6,7-dimethyl-8-ribityllumazine synthase solution. Assays were performed at 30 °C for 20 min and were monitored photometrically at 410 nm (Figure 3.22, **A**).

3.2.1.4 Riboflavin synthase of *Aquifex aeolicus*

The *ribC* gene of *A. aeolicus* specifies a riboflavin synthase comprising 207 amino acid residues. The recombinant riboflavin synthase is expressed efficiently in a recombinant *E. coli* strain and can be easily purified by Ni⁺-column chromatography due to the 6-histidine tag present at the C-terminus (see Methods 2.3.4.1.4). The resulting protein appeared approximately 90 % pure, with an apparent subunit mass of about 24 kDa as judged by SDS-PAGE (Figure 3.23, **A**). Riboflavin synthase activity was confirmed by the conversion of 6,7-dimethyl-8-ribityllumazine (**10**) to riboflavin (**11**) as shown in the Figure 3.23 (**B**, **C**). The assay mixture (0.5 ml) contained 100 mM Tris-HCl (pH 7.0), 100 mM sodium chloride, 0.02 % NaN₃, 0.17 mM 6,7-dimethyl-8-ribityllumazine (**10**) and 10 μl of riboflavin synthase solution. The time resolved assay was performed at 37 °C for 20 min (Figure 3.23, **B**).

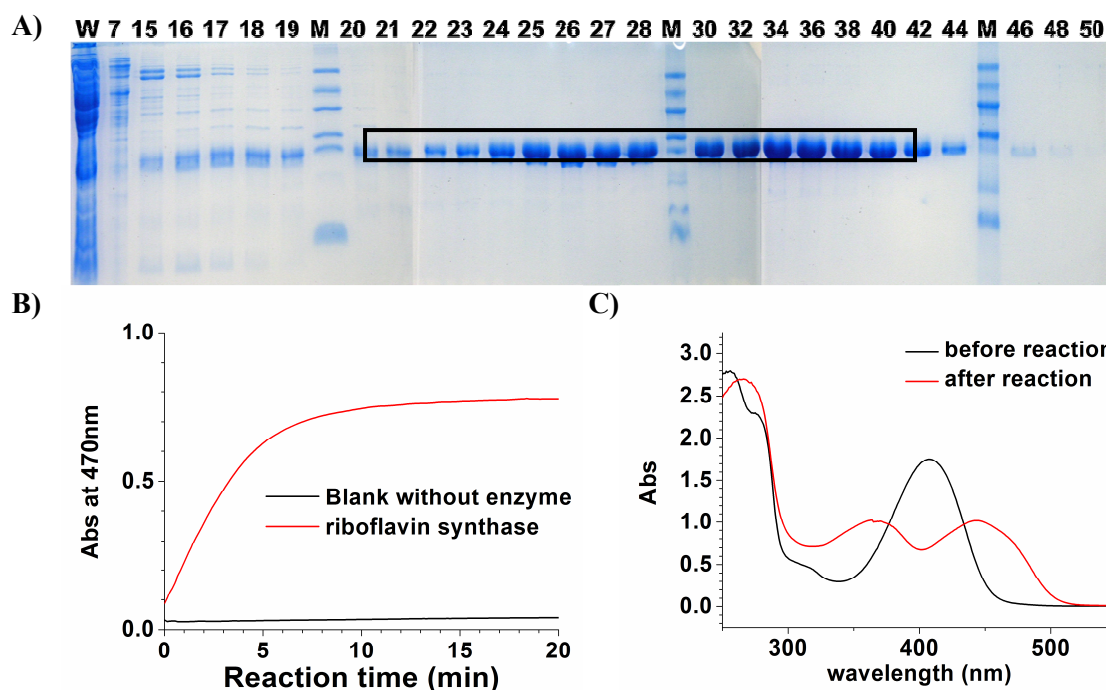


Figure 3.23 Analysis of recombinant riboflavin synthase. **A**) SDS-PAGE (W is flow through. M is protein size marker; lanes 7 to 50 are elution fractions, the target protein is indicated with black box), **B**) and **C**) testing of isolated protein for riboflavin synthase activity.

3.2.1.5 Flavokinase of *Schizosaccharomyces pombe*

The *fmn1* gene of *Schizosaccharomyces pombe* specifies a flavokinase (riboflavin kinase) comprising 163 amino acid residues. The recombinant plasmid (pNCO-FKSSP) containing *fmn1* gene of *S. pombe* was obtained from Dr. Monika Joshi (TUM, Munich, Germany). The recombinant riboflavin synthase is expressed efficiently in a recombinant *E. coli* strain and can be easily purified by ion exchange chromatography on Q-Sepharose column (see Methods 2.3.4.1.5). The resulting protein appeared approximately 80% pure, with an apparent subunit mass of 24 kDa as judged by SDS-PAGE (Figure 3.24, A).

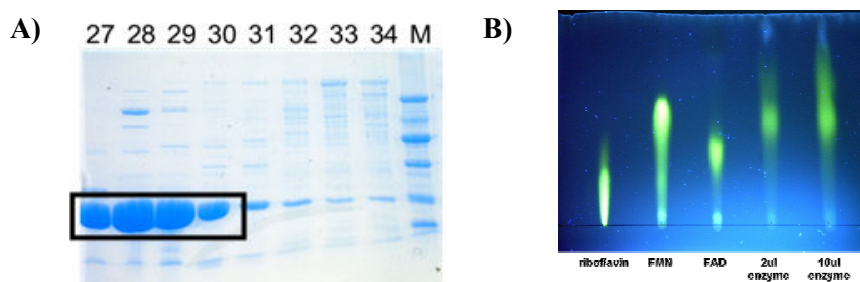


Figure 3.24 Purification of recombinant flavokinase. **A)** SDS-PAGE (M is protein size marker, Fractions 27 to 30 are contain flavokinase (black box), **B)** analysis of flavokinase reaction products.

The activity of flavokinase was confirmed by the conversion of riboflavin to FMN as shown in the Figure 3.24. The assay mixture (0.5 ml) contained 100 mM Tris (pH 8.0), 10 mM magnesium chloride, 0.1 mM riboflavin, 0.1 mM ATP and 2 μ l or 10 μ l flavokinase. The assay product was also monitored by TLC (prepared as described under methods 2.3.5.3).

3.2.1.6 Bifunctional Flavokinase/FAD synthetase of *Enterococcus faecalis*

The *ribF* gene of *E. faecalis* specifies a bifunctional flavokinase/FAD synthetase comprising 316 amino acid residues. The bifunctional flavokinase/FAD synthetase was amplified by PCR using oligonucleotides EFFADS-*Bam*HI and EFFADS-*Hind*III as primers (see Methods 2.3.1.7). The amplificate was digested with *Bam*HI and *Hind*III restriction enzymes and the resulting fragment was cloned into the vector pET22-HC, which had been treated with the same restriction enzymes. The vector pET22-HC contains a DNA fragment specifying a hisactophilin, an actin-binding protein of approximately 200 amino acids, 31 of them are histidine, as well as a TEV cleavage site (ENLYFQG). The recombinant chimeric gene for hisactophilin-bifunctional flavokinase/FAD synthetase (pET22-HCEFFADS) was expressed efficiently in a recombinant *E. coli* strain and resulting protein can be easily purified by Ni⁺-column chromatography due to the hisactophilin present at its the N-terminus

(see Methods 2.3.4.2). The recombinant chimeric protein appeared approximately 80 % pure, with an apparent subunit mass of 50 kDa as judged by SDS-PAGE (Figure 3.25).



Figure 3.25 Purification of the recombinant bifunctional flavokinase/FAD synthetase. (M is protein size, W1 and W2 are flow through from Ni⁺-column, fraction 18 to 34 are contain the bifunctional Flavokinase/FAD synthetase (black box))

The activity of flavokinase was determined by the conversion of riboflavin to FAD. The assay mixture (0.5 ml) contained 100 mM Tris (pH 8), 10 mM magnesium chloride, 0.1 mM riboflavin, 0.1 mM ATP and 10 µl bifunctional flavokinase/FAD synthase. Assays were performed at 30 °C for 20 min. Assay mixture were analyzed by TLC as described under methods 2.3.5.4. Under these conditions the flavokinase and FAD- synthetase activity of the enzyme has been confirmed (data not shown).

3.2.1.7 Enzyme storage

Each of the recombinant enzymes was concentrated by ultrafiltration and stored in 50 mM Tris-HCl (pH 7) containing 1 mM DTT and 0.02 % NaN₃ at -80 °C. Under these conditions, the enzymes did not lose activity after storage for 6 months.

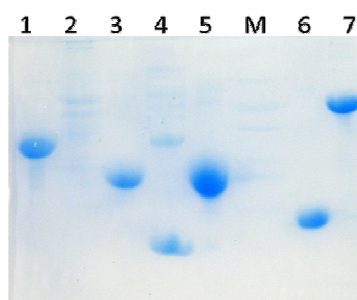


Figure 3.26 SDS-PAGE analyses of the enzymes used for enzyme-assisted riboflavin synthesis. 1, ribose kinase; 2, pentose phosphate isomerase (commercial protein); 3, 3,4-dihydroxy-2-butanone 4-phosphate synthase; 4; 6,7-dimethyl-8-ribityllumazine synthase; 5, riboflavin synthase; 6, Flavokinase; 7, FAD synthase; H, pyruvate kinase (commercial protein); M, protein size marker.

3.2.2 Preparation of 5-amino-6-ribitylamino-2,4(1*H*,3*H*)-pyrimidinedione (7)

5-Amino-6-ribitylamino-2,4(1*H*,3*H*)-pyrimidinedione (7) was prepared from 5-nitro-6-ribitylamino-2,4(1*H*,3*H*)-pyrimidinedione (33) as described by Dr. Klaus Kis [24]. The reaction mixture contained 0.1 M 5-nitro-6-ribitylamino-2,4(1*H*,3*H*)-pyrimidinedione (1.5 g) and 180 mg palladium/charcoal (10 %) resuspended in 50 ml D₂O in a 250 ml round-bottom flask was hydrogenated for 48 h at room temperature and atmospheric pressure. DTT was added to a final concentration of 100 mM and aliquots (2 ml) were stored at -80 °C [136].

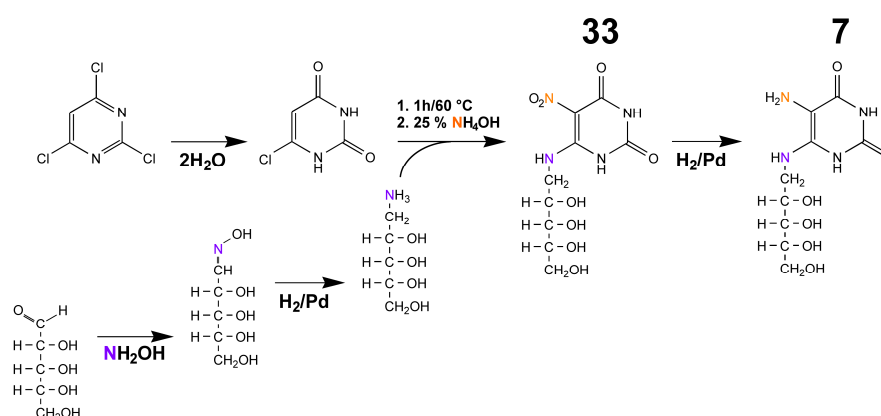


Figure 3.27 Preparation of 5-amino-6-ribitylamino-2,4(1*H*,3*H*)-pyrimidinedione (7).

The product yield was estimated enzymatically by conversion of 5-amino-6-ribitylamino-2,4(1*H*,3*H*)-pyrimidinedione (7) to 6,7-dimethyl-8-ribityllumazine. The reaction mixture (0.5 ml) contained 100 mM Tris 100 mM Tris-HCl (pH 7), 100 mM NaCl, 1 mM DTT, 0.02% NaN₃, 0.25 mM 3,4-dihydroxy-2-butanone 4-phosphate, and 0.5 mg 6,7-dimethyl-8-ribityllumazine synthase of *Bacillus subtilis*. A dilution series of the 5-amino-6-ribitylamino-2,4(1*H*,3*H*)-pyrimidinedione (7) obtained after hydrogenation, was prepared in order to determine the concentration of 7 (Figure 3.28). The mixture was incubated at 37 °C for 70 min and UV/VIS spectra were recorded thereafter (Figure 3.28). The reaction yield was around 70 %.

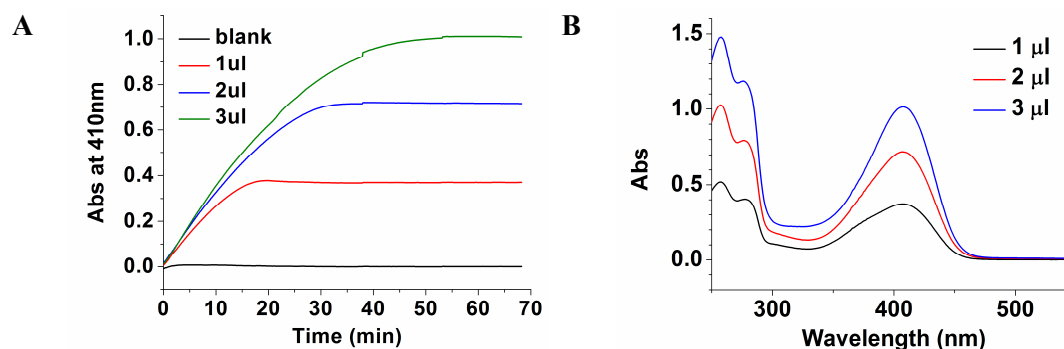


Figure 3.28 Analysis of synthesized 5-amino-6-ribitylamino-2,4(1*H*,3*H*)-pyrimidinedione. A, reaction mixture monitored photometrically at 410nm; B, UV/VIS spectral analysis of the final reaction product.

3.2.3 One-pot synthesis of riboflavin

These enzymes can be designed for efficient purification by affinity chromatography with acceptable purity. The concentrated enzymes were stored in 50 mM Tris-HCl (pH 7) containing 1 mM DTT and 0.02 % NaN_3 at 80 °C. Under these conditions, the enzyme did not lose activity after storage for 6 months. The final concentration of every enzyme, which is present in one-pot reaction mixture, was optimized by enzyme titration as shown in Figure 3.29. For every enzyme a dilution series was prepared as shown in Figure 3.29. As shown in Figure 3.29, the concentration of 3,4-dihydroxy-2-butanone-4-phosphate synthase (Figure 3.29, I) a limiting factor of the reaction already after a second dilution step. On the other hands, it is clear the concentration of ribose kinase (Figure 3.29, S) or pyruvate kinase (Figure 3.29, Q) at the beginning of titration is still very excessive and could be reduced by factor of 8, respectively.

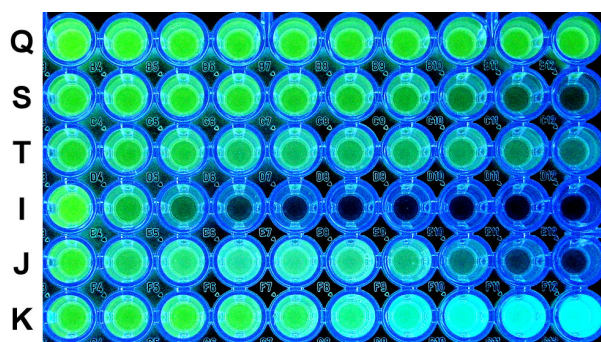


Figure 3.29 Titration of recombinant and commercially available enzymes for one-pot synthesis reaction. Rows: S = Ribose kinase, T = ribose-5-phosphate isomerase, I = 3,4-dihydroxy-2-butanone-4-phosphate synthase, J = 6,7-dimethyl-8-ribityllumazine, E = riboflavin synthase, Q = pyruvate kinase. Enzymes were titrated in well from left to right with a dilution step 1:2.

When the optimized one-pot reaction was scaled up to 50 ml, the unexpected absorption band (340 nm) was detected in the UV/VIS spectrum of the reaction mixture. It was observed in reaction mixtures designed for the production of 6,7-dimethyl-8-ribityllumazine (Figure 3.30) or riboflavin (Figure 3.31). This absorbance band increased with incubation time (black arrows in Figure 3.30 and 3.31). The reaction mixture subsequently was analyzed by TLC.

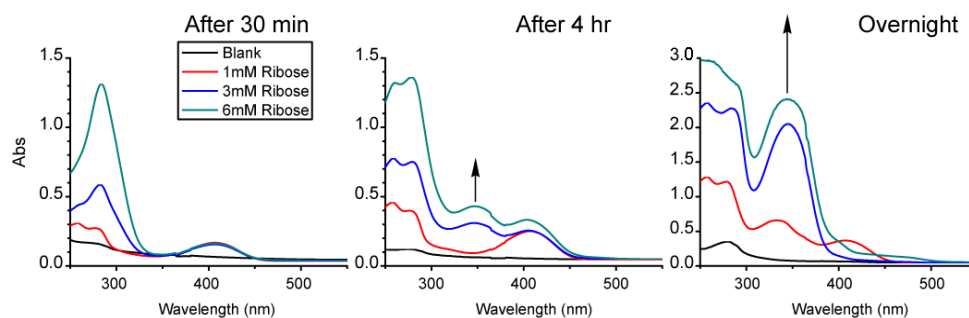


Figure 3.30 UV/VIS spectra of 6,7-dimethyl-8-ribityllumazine synthase reaction mixture producing reaction mixture taken in the course of fraction.

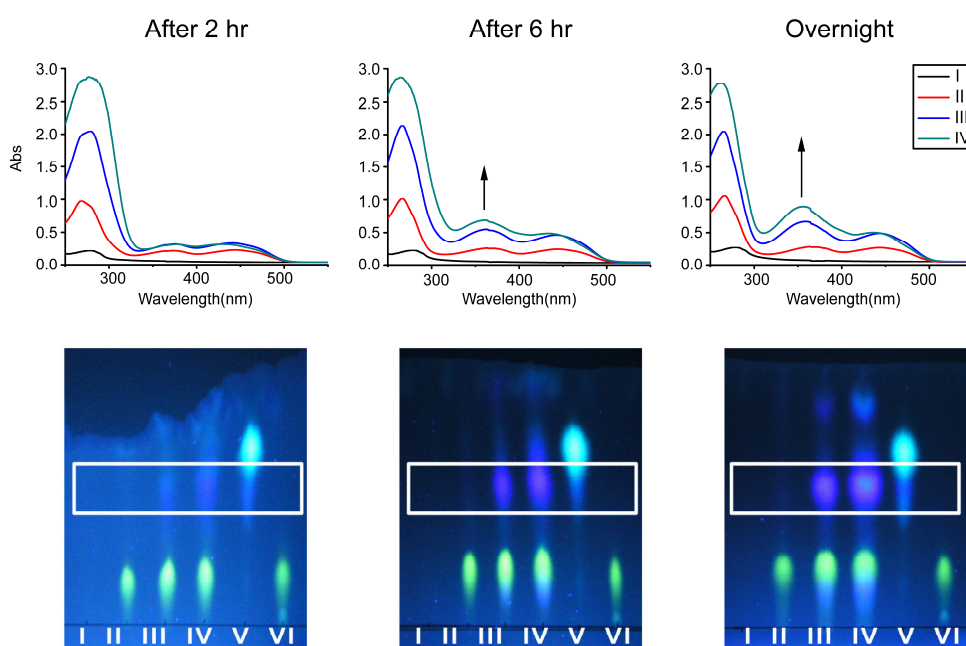


Figure 3.31 One-pot riboflavin synthesis. Top, UV/VIS spectra taken in the course of reaction; bottom, TLC analysis. I, reaction without ribose; II, reaction with 1 mM ribose; III, reaction with 3 mM ribose; IV, reaction with 6 mM ribose; V, 6,7-dimethyl-8-ribityllumazine standard; VI, riboflavin standard. White box indicates an additional fluorescent spot presumably 5-nitro-6-ribitylamino-2,4(1*H*,3*H*)-pyrimidinedione..

5-Amino-6-ribitylamino-2,4(1*H*,3*H*)-pyrimidinedione can be easily oxidized [137, 138]. We assumed that oxidation of 5-amino-6-ribitylamino-2,4(1*H*,3*H*)-pyrimidinedione takes place in the one-pot reaction mixture and resulting compound, 5-nitro-6-ribitylamino-2,4(1*H*,3*H*)-pyrimidinedione, inhibits 6,7-dimethyl-8-ribityllumazine synthase diminishing the reaction yield. When the reaction was run under oxygen-free conditions in a glove box, no 5-amino-6-ribitylamino-2,4(1*H*,3*H*)-pyrimidinedione remained at the end of incubation. Moreover, it has been shown that the high reaction yield remained the same in the temperature interval between 25 °C to 37 °C (around 80 %) (Figure 3.32).

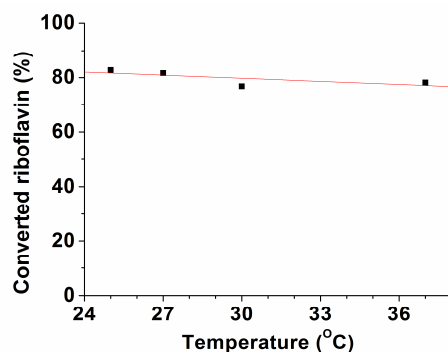


Figure 3.32 Temperature dependence of riboflavin yield.

3.2.4 Preparation of deuterated riboflavin

The overall reaction comprises five enzyme-catalyzed reaction steps for the synthesis of riboflavin (**11**), namely ribose kinase (**S**), ribose phosphate isomerase (**T**), 3,4-dihydroxy-2-butanone 4-phosphate synthase (**I**), 6,7-dimethyl-8-ribityllumazine synthase (**J**) and riboflavin synthase (**K**). Moreover, the overall reaction contains pyruvate kinase for the recycling of ADP (Figure 3.33).

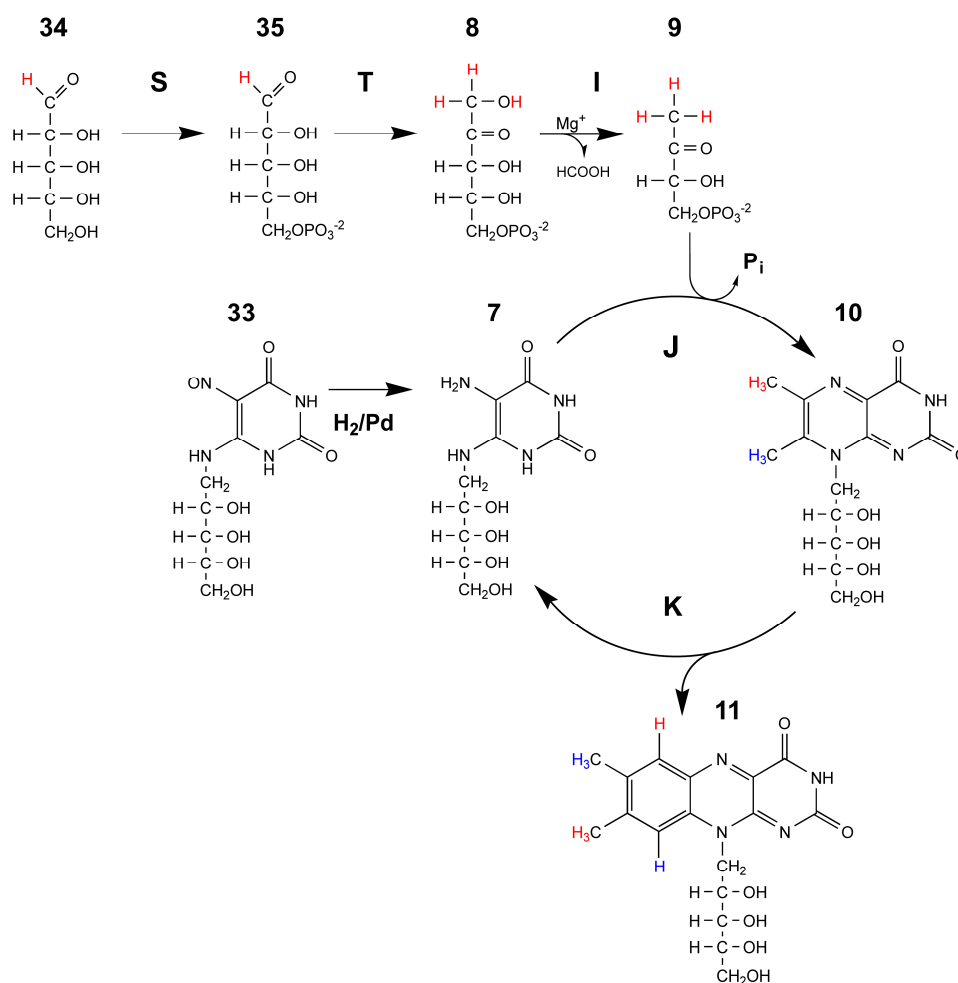


Figure 3.33 Enzymatic syntheses of deuterated riboflavin.

3.2.4.1 Attempted synthesis of [6,8 α - $^2\text{H}_2$]riboflavin

An attempt was made to prepare [6,8 α - $^2\text{H}_2$]riboflavin from [1- $^2\text{H}_1$]ribose using an approach resembling 2.3.5.2.1. The basic idea was to convert [1- $^2\text{H}_1$]ribose into [1- $^2\text{H}_1$]3,4-dihydroxy-2-butanone 4-phosphat that should then be converted rapidly *in situ* into [6- $^2\text{H}_1$]6,7-dimethyl-8-ribityllumazine. Treatment with riboflavin synthase should then afford the desired riboflavin isotopologue. For reasons that are as yet not understood, the deuterium label was lost in transit, and only unlabeled riboflavin was formed. One of the reason for failed labeling of riboflavin could be that ribose isomerase, the enzyme that catalyze interconversion of D-ribose 5-phosphate to D-ribulose 5-phosphate is too fast in comparison with the enzymes catalyzing downstream reaction steps. As the consequence, the deuterium at C-1 of the proffered D-ribose could be washed out and replaced by protium at this reaction step.

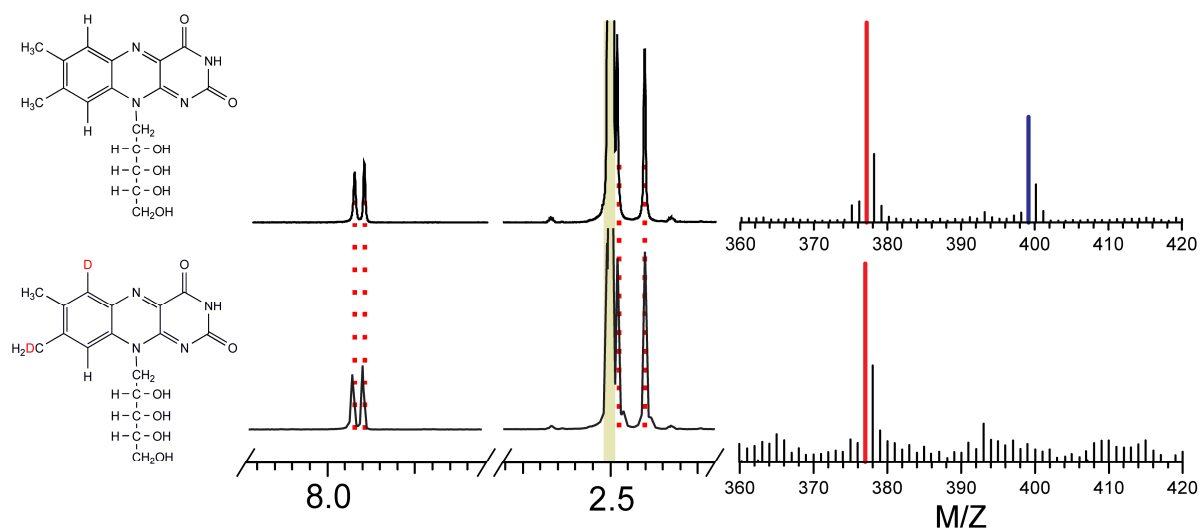


Figure 3.34 NMR and mass spectra of authentic riboflavin (top) and riboflavin synthesized from [1- $^2\text{H}_1$]ribose (bottom). Expected labeling pattern of riboflavin is shown in the left part, ^1H -NMR spectra in the middle part, FAB mass spectra in the right part of the Figure. Red lines in mass spectrum indicate $[\text{M}+\text{H}]^+$ signal and blue lines indicate $[\text{M}+\text{Na}]^+$ signal.

According to ^1H -NMR spectrum and FAB mass spectrum, there is no difference between the unlabeled riboflavin and riboflavin synthesized from [1- $^2\text{H}_1$]ribose (Figure 3.34). ^1H -NMR signals from H-6 and H-8 α are present in the ^1H -NMR spectrum and their relative integration value had no change by comparison with unlabeled riboflavin. Moreover, FAB mass spectrum revealed in that case a signal of 267.2 Daltons (Figure 3.34).

3.2.4.2 Preparation of [6,7 α ,8 α ,9-²H₈]riboflavin

It is convenient to perform all reactions simultaneously as a one-pot reaction (Method 2.3.5.2.2). The one-pot enzyme-assisted reaction was scaled up to 50 ml volume. D₂O was used as reaction solvent instead of H₂O and 5 mM D-ribose (37.5 mg) was used as starting material. Incubation of the reaction mixture for 48 hours at room temperature in an oxygen-free atmosphere afforded deuterated riboflavin (2.3 mM; 43.2 mg) with a yield of 45 % based on the proffered D-ribose. As shown in the Figure 3.35, the product contained mainly riboflavin (white box), unreacted substrate 5-amino-6-ribitylamino-2,4(1*H*,3*H*)-pyrimidinedione, and some minor fluorescent bands (blue fluorescence on the TLC; Figure 3.35, A). To remove the contaminants, riboflavin was recrystallized and purified using cation exchange chromatography (Dowex 50 WX8).

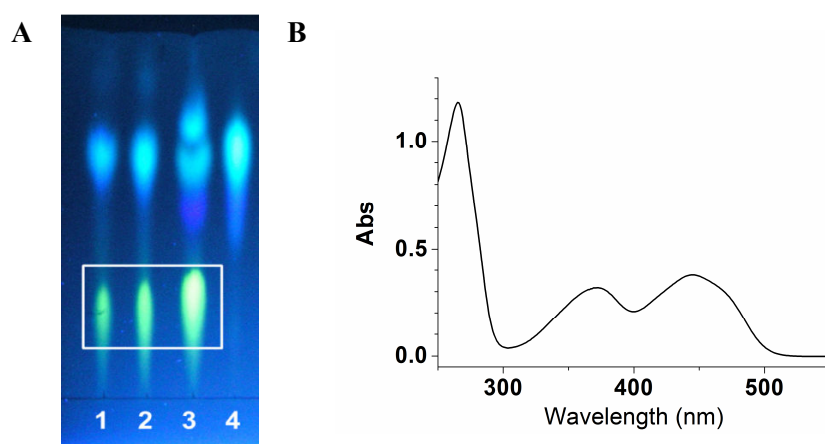


Figure 3.35 TLC chromatogram (A) and UV/VIS spectrum of the [6,7 α ,8 α ,9-²H₈]riboflavin (B). **1**, after 1.5 hr reaction product; **2**, after 3 hr reaction product; **3**, after 24 hr reaction product; **4**, 6,7-dimethyl-8-ribityllumazine standard; white box, riboflavin (A).

The riboflavin molecule comprises 20 hydrogen atoms that can be classified into two groups according to the exchangeability. Fifteen nonexchangeable hydrogen atoms are bound to carbon. The five hydrogen atoms bound at heteroatoms (NH-3, OH-2', 3', 4', 5') are exchangeable. The product of the one-pot riboflavin synthesis reaction in D₂O solvent should be therefore [3,6,7 α ,8 α ,9,2',3',4',5'-²H₁₃]riboflavin. At the last reaction step (conversion of lumazine to riboflavin) exchangeable deuteriums can be replaced by hydrogen. Therefore, the isolated product should be [6,7 α ,8 α ,9-²H₈]riboflavin (**8**). The labeling pattern of produced riboflavin was characterized by FAB mass spectrometry and ¹H-NMR spectrometry using [U-¹H₂₀]riboflavin as unlabeled standard (Figure 3.36). Four signals of H-7 α (2.39 ppm), H-8 α (2.47 ppm), H-6 (7.86 ppm), H-9 (7.9 ppm) are not present in the ¹H-NMR spectrum of synthesized riboflavin (Figure 3.36). On the FAB mass spectrum, the signal for riboflavin was detected at 376.2 Daltons and for deuterated [6,7 α ,8 α ,9-²H₈]riboflavin (**8**) as expected at 384.1 Daltons (8 Daltons higher than riboflavin) (Figure 3.36).

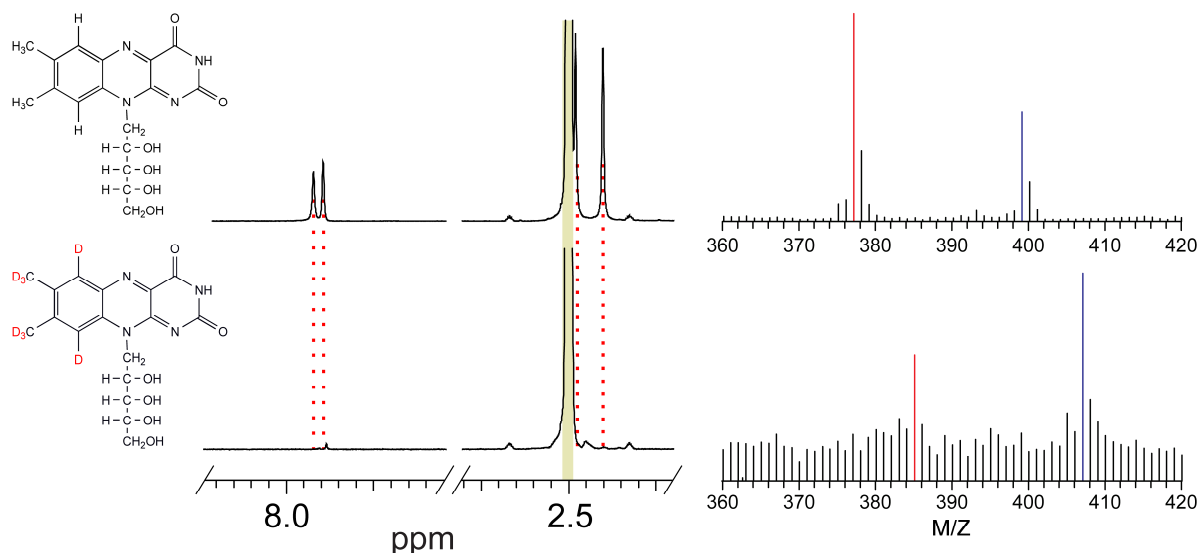


Figure 3.36 NMR and mass spectra of unlabeled riboflavin (top) and synthesized $[6,7\alpha,8\alpha,9-^2\text{H}_8]$ riboflavin (bottom). Labeling pattern of riboflavin is shown in the left part, ^1H -NMR spectra are shown in the middle part, FAB mass spectra are shown in the right part. Red lines in the mass spectrum indicate $[\text{M}+\text{H}]^+$ signal, blue lines indicate $[\text{M}+\text{Na}]^+$ signal.

3.2.4.3 Preparation of $[7\alpha,9-^2\text{H}_4]$ riboflavin

The hydrogen atoms bound at C-7 α (blue hydrogen atoms in Figure 3.33) of 6,7-dimethyl-8-ribityllumazine (**7**), which serves as the direct biosynthetic precursor of riboflavin, can be non-enzymatically exchanged with the solvent D_2O [139] and this exchange is accelerated by riboflavin synthase. $[7\alpha-^2\text{H}_3]$ 6,7-Dimethyl-8-ribityllumazine was subjected to dismutation by riboflavin synthase (**E**) affording one molecule of $[7\alpha,9-^2\text{H}_4]$ riboflavin and one molecule of 5-amino-6-ribitylamino-2,4-pyrimidinedione (**6**) (Figure 3.33). During deuterium exchange, the color of the solution slowly changed to brown, probably due to autoxidation. It is therefore preferable to perform the exchange and the enzyme treatment under anaerobic conditions. The product, $[7\alpha,9-^2\text{H}_4]$ riboflavin, precipitates from the reaction mixture and can be harvested by centrifugation. The yield is around 90 %. The crude product can be purified by recrystallization from.

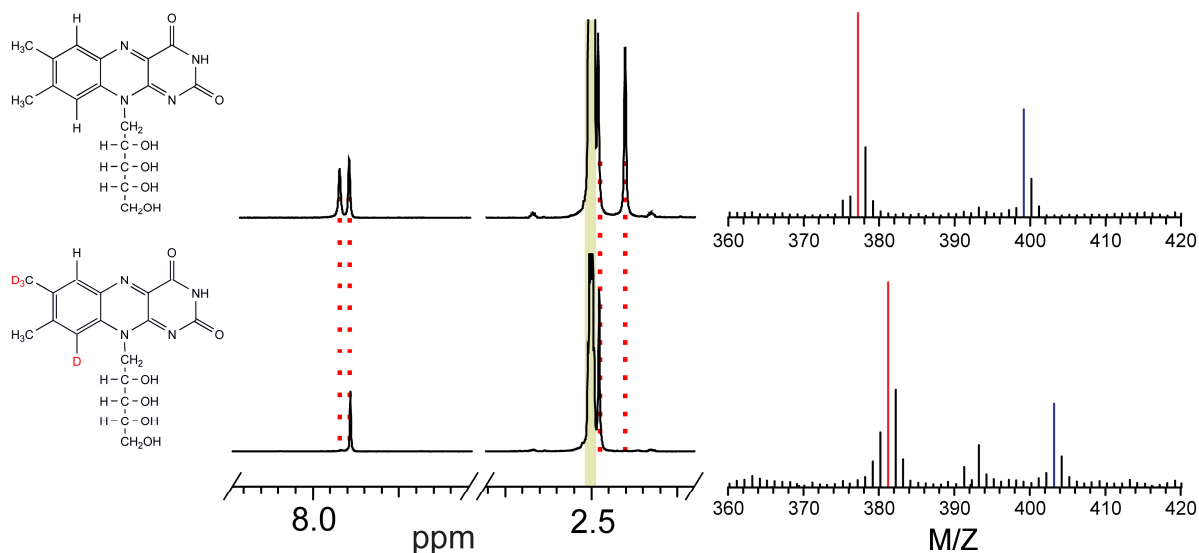


Figure 3.37 NMR and mass spectra of unlabeled riboflavin (top) and synthesized $[7\alpha,9-^2\text{H}_4]$ riboflavin (bottom). Labeling pattern of riboflavin is shown in the left part, ^1H -NMR spectra are shown in the middle part, FAB mass spectra are shown in the right part. Red lines in mass spectrum indicate $[\text{M}+\text{H}]^+$ signal and blue lines indicate $[\text{M}+\text{Na}]^+$ signal.

NMR and mass spectrometry data confirmed that the final product is $[7\alpha,9-^2\text{H}_4]$ riboflavin. The signal of H-7 α (2.39 ppm), 9 (7.9 ppm) were not observable in the ^1H -NMR spectrum (Figure 3.37). On the FAB mass spectrum, riboflavin was detected at 376.2 Daltons and synthesized riboflavin was detected at 380.2 Daltons (4 Daltons heavier than unlabeled riboflavin) (Figure 3.37).

3.2.4.4 Preparation of $[6,8\alpha-^2\text{H}_4]$ riboflavin

$[6,8\alpha-^2\text{H}_4]$ Riboflavin was obtained by a combination of the methods described above. $[6\alpha,7\alpha-^2\text{H}_6]$ 6,7-Dimethyl-8-ribityllumazine (prepared according to 3.2.4.2) was used as starting material. Treatment with water resulted in the removal of deuterium from the 7 α methyl group. The resulting $[6\alpha-^2\text{H}_3]$ 6,7-dimethyl-8-ribityllumazine was then converted to riboflavin by treatment with riboflavin synthase. More specifically, $[6\alpha,7\alpha-^2\text{H}_6]$ 6,7-dimethyl-8-ribityllumazine (prepared according to 3.2.4.2) was obtained from ribose and 5-amino-6-ribitylamino-2,4(1*H*,3*H*)-pyrimidinedione as substrates and the reaction yield was about 50 % based on the proffered ribose. The reaction product was treated with water under anaerobic conditions for 2 days. Riboflavin synthase was then added in order to convert the resulting $[6\alpha-^2\text{H}_3]$ 6,7-dimethyl-8-ribityllumazine into riboflavin. The second step involved the loss of about 50 % of the 6,7-dimethyl-8-ribityllumazine intermediate for unexplained reasons (Figure 3.38).

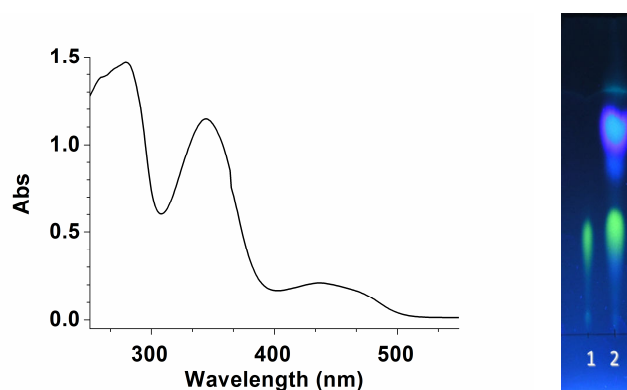


Figure 3.38 Optical spectrum (left part) and TLC analysis (right part) of synthesized [6,8 α - $^2\text{H}_4$]riboflavin in reaction mixture.

The synthesized product, [6,8 α - $^2\text{H}_4$]riboflavin, was purified by HPLC using a RP18 (250 \times 4 mm, 5 μl) column. Riboflavin was eluted with 40 % of methanol after 4 min (1 ml/min flow) (Figure 3.39).

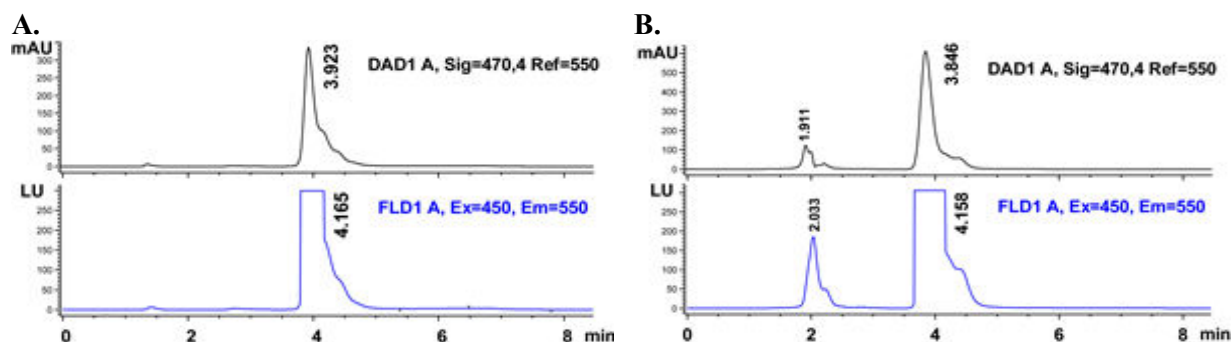


Figure 3.39 Purification by HPLC of unlabeled riboflavin (**A**) and [6,8 α - $^2\text{H}_4$]riboflavin (**B**). Purification was monitored with diode array detection (DAD) (black line) at 470 nm and fluorescence detection (FLD) with excitation at 450 and emission at 550 nm (blue line).

UV/VIS spectrum (Figure 3.40) indicated that [6,8 α - $^2\text{H}_4$]riboflavin purified by HPLC should be very pure (> 90 %). The synthesized riboflavin sample was lyophilized and dissolved in 99 % DMSO for ^1H -NMR measurements.

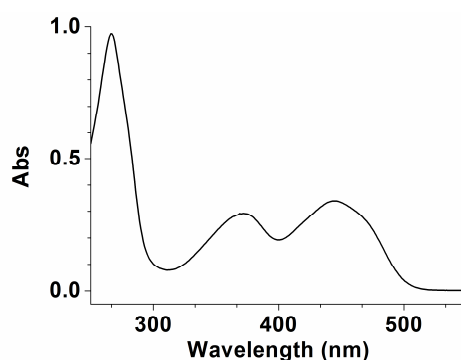


Figure 3.40 UV/VIS spectrum of [6,8 α - $^2\text{H}_4$]riboflavin after purification.

The yield of purified $[6,8\alpha\text{-}^2\text{H}_4]$ riboflavin was only 3 mg. However, FAB mass spectrometry confirmed the structure of the product as $[6,8\alpha\text{-}^2\text{H}_4]$ riboflavin. The riboflavin signal was detected at 376.2 Daltons and deuterated riboflavin was detected at 380.2 Daltons (4 Daltons bigger than riboflavin) (Figure 3.41).

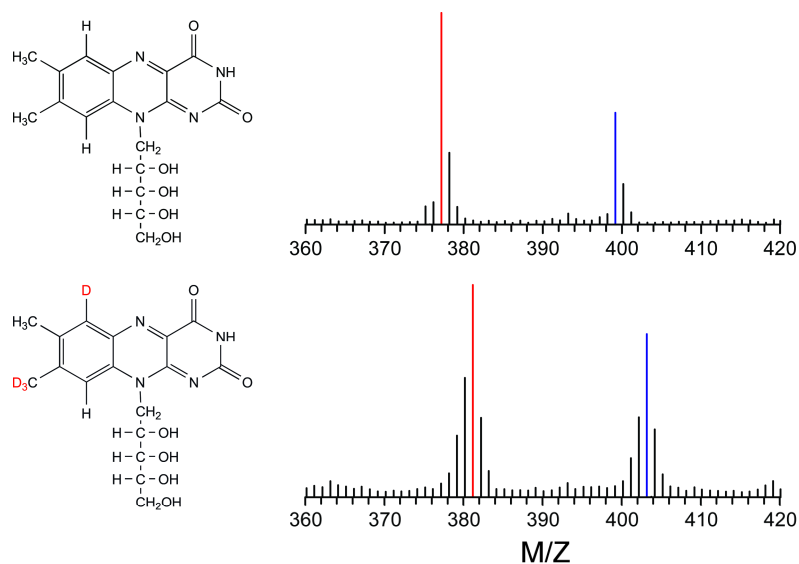


Figure 3.41 Mass spectra of unlabeled riboflavin (top) and synthesized $[6,8\alpha\text{-D}_4]$ riboflavin (bottom). Labeling pattern of riboflavin is shown in the left part, FAB mass spectra are shown in the right part. Red lines in mass spectrum indicate $[M+H]^+$ signal and blue lines indicate $[M+Na]^+$ signal.

Table 3.7 Data of FAD mass spectrometry of riboflavin isotopologues (M/Z).

	Riboflavin	[6,8 α - ² H ₂] riboflavin	[7 α ,9- ² H ₄] riboflavin	[6,8 α - ² H ₄] Riboflavin	[6,7 α ,8 α ,9- ² H ₈] Riboflavin
[M+H] ⁺	377.2	377.2	381.2	381.2	385.1
[M+Na] ⁺	399.2	-	403.2	403.2	407.1
Mass	376.2	376.2	380.2	380.2	384.1

Table 3.8 ¹H-NMR chemical shifts of riboflavin isotopologues. Internal standard is DMSO (2.5 ppm).

H position	Riboflavin		[7 α ,9- ² H ₄]riboflavin		[6,7 α ,8 α ,9- ² H ₈]riboflavin	
	ppm	Integration	ppm	Integration	ppm	Integration
7 α	2.39	2.74	-		-	
8 α	2.47	3.00	2.48	3.19	-	
5	3.46	1.05	3.46	1.28	3.49	1.01
3', 4', 5'a	3.64	3.01	3.63	3.50	3.63	2.77
2'	4.26	1.00	4.26	1.24	4.24	1.01
5'-OH	4.47	1.00	4.48	0.84	-	
1'a	4.62	0.95	4.62	1.20	4.63	0.96
2'-OH	4.79	1.00	4.79	0.86	-	
4'-OH	4.8	1.01	4.86	0.82	-	
1'b	4.92	0.96	4.93	1.21	4.91	1.05
3'-OH	5.10	1.00	5.11	0.82		
6	7.86	0.99	7.86	1.00	-	
9	7.90	1.00	-		-	
3	11.32	0.95	11.30	0.81	-	

3.3 LOV2 domain from *Avena sativa*

Prof. Stefan Weber, Dr. Erik Schleicher (Albert-Ludwigs-Universität Freiburg, Freiburg, Germany) and coworkers have studied the temperature dependence of the 1H ENDOR spectra of LOV2 domains.

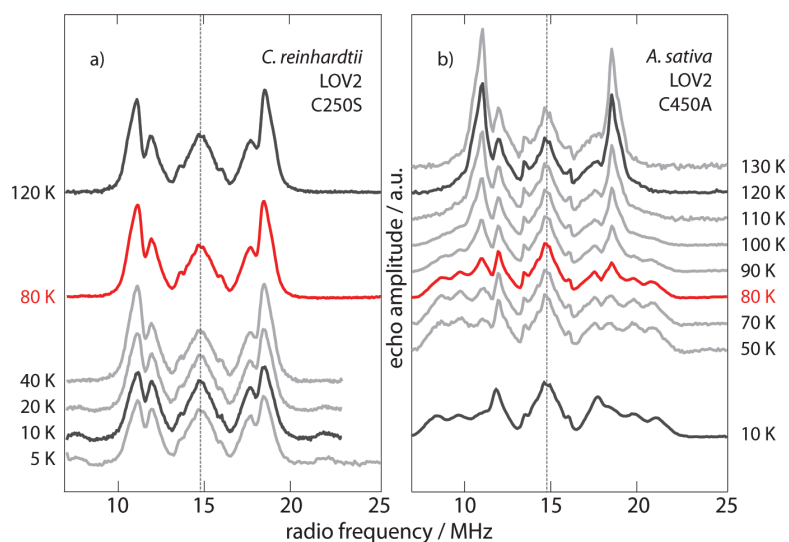


Figure 3.42 Temperature series of pulsed X-band proton ENDOR spectra obtained from different LOV sample. In each panel, the spectra at 120, 80 and 10 K are highlighted in order to emphasize the very different temperature behavior of (a) the *Cr*LOV2 C250S neutral radical and (b) the *As*LOV2 C450A neutral radical (from Richard, 2010 [140]).

The data revealed unexpected differences between LOV2 domains from *Avena sativa* (oats) and *Chlamydomonas reinhardtii*. The authors suggested that the rotation of the position 8 methyl group of the protein-bound FMN radical of *A. sativa* starts to freeze out at about 100 K, whereas this process starts at much lower temperatures in the *C. reinhardtii* protein. Whereas the protein domains from the two different organisms show the same protein fold, some amino acids in the vicinity of the 8-methyl group of the bound cofactor are different, and the different temperature behavior was tentatively ascribed to these differences. Studies with mutants of the *A. sativa* protein appeared to support this interpretation.

In order to further investigate the supposed correlation between the rotational properties of the flavin cofactor's methyl group and the temperature characteristics of the ENDOR signal, it was desirable to modify the physical character of the methyl group *per se*. More specifically, the angular momentum of the methyl group can be increased by the substitution of the hydrogen atoms by deuterium. Moreover, since carbon-deuterium bonds are slightly shorter than carbon-hydrogen bonds, the replacement of hydrogen by deuterium should result in a slight contraction of the methyl substituent. The deuterated riboflavin samples whose synthesis has been described in the previous passage can now be used for this purpose.

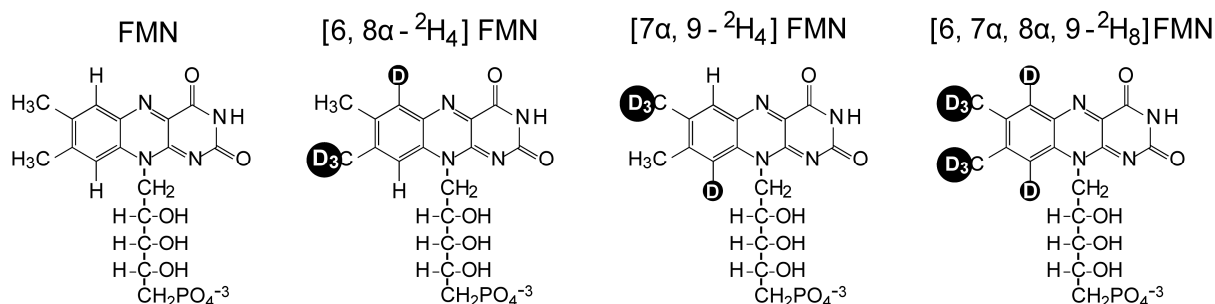


Figure 3.43 FMN isotopologues used for reconstitution of LOV domain.

The deuterated riboflavin (3 mg) samples were incubated in 20 ml of buffer which is already containing 100 mM Tris-HCl, pH 7.0, 20 mM magnesium chloride, 0.02 % sodium azide, 5 mM DTT, 0.5 mM ATP, 6 mM phosphoenol pyruvate, 0.5 mM riboflavin or isotope-labeled riboflavin, 1 unit of inorganic pyrophosphatase from baker's yeast (Sigma), 5 units of pyruvate kinase from rabbit muscle (Sigma) and 2 mg flavokinase (see Method 2.3.5.3). Riboflavin and riboflavin isotopologues were converted to FMN by treatment with riboflavin kinase. The resulting deuterated FAD isotopologues (Figure 3.43) were then incorporated into LOV domains. The protein-cofactor complexes are currently under investigation in the research group of Prof. Stefan Weber in Freiburg.

3.3.1 Isolation and reconstitution of LOV2 domain from *Avena sativa*

The hisactophilin-LOV2 fusion proteins were expressed efficiently in a recombinant *E. coli* strain. Due to many histidine residues present in the hisactophilin domain, the fusion protein can be purified on Ni⁺-column. After loading the fusion protein to a Ni⁺-column, which was washed with buffer containing 6 M guanidine-HCl to release protein-bound FMN, and the resulting apoprotein was reconstituted on the column with one of the FMN isotopologues, The reconstituted protein was then eluted from the column with imidazole (see Methods 2.3.5.3).

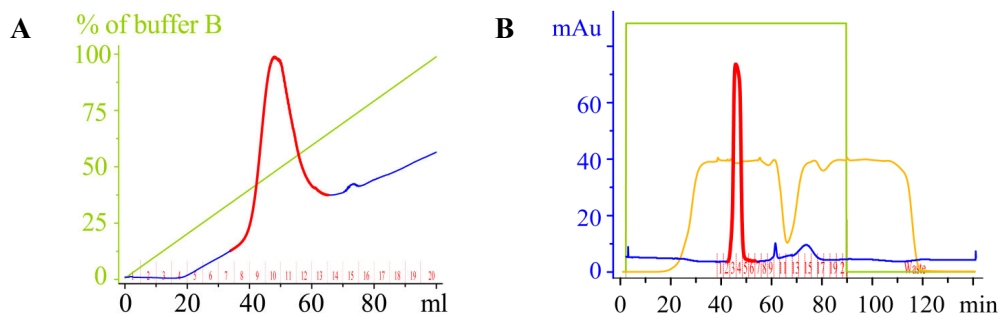


Figure 3.44 Purification of LOV2 C450A domain by nickel affinity chromatography; elution from the Ni⁺-column (A) and elution from desalting column (B). (the desired fractions with protein).

The eluent was treated with thrombin in order to split the fusion protein. The resulting protein mixture was passed again through a Ni⁺-column. Whereas LOV2 domain passed the column, the hisactophilin part remained bound. The eluent was passed thereafter through a desalting column in order to transfer the reconstituted LOV2 domain to the appropriate buffer. The SDS-PAGE of the purified protein is shown in Figure 3.44, **B**. The fusion protein of hisactophilin and LOV2 wild type long clone domain from *A. sativa* contains 288 amino acids and has a mass of about 27 kDa (black box in Figure 3.44). After thrombin cleavage, the remaining LOV2 domain part contained 160 amino acids and had a molecular mass of about 14 kDa (red box in Figure 3.45).

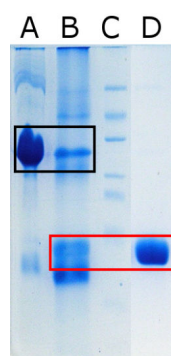


Figure 3.45 SDS polyacrylamide gel (15 %); A, Fusion protein of hisactophilin and LOV2 wild type domain from *A. sativa*; B, same after thrombin cleavage; C; protein marker (66 kDa, 45 kDa, 36 kDa, 30 kDa, 20 kDa, 13 kDa); D, purified LOV2 domain from *A. sativa*.

3.3.2 Optical spectroscopy of LOV2 domain from *Avena sativa*

The recombinant LOV2 C450A long clone of *A. sativa* has absorbance maxima at 378 and 447 nm, characteristic for FMN in the oxidized state (Figure 3.46). Shoulders at 422 and 474 nm are vibrational contributions that are well resolved. This is indicative of tight binding between the noncovalently bound FMN, and the highly ordered protein structure, as well as of the nonpolar nature of the flavin binding pocket.

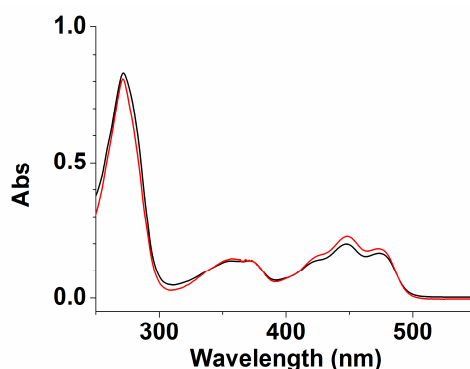


Figure 3.46 Optical spectra of the fusion protein hisactophilin plus either LOV2 C450A long clone domain from *A. sativa* (black) or LOV2 C450A long clone domain from *A. sativa* (red).

3.3.3 ENDOR spectroscopy of LOV2 domain from phototropin of *Avena sativa*

ENDOR spectra of the LOV domains reconstituted with partially deuterated FMN were measured by Richard Brosi (Freie Universität Berlin, Berlin, Germany) and Dr. Erik Schleicher (Albert-Ludwigs-Universität Freiburg, Freiburg, Germany) (Figure 3.47 and 3.48).

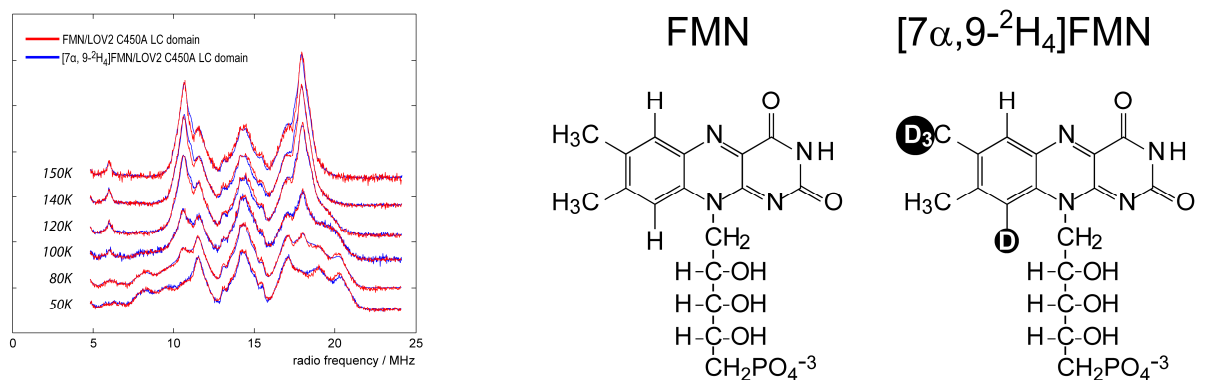


Figure 3.47 Temperature series of pulsed X-band ENDOR spectra obtained with LOV2 C450A long clone domain *A. sativa* complexes with FMN (red) or [7 α ,9- 2 H $_4$]FMN (blue), temperature of 50, 80, 100, 120, 140 and 150K (spectra were measured by Richard Brosi (Freie Universität Berlin, Berlin, Germany) and Dr. Erik Schleicher (Albert-Ludwigs-Universität Freiburg, Freiburg, Germany)).

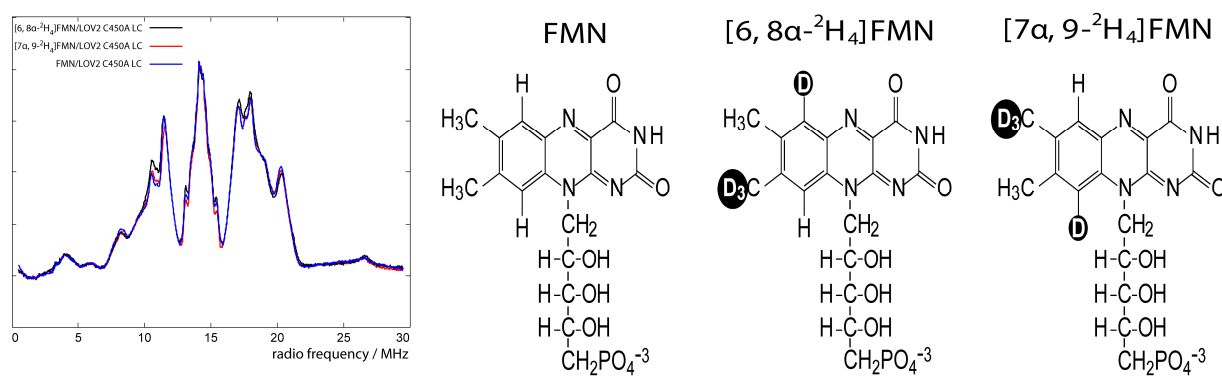


Figure 3.48 Pulsed X-band proton Davies 2 H ENDOR spectra of LOV2 C450A LC domain complexes with FMN (blue), [6,8 α - 2 H $_4$]FMN (black) and [7 α ,9- 2 H $_4$]FMN (red) at 80 K (spectra were measured by Richard Brosi (Freie Universität Berlin, Berlin, Germany) and Dr. Erik Schleicher (Albert-Ludwigs-Universität Freiburg, Freiburg, Germany)). Differences between the traces are valid and experimentally significant but have yet to be interpreted in more detail.

This work in progress has already established that (i) 2 H ENDOR signals can be recorded with LOV domains carrying methyl-deuterated FMN and (ii) at least some changes have already been observed for the temperature characteristic of the 1 H ENDOR spectra of partially deuterated samples.

Assigning the vibrational spectra of protein-bound FAD in the ground state and the optically excited S1 state

3.4 BLUF domain from *Rhodobacter sphaeroides*

3.4.1 Preparation of isotope-labeled FAD and AppA_{BLUF}

[U-¹⁵N₄]FAD, [U-¹³C₁₇]FAD, [6,7,7 α ,8 α ,9,9 α -¹³C₈]FAD, [2-¹³C₁]FAD, [4,10 α -¹³C₂]FAD and [4-¹⁸O₁]FAD were prepared by treatment of the cognate riboflavin isotopologues with the bifunctional flavokinase/FAD synthase of *Enterococcus faecalis* (Methods 2.3.5.4). The treatment products were isolated by HPLC. The purified FAD samples were lyophilized. The purity was more than 90 % as judged by TLC analysis. Final FAD samples were lyophilized and shipped to the laboratory of Prof. Peter Tonge (Stony Brook University, Stony Brook, New York, USA).

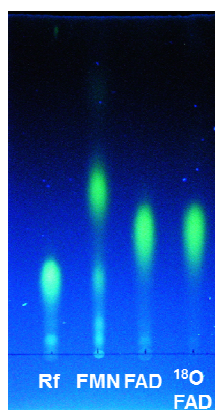


Figure 3.49 TLC analyses of purified flavin isotopologues.

The recombinant AppA_{BLUF} from *Rhodobacter sphaeroides* is a relatively hydrophobic protein. Specially, the flavin binding pocket of the AppA_{BLUF} is lined by very hydrophobic side chains (Y21, L34, I37, V38, A43, G52, L54, Y56, F61, L65, V75, M76, I79, V88, I90, W104), with a few polar or charged residues (Q63, Q42, Q80, and H85) that could be important for establishing of specific contacts with the flavin ligand. From these residues, almost all are conserved within the BLUF domain family, suggesting that they specifically involved in flavin binding.

As shown in Figure 3.50, most of the overexpressed AppA_{BLUF} protein forms inclusion bodies. Attempts to exchange the FAD cofactor of recombinant AppA_{BLUF} protein after partial denaturation with urea or guanidine-HCl were unsuccessful. The labeled FAD samples were therefore sent to the laboratory of Prof. Peter Tonge (Stony Brook University, New York, USA), where they were incorporated into AppA_{BLUF} protein under non-denaturing conditions.

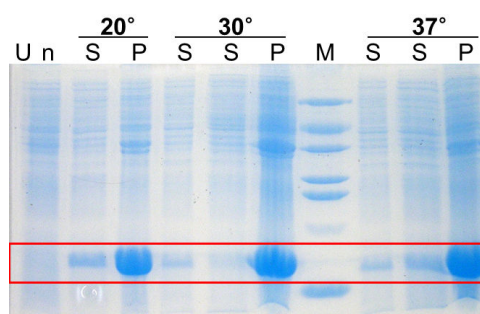


Figure 3.50 Expression of the AppA_{BLUF} from *Rhodobacter sphaeroides* at different cultivation temperatures (20, 30 and 37 °C). M indicates protein size marker, Un and S indicate crude extract obtained from un-induced cell, respectively, induced *E. coli* culture. P indicates respective cell pellet. Box indicates a gel region characteristic for the target protein.

3.4.2 Time-resolved infrared spectroscopy of FAD and BLUF domain

The reconstituted BLUF domains were used for ultrafast time resolved infrared (TRIR) spectroscopy. These measurements were performed in the laboratory of Prof. Stephen R. Meech (University of East Anglia, Norwich, UK). The main results obtained in the partner group are only summarized briefly below.

The TRIR spectra of dark (dAppA_{BLUF}) and light-adapted (lAppA_{BLUF}) AppA_{BLUF} contain a wealth of information on the early structural changes that accompany protein photoexcitation [93]. Isotope-labeling of FAD and riboflavin has enabled the assignment of various ground and excited state modes seen in the TRIR spectra of AppA_{BLUF} (data from Allison Haigney, Stony Brook University, New York, USA). In Figure 3.51 the transient vibrational spectra at a 3 ps time delay after excitation of FAD and [2-¹³C₁]-FAD are shown and compared with DFT calculations of the ground state IR transmission spectrum. Experimental data were recorded in H₂O and calculations were made with a proton at N3. The experimental spectra in Figure 3.51 are difference spectra of the excited state minus un-excited (ground) state transmission where the negative modes are associated with loss of the ground state and referred to as bleaches and the positive modes are associated with the newly generated excited state. The main observed effect of isotopic substitution is a shift in the band with the second highest frequency from 1663 cm⁻¹ to 1625 cm⁻¹.

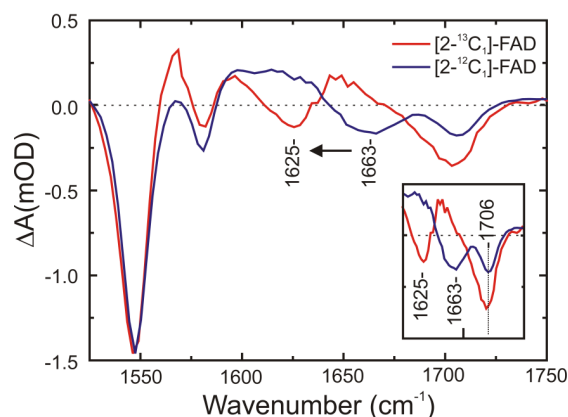


Figure 3.51 TRIR and calculated spectra of unlabeled FAD and $[2-^{13}\text{C}_1]$ -FAD in H_2O . FAD concentration was 6 mM in phosphate buffer, pH 8, and the TRIR spectra were recorded with a time delay of 3 ps (the spectrum was measured by Allison Haigney [85]).

The TRIR spectra of $[\text{U}-^{13}\text{C}_{17}]$ -FAD are shown in Figure 3.52. The 1700 cm^{-1} bleach assigned to the $\text{C4}=\text{O}$ is shifted by 40 wavenumbers to 1660 cm^{-1} which is in agreement with data obtained for the $[4,10\text{a}-^{13}\text{C}_2]$ isotopologue where this bleach appears at 1664 cm^{-1} . In addition to the effect on the 1700 cm^{-1} bleach, the 1606 cm^{-1} transient also shifts by 38 cm^{-1} to 1568 cm^{-1} . This band is assigned to the ribose group of FAD, an assignment that is supported by the observation that this band is absent in the TRIR spectra of lumiflavin where ribose adenosine diphosphate is replaced by a methyl group [96]. Figure 3.52 also demonstrates that the 1581 cm^{-1} and 1549 cm^{-1} bleaches shift to 1536 cm^{-1} and 1507 cm^{-1} , respectively upon uniform ^{13}C labeling of FAD. This is in agreement with these modes being assigned to the $\text{C}=\text{C}$ and $\text{C}=\text{N}$ stretching vibrations.

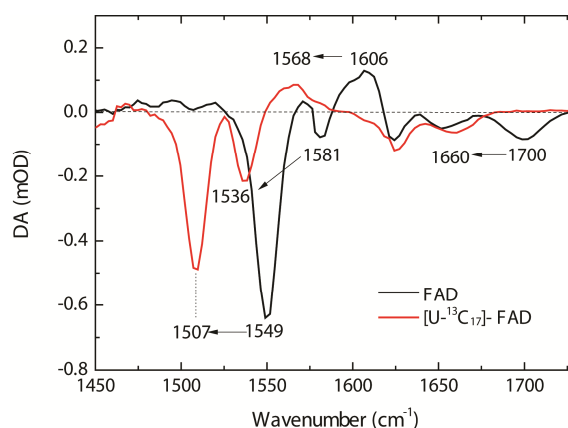


Figure 3.52 TRIR and calculated spectra of unlabeled FAD and $[\text{U}-^{13}\text{C}_{17}]$ -FAD in D_2O . TRIR spectra of 3 mM FAD (black) $[\text{U}-^{13}\text{C}_{17}]$ -FAD (red) in pH 8 phosphate buffer recorded with a time delay of 3 ps (the spectrum was measured by Allison Haigney [85]).

3.5 DNA photolyase from *Thermus thermophilus*

The CPD photolyase from *Thermus thermophilus* contains 420 amino acids. A semisynthetic DNA fragment encoding this enzyme was cloned into the vector pET22b⁺. The resulting construct directed the synthesis of a protein with a 6-histidine tag at its C-terminal end (see methods 2.3.1.9). The crude extract from recombinant *E. coli* culture showed no visible expression as judged by SDS-PAGE (Figure 3.53, **B**, lane 3). Nevertheless, the CPD photolyase was expressed and could be purified using a Ni⁺-column. Selected protein fractions were combined and applied once again to the Ni⁺-column. The column was washed with buffer containing 6 M guanidine-HCl to release the protein-bound FAD, and the resulting apoprotein was reconstituted on the column with FAD isotopologue. The reconstituted CPD photolyase was eluted from the column with imidazole (Figure 3.53, **B**).

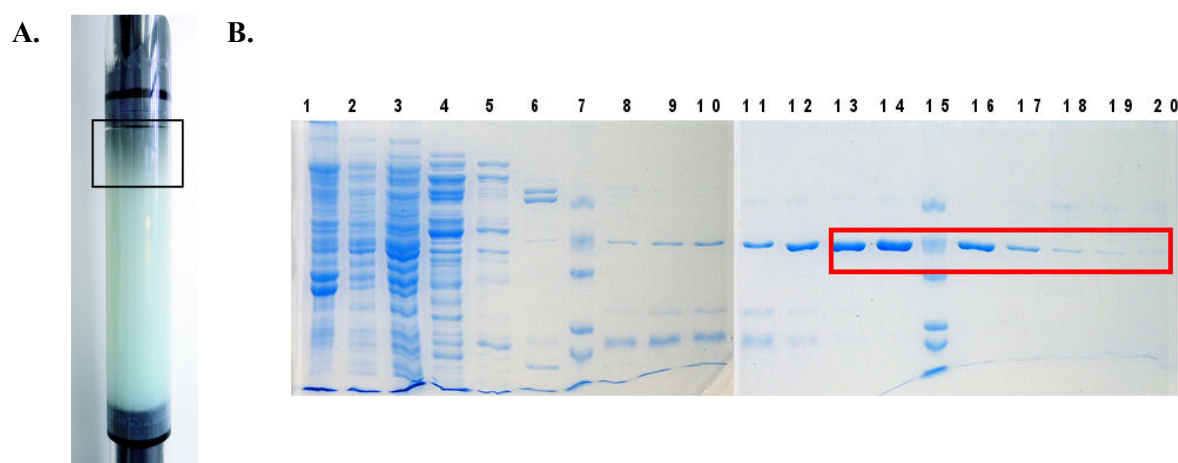


Figure 3.53 Isolation of CPD photolyase of *Thermus thermophilus*. **A**, CPD photolyase bound Ni⁺-column (dark band); **B**, 15 % SDS-PAGE (line 7 and 15 are protein size marker, box indicates target protein collected for further investigation).

The resulting protein appeared to be approximately 90 % pure as judged by SDS-PAGE with an apparent mass of 48 kDa (Figure 3.53, **B**). Reconstituted CPD photolyase has one chromophore-FAD. CPD photolyase appears on the Ni⁺-column as a dark grey band (Figure 3.53, **A**) under oxygen free conditions during the enzyme purification. It has been shown earlier that flavin in the CPD photolyase can be found in three different oxidation states: fully reduced (FADH₂), neutral radical (FADH[•]), and fully oxidized (FAD_{ox}) [105]. Figure 3.54 shows the absorption spectrum of the purified enzyme containing FAD. The neutral flavin radical complex of photolyase displays a characteristic absorption spectrum with two closely spaced bands at 561 and 600 (Figure 3.54, **B**; box). The flavin chromophore is easily oxidized by further dialysis (absorption spectrum shown in black in Figure 3.54, **B**). Prolonged storage of the enzyme without a reducing reagent resulted in the further oxidation of the flavin to the fully oxidized form. Both the neutral radical and fully oxidized forms of the enzyme can

be reduced to the FADH^2 by irradiation with UV/visible light under anaerobic conditions in the presence of DTT.

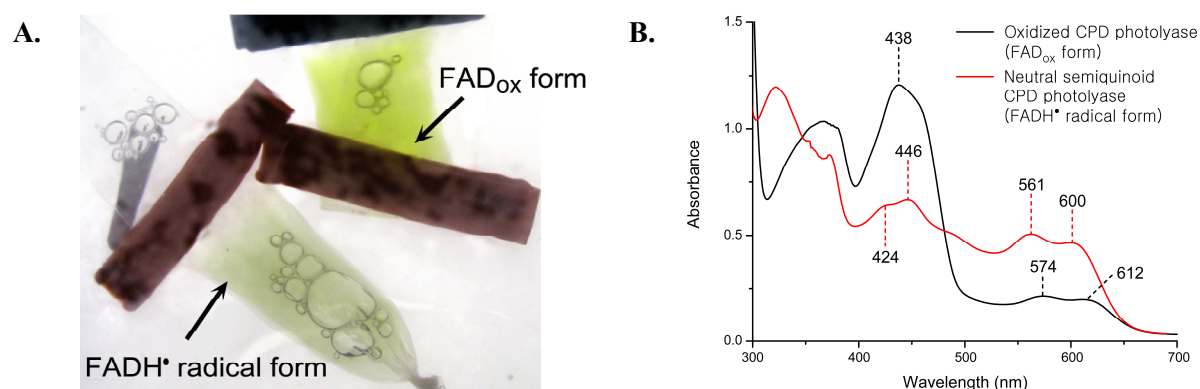


Figure 3.54 Isolated CPD photolyase of *Thermus thermophilus*. (**A**, Enzyme solution after dialysis; **B**, absorbance spectra of the enzyme in oxidized or radical form).

Following the procedure developed by Jorns et al. [141]), the enzyme activity was measured by monitoring the repair of T\diamondT dimer by DNA photolyase. UV-irradiated single-strand oligo-(dT)₁₈ DNA was used as a substrate. The photorepair was performed by illuminating the mixture containing 5 % acetone at pH 8 with white light, and the repair of the T\diamondT by DNA photolyase was monitored by changes in the absorption band at 266 nm (Figure 3.55, **B**) The data shown in the Figure 3.55 suggest that the photorepair reaction catalyzed by isolated and reconstituted CPD photolyase was almost completed already in 30 min after start.

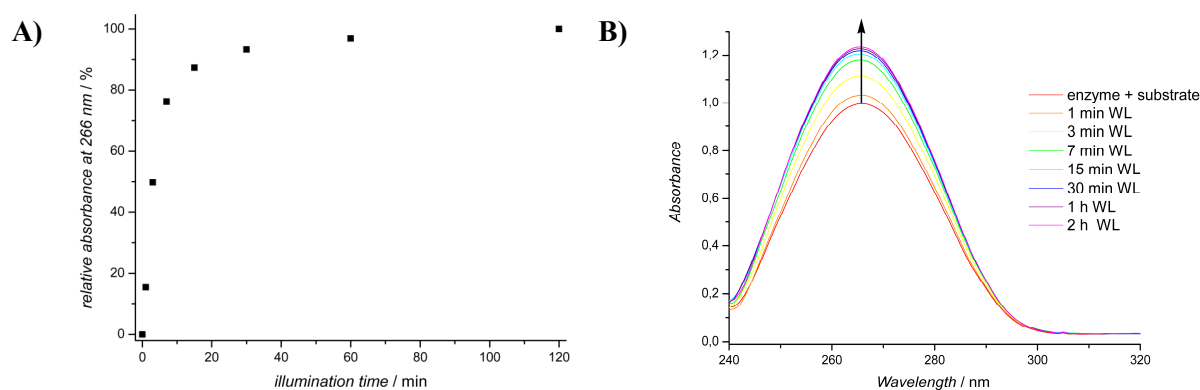


Figure 3.55 Enzyme activity test of CPD photolyase from *Thermus thermophilus* (the data were recorded and evaluated by Dr. Erik Schleicher (Albert-Ludwigs-Universität Freiburg, Freiburg, Germany)).

4 Reference

1. Kuhn, R., Wagner-Jauregg, T., Ber. deutsch. chem. Ges., 1933. 66,: p. 1577.
2. Karrer, P., *Vitamine A, C und B2*. Monatshefte für Chemie / Chemical Monthly, 1935. 66(1): p. 367-392.
3. Theorell, H., *Preparation in pure state of the effect group of yellow enzymes*. Biochemische Zeitschrift, 1935(275): p. 344 - 346.
4. Kuhn, R., H. Rudy, and F. Weygand, *Synthese der Lactoflavin-5'-Phosphorsäure*. Berichte der deutschen chemischen Gesellschaft (A and B Series), 1936. 69(6): p. 1543-1547.
5. Brown, G.M. and J.J. Reynolds, *BIOGENESIS OF WATER-SOLUBLE VITAMINS*. Annual Review of Biochemistry, 1963. 32: p. 419-&.
6. Plaut, G.W., C.M. Smith, and W.L. Alworth, *Biosynthesis of water-soluble vitamins*. Annu Rev Biochem, 1974. 43(0): p. 899-922.
7. Bacher, A., et al., *Biosynthesis of vitamin b2 (riboflavin)*. Annu Rev Nutr, 2000. 20: p. 153-67.
8. Bacher, A., et al., *Biosynthesis of riboflavin*. Vitam Horm, 2001. 61: p. 1-49.
9. Fischer, M. and A. Bacher, *Biosynthesis of flavocoenzymes*. Nat Prod Rep, 2005. 22(3): p. 324-50.
10. Fischer, M. and A. Bacher, *Biosynthesis of vitamin B2 in plants*. Physiologia Plantarum, 2006. 126(3): p. 304-318.
11. Fischer, M. and A. Bacher, *Biosynthesis of vitamin B2: Structure and mechanism of riboflavin synthase*. Arch Biochem Biophys, 2008. 474(2): p. 252-65.
12. Fischer, M. and A. Bacher, *Biosynthesis of vitamin B2: a unique way to assemble a xylene ring*. Chembiochem, 2011. 12(5): p. 670-80.
13. Foor, F. and G.M. Brown, *Purification and properties of guanosine triphosphate cyclohydrolase II from Escherichia coli*. J Biol Chem, 1975. 250(9): p. 3545-51.
14. Graham, D.E., H. Xu, and R.H. White, *A member of a new class of GTP cyclohydrolases produces formylaminopyrimidine nucleotide monophosphates*. Biochemistry, 2002. 41(50): p. 15074-84.
15. Grochowski, L.L., H. Xu, and R.H. White, *An iron(II) dependent formamide hydrolase catalyzes the second step in the archaeal biosynthetic pathway to riboflavin and 7,8-didemethyl-8-hydroxy-5-deazariboflavin*. Biochemistry, 2009. 48(19): p. 4181-8.
16. Spoonamore, J.E., et al., *Evolution of new function in the GTP cyclohydrolase II proteins of Streptomyces coelicolor*. Biochemistry, 2006. 45(39): p. 12144-55.
17. Horst, F. and J.A. Nunley, 2nd, *Ankle arthrodesis*. J Surg Orthop Adv, 2004. 13(2): p. 81-90.
18. Burrows, R.B. and G.M. Brown, *Presence of Escherichia coli of a deaminase and a reductase involved in biosynthesis of riboflavin*. J Bacteriol, 1978. 136(2): p. 657-67.
19. Bacher, A. and F. Lingens, *Biosynthesis of riboflavin. Formation of 2,5-diamino-6-hydroxy-4-(1'-D-ribitylamino)pyrimidine in a riboflavin auxotroph*. J Biol Chem, 1970. 245(18): p. 4647-52.
20. Hollander, I. and G.M. Brown, *Biosynthesis of riboflavin: reductase and deaminase of Ashbya gossypii*. Biochem Biophys Res Commun, 1979. 89(2): p. 759-63.
21. Richter, G., et al., *Biosynthesis of riboflavin: cloning, sequencing, and expression of the gene coding for 3,4-dihydroxy-2-butanone 4-phosphate synthase of Escherichia coli*. J Bacteriol, 1992. 174(12): p. 4050-6.
22. Volk, R. and A. Bacher, *Studies on the 4-carbon precursor in the biosynthesis of riboflavin. Purification and properties of L-3,4-dihydroxy-2-butanone-4-phosphate synthase*. J Biol Chem, 1990. 265(32): p. 19479-85.
23. Volk, R. and A. Bacher, *Biosynthesis of riboflavin. Studies on the mechanism of L-3,4-dihydroxy-2-butanone 4-phosphate synthase*. J Biol Chem, 1991. 266(31): p. 20610-8.
24. Kis, K., R. Volk, and A. Bacher, *Biosynthesis of riboflavin. Studies on the reaction mechanism of 6,7-dimethyl-8-ribityllumazine synthase*. Biochemistry, 1995. 34(9): p. 2883-92.
25. Keller, P.J., et al., *Biosynthesis of riboflavin: mechanism of formation of the ribitylamino linkage*. Biochemistry, 1988. 27(4): p. 1117-20.
26. Nielsen, P., et al., *Biosynthesis of riboflavin. Enzymatic formation of 6,7-dimethyl-8-ribityllumazine from pentose phosphates*. J Biol Chem, 1986. 261(8): p. 3661-9.

27. Kis, K., K. Kugelbrey, and A. Bacher, *Biosynthesis of riboflavin. The reaction catalyzed by 6,7-dimethyl-8-ribityllumazine synthase can proceed without enzymatic catalysis under physiological conditions.* J Org Chem, 2001. 66(8): p. 2555-9.
28. Plaut, G.W., *Studies on the stoichiometry of the enzymic conversion of 6,7-dimethyl-8-ribityllumazine to riboflavin.* J Biol Chem, 1960. 235: p. PC41-2.
29. Plaut, G.W., *Studies on the nature of the enzymic conversion of 6,7-dimethyl-8-ribityllumazine to riboflavin.* J Biol Chem, 1963. 238: p. 2225-43.
30. Wacker, H., et al., *4-(1'-D-Ribitylamino)-5-Amino-2,6-Dihydroxypyrimidine, the Second Product of the Riboflavin Synthetase Reaction.* J Biol Chem, 1964. 239: p. 3493-7.
31. Rowan, T. and H.C.S. Wood. *The Biosynthesis of Riboflavin.* in Proc. Chem. Soc. 1963. London: RSC Publishing.
32. Beach, R. and G.W. Plaut, *The formation of riboflavin from 6,7-dimethyl-8-ribityllumazine in acid media.* Tetrahedron Lett, 1969. 40: p. 3489-92.
33. Paterson, T. and H.C. Wood, *The biosynthesis of pteridines. VI. Studies of the mechanism of riboflavin biosynthesis.* J Chem Soc [Perkin 1], 1972. 8: p. 1051-6.
34. Eberhardt, S., et al., *Biosynthesis of riboflavin: an unusual riboflavin synthase of Methanobacterium thermoautotrophicum.* J Bacteriol, 1997. 179(9): p. 2938-43.
35. Fischer, M., et al., *Evolution of vitamin B2 biosynthesis: structural and functional similarity between pyrimidine deaminases of eubacterial and plant origin.* J Biol Chem, 2004. 279(35): p. 36299-308.
36. Ramsperger, A., et al., *Crystal structure of an archaeal pentameric riboflavin synthase in complex with a substrate analog inhibitor: stereochemical implications.* J Biol Chem, 2006. 281(2): p. 1224-32.
37. Beach, R.L. and G.W. Plaut, *Stereospecificity of the enzymatic synthesis of the o-xylene ring of riboflavin.* J Am Chem Soc, 1970. 92(9): p. 2913-6.
38. Illarionov, B., W. Eisenreich, and A. Bacher, *A pentacyclic reaction intermediate of riboflavin synthase.* Proc Natl Acad Sci U S A, 2001. 98(13): p. 7224-9.
39. Kim, R.R., et al., *Mechanistic insights on riboflavin synthase inspired by selective binding of the 6,7-dimethyl-8-ribityllumazine exomethylene anion.* J Am Chem Soc, 2010. 132(9): p. 2983-90.
40. Paterson, T. and H.C. Wood, *The biosynthesis of pteridines. VI. Studies of the mechanism of riboflavin biosynthesis.* J Chem Soc Perkin 1, 1972. 8: p. 1051-6.
41. Plaut, G.W.E. and R.L. Beach. *Substrate specificity and stereospecific mode of action of riboflavin synthase.* in *Flavins Flavoproteins, Proc. Int. Symp., 5th.* 1976.
42. Gerhardt, S., et al., *Studies on the reaction mechanism of riboflavin synthase: X-ray crystal structure of a complex with 6-carboxyethyl-7-oxo-8-ribityllumazine.* Structure, 2002. 10(10): p. 1371-81.
43. Schott, K., et al., *Riboflavin synthases of Bacillus subtilis. Purification and amino acid sequence of the alpha subunit.* J Biol Chem, 1990. 265(8): p. 4204-9.
44. Liao, D.I., et al., *Crystal structure of riboflavin synthase.* Structure, 2001. 9(5): p. 399-408.
45. Cushman, M., et al., *Synthesis of epimeric 6,7-bis(trifluoromethyl)-8-ribityllumazine hydrates. Stereoselective interaction with the light riboflavin synthase of Bacillus subtilis.* The Journal of Organic Chemistry, 1991. 56(15): p. 4603-4608.
46. Eberhardt, S., et al., *Domain structure of riboflavin synthase.* Eur J Biochem, 2001. 268(15): p. 4315-23.
47. Truffault, V., et al., *The solution structure of the N-terminal domain of riboflavin synthase.* J Mol Biol, 2001. 309(4): p. 949-60.
48. Meining, W., et al., *The structure of the N-terminal domain of riboflavin synthase in complex with riboflavin at 2.6A resolution.* J Mol Biol, 2003. 331(5): p. 1053-63.
49. Spencer, R., J. Fisher, and C. Walsh, *Preparation, characterization, and chemical properties of the flavin coenzyme analogues 5-deazariboflavin, 5-deazariboflavin 5'-phosphate, and 5-deazariboflavin 5'-diphosphate, 5'leads to 5'-adenosine ester.* Biochemistry, 1976. 15(5): p. 1043-53.
50. Karthikeyan, S., et al., *Crystal structure of human riboflavin kinase reveals a beta barrel fold and a novel active site arch.* Structure, 2003. 11(3): p. 265-73.
51. Manstein, D.J., et al., *Absolute stereochemistry of flavins in enzyme-catalyzed reactions.* Biochemistry, 1986. 25(22): p. 6807-16.

52. Sandoval, F.J. and S. Roje, *An FMN hydrolase is fused to a riboflavin kinase homolog in plants*. J Biol Chem, 2005. 280(46): p. 38337-45.
53. Illarionov, B., et al., *Rapid preparation of isotopolog libraries by in vivo transformation of ¹³C-glucose. Studies on 6,7-dimethyl-8-ribityllumazine, a biosynthetic precursor of vitamin B₂*. J Org Chem, 2004. 69(17): p. 5588-94.
54. Romisch, W., et al., *Rapid one-pot synthesis of riboflavin isotopomers*. J Org Chem, 2002. 67(25): p. 8890-4.
55. Massey, V., *The chemical and biological versatility of riboflavin*. Biochem Soc Trans, 2000. 28(4): p. 283-96.
56. Briggs, W.R. and E. Huala, *Blue-light photoreceptors in higher plants*. Annu Rev Cell Dev Biol, 1999. 15: p. 33-62.
57. Sancar, A., *Mechanisms of DNA excision repair*. Science, 1994. 266(5193): p. 1954-6.
58. Mewies, M., W.S. McIntire, and N.S. Scrutton, *Covalent attachment of flavin adenine dinucleotide (FAD) and flavin mononucleotide (FMN) to enzymes: the current state of affairs*. Protein Sci, 1998. 7(1): p. 7-20.
59. Losi, A., E. Ternelli, and W. Gartner, *Tryptophan fluorescence in the Bacillus subtilis phototropin-related protein YtvA as a marker of interdomain interaction*. Photochem Photobiol, 2004. 80: p. 150-3.
60. Briggs, W.R., et al., *The phototropin family of photoreceptors*. Plant Cell, 2001. 13(5): p. 993-7.
61. Gomelsky, M. and G. Klug, *BLUF: a novel FAD-binding domain involved in sensory transduction in microorganisms*. Trends Biochem Sci, 2002. 27(10): p. 497-500.
62. van der Horst, M.A. and K.J. Hellingwerf, *Photoreceptor proteins, "star actors of modern times": a review of the functional dynamics in the structure of representative members of six different photoreceptor families*. Acc Chem Res, 2004. 37(1): p. 13-20.
63. Lin, W. and H. Frei, *Anchored metal-to-metal charge-transfer chromophores in a mesoporous silicate sieve for visible-light activation of titanium centers*. J Phys Chem B, 2005. 109(11): p. 4929-35.
64. Essen, L.O., *Photolyases and cryptochromes: common mechanisms of DNA repair and light-driven signaling?* Curr Opin Struct Biol, 2006. 16(1): p. 51-9.
65. Huala, E., et al., *Arabidopsis NPH1: a protein kinase with a putative redox-sensing domain*. Science, 1997. 278(5346): p. 2120-3.
66. Christie, J.M., et al., *LOV (light, oxygen, or voltage) domains of the blue-light photoreceptor phototropin (nph1): binding sites for the chromophore flavin mononucleotide*. Proc Natl Acad Sci U S A, 1999. 96(15): p. 8779-83.
67. Losi, A., et al., *First evidence for phototropin-related blue-light receptors in prokaryotes*. Biophys J, 2002. 82(5): p. 2627-34.
68. Taylor, B.L. and I.B. Zhulin, *PAS domains: internal sensors of oxygen, redox potential, and light*. Microbiol Mol Biol Rev, 1999. 63(2): p. 479-506.
69. Crosson, S. and K. Moffat, *Structure of a flavin-binding plant photoreceptor domain: insights into light-mediated signal transduction*. Proc Natl Acad Sci U S A, 2001. 98(6): p. 2995-3000.
70. Crosson, S. and K. Moffat, *Photoexcited structure of a plant photoreceptor domain reveals a light-driven molecular switch*. Plant Cell, 2002. 14(5): p. 1067-75.
71. Fedorov, R., et al., *Crystal structures and molecular mechanism of a light-induced signaling switch: The Phot-LOV1 domain from Chlamydomonas reinhardtii*. Biophys J, 2003. 84(4): p. 2474-82.
72. Crosson, S., S. Rajagopal, and K. Moffat, *The LOV domain family: photoresponsive signaling modules coupled to diverse output domains*. Biochemistry, 2003. 42(1): p. 2-10.
73. Kottke, T., et al., *Irreversible photoreduction of flavin in a mutated Phot-LOV1 domain*. Biochemistry, 2003. 42(33): p. 9854-62.
74. Salomon, M., et al., *An optomechanical transducer in the blue light receptor phototropin from Avena sativa*. Proc Natl Acad Sci U S A, 2001. 98(22): p. 12357-61.
75. Kasahara, M., et al., *Photochemical properties of the flavin mononucleotide-binding domains of the phototropins from Arabidopsis, rice, and Chlamydomonas reinhardtii*. Plant Physiol, 2002. 129(2): p. 762-73.
76. Swartz, T.E., et al., *The photocycle of a flavin-binding domain of the blue light photoreceptor phototropin*. J Biol Chem, 2001. 276(39): p. 36493-500.

77. Salomon, M., et al., *Photochemical and mutational analysis of the FMN-binding domains of the plant blue light receptor, phototropin*. *Biochemistry*, 2000. 39(31): p. 9401-10.
78. Christie, J.M., *Phototropin blue-light receptors*. *Annu Rev Plant Biol*, 2007. 58: p. 21-45.
79. Eisenreich, W., et al., *¹³C Isotopologue editing of FMN bound to phototropin domains*. *FEBS J*, 2007. 274(22): p. 5876-90.
80. Schleicher, E., et al., *On the reaction mechanism of adduct formation in LOV domains of the plant blue-light receptor phototropin*. *J Am Chem Soc*, 2004. 126(35): p. 11067-76.
81. Corchnoy, S.B., et al., *Intramolecular proton transfers and structural changes during the photocycle of the LOV2 domain of phototropin I*. *J Biol Chem*, 2003. 278(2): p. 724-31.
82. Harper, S.M., J.M. Christie, and K.H. Gardner, *Disruption of the LOV-Jalpha helix interaction activates phototropin kinase activity*. *Biochemistry*, 2004. 43(51): p. 16184-92.
83. Salomon, M., et al., *Mapping of low- and high-fluence autophosphorylation sites in phototropin I*. *Biochemistry*, 2003. 42(14): p. 4217-25.
84. Masuda, S. and C.E. Bauer, *AppA is a blue light photoreceptor that antirepresses photosynthesis gene expression in Rhodospirillum rubrum*. *Cell*, 2002. 110(5): p. 613-23.
85. Haigney, A., et al., *Ultrafast infrared spectroscopy of an isotope-labeled photoactivatable flavoprotein*. *Biochemistry*, 2011. 50(8): p. 1321-8.
86. Laan, W., et al., *Initial characterization of the primary photochemistry of AppA, a blue-light-using flavin adenine dinucleotide-domain containing transcriptional antirepressor protein from Rhodospirillum rubrum: a key role for reversible intramolecular proton transfer from the flavin adenine dinucleotide chromophore to a conserved tyrosine?* *Photochem Photobiol*, 2003. 78(3): p. 290-7.
87. Masuda, S., K. Hasegawa, and T.A. Ono, *Light-induced structural changes of apoprotein and chromophore in the sensor of blue light using FAD (BLUF) domain of AppA for a signaling state*. *Biochemistry*, 2005. 44(4): p. 1215-24.
88. Unno, M., et al., *Light-induced structural changes in the active site of the BLUF domain in AppA by Raman spectroscopy*. *J Phys Chem B*, 2005. 109(25): p. 12620-6.
89. Anderson, S., et al., *Structure of a novel photoreceptor, the BLUF domain of AppA from Rhodospirillum rubrum*. *Biochemistry*, 2005. 44(22): p. 7998-8005.
90. Grinstead, J.S., et al., *The solution structure of the AppA BLUF domain: insight into the mechanism of light-induced signaling*. *Chembiochem*, 2006. 7(1): p. 187-93.
91. Jung, A., et al., *Structure of a bacterial BLUF photoreceptor: insights into blue light-mediated signal transduction*. *Proc Natl Acad Sci U S A*, 2005. 102(35): p. 12350-5.
92. Unno, M., S. Kikuchi, and S. Masuda, *Structural refinement of a key tryptophan residue in the BLUF photoreceptor AppA by ultraviolet resonance Raman spectroscopy*. *Biophys J*, 2010. 98(9): p. 1949-56.
93. Stelling, A.L., et al., *Ultrafast structural dynamics in BLUF domains: transient infrared spectroscopy of AppA and its mutants*. *J Am Chem Soc*, 2007. 129(50): p. 15556-64.
94. Gauden, M., et al., *Photocycle of the flavin-binding photoreceptor AppA, a bacterial transcriptional antirepressor of photosynthesis genes*. *Biochemistry*, 2005. 44(10): p. 3653-62.
95. Gauden, M., et al., *On the role of aromatic side chains in the photoactivation of BLUF domains*. *Biochemistry*, 2007. 46(25): p. 7405-15.
96. Kondo, M., et al., *Ultrafast vibrational spectroscopy of the flavin chromophore*. *J Phys Chem B*, 2006. 110(41): p. 20107-10.
97. Domratcheva, T., et al., *Molecular models predict light-induced glutamine tautomerization in BLUF photoreceptors*. *Biophys J*, 2008. 94(10): p. 3872-9.
98. Sadeghian, K., M. Bocola, and M. Schutz, *A conclusive mechanism of the photoinduced reaction cascade in blue light using flavin photoreceptors*. *J Am Chem Soc*, 2008. 130(37): p. 12501-13.
99. Friedberg, E.C., et al., *DNA repair and mutagenesis*. 1995, Washington, DC: ASM press.
100. Sancar, G.B., *DNA photolyases: physical properties, action mechanism, and roles in dark repair*. *Mutat Res*, 1990. 236(2-3): p. 147-60.
101. Sancar, A., *Structure and Function of DNA Photolyase and Cryptochrome Blue-Light Photoreceptors*. *Chemical Reviews*, 2003. 103(6): p. 2203-2238.
102. Blackburn, G.M. and R.J.H. Davies, *The structure of thymine photo-dimer*. *Chemical Communications (London)*, 1965(11): p. 215-216.

103. Blackburn, G.M. and R.J. Davies, *The structure of DNA-derived thymine dimer*. Biochem Biophys Res Commun, 1966. 22(6): p. 704-6.
104. Otsoshi, E., et al., *Respective roles of cyclobutane pyrimidine dimers, (6-4)photoproducts, and minor photoproducts in ultraviolet mutagenesis of repair-deficient xeroderma pigmentosum A cells*. Cancer Res, 2000. 60(6): p. 1729-35.
105. Sancar, A., *Structure and function of DNA photolyase*. Biochemistry, 1994. 33(1): p. 2-9.
106. Sancar, G.B., *Enzymatic photoreactivation: 50 years and counting*. Mutat Res, 2000. 451(1-2): p. 25-37.
107. Nakajima, S., et al., *Cloning and characterization of a gene (UVR3) required for photorepair of 6-4 photoproducts in Arabidopsis thaliana*. Nucleic Acids Res, 1998. 26(2): p. 638-44.
108. Todo, T., *Functional diversity of the DNA photolyase/blue light receptor family*. Mutat Res, 1999. 434(2): p. 89-97.
109. Schleicher, E., et al., *Light-induced reactions of Escherichia coli DNA photolyase monitored by Fourier transform infrared spectroscopy*. FEBS J, 2005. 272(8): p. 1855-66.
110. Jorns, M.S., et al., *Action mechanism of Escherichia coli DNA photolyase. II. Role of the chromophores in catalysis*. J Biol Chem, 1987. 262(1): p. 486-91.
111. Sancar, G.B., et al., *Action mechanism of Escherichia coli DNA photolyase. I. Formation of the enzyme-substrate complex*. J Biol Chem, 1987. 262(1): p. 478-85.
112. Payne, G., et al., *The active form of Escherichia coli DNA photolyase contains a fully reduced flavin and not a flavin radical, both in vivo and in vitro*. Biochemistry, 1987. 26(22): p. 7121-7.
113. Kim, S.T., et al., *Time-resolved EPR studies with DNA photolyase: excited-state FADH0 abstracts an electron from Trp-306 to generate FADH-, the catalytically active form of the cofactor*. Proc Natl Acad Sci U S A, 1993. 90(17): p. 8023-7.
114. Kim, S.T. and A. Sancar, *Photochemistry, photophysics, and mechanism of pyrimidine dimer repair by DNA photolyase*. Photochem Photobiol, 1993. 57(5): p. 895-904.
115. Ueda, T., et al., *NMR study of repair mechanism of DNA photolyase by FAD-induced paramagnetic relaxation enhancement*. J Biol Chem, 2004. 279(50): p. 52574-9.
116. Komori, H., et al., *Crystal structure of thermostable DNA photolyase: pyrimidine-dimer recognition mechanism*. Proc Natl Acad Sci U S A, 2001. 98(24): p. 13560-5.
117. Klare, J.P., et al., *Effects of solubilization on the structure and function of the sensory rhodopsin II/transducer complex*. J Mol Biol, 2006. 356(5): p. 1207-21.
118. Dower, W.J., J.F. Miller, and C.W. Ragsdale, *High efficiency transformation of E. coli by high voltage electroporation*. Nucleic Acids Res, 1988. 16(13): p. 6127-45.
119. Bullock, W.O., J.M. Fernandez, and J.M. Short, *XII-Blue: A High Efficiency Plasmid Transforming recA Escherichia coli Strain With Beta-Galactosidase Selection*. Biotechniques, 1987. 5: p. 376-379.
120. Stueber, D., H. Matile, and G. Garotta, *System for high level production in Escherichia coli and rapid application to epitope mapping, preparation of antibodies and structurefunction analysis*. immunological Methods, 1990. IV: p. 121-152.
121. Ostanin, K., et al., *Overexpression, site-directed mutagenesis, and mechanism of Escherichia coli acid phosphatase*. J Biol Chem, 1992. 267(32): p. 22830-6.
122. Fischer, M., et al., *Design of Biofunctional Assemblies on Solids through Recombinant Spherical Bacterial Protein Lumazine Synthase*. Chemphyschem, 2001. 2(10): p. 623-627.
123. Laemmli, U.K., *Cleavage of structural proteins during the assembly of the head of bacteriophage T4*. Nature, 1970. 227(5259): p. 680-5.
124. Read, S.M. and D.H. Northcote, *Minimization of variation in the response to different proteins of the Coomassie blue G dye-binding assay for protein*. Anal Biochem, 1981. 116(1): p. 53-64.
125. Plaut, G.W.E., ed. *Metabolism of water-soluble vitamins: The biosynthesis of riboflavin*. In: Florkin, M., Stotz, E.H. Comprehensive Biochemistry. Vol. 21. 1971, Elsevier, Amsterdam. 11-45.
126. Koziol, J., *Fluorometric analyses of riboflavin and its coenzymes*. . Methods Enzymol, 1971. 18B: p. 253-285.
127. Hinkson, J.W., *Azotobacter free-radical flavoprotein. Preparation and properties of the apoprotein*. Biochemistry, 1968. 7(7): p. 2666-72.
128. Jorns, M.S., et al., *Chromophore function and interaction in Escherichia coli DNA photolyase: reconstitution of the apoenzyme with pterin and/or flavin derivatives*. Biochemistry, 1990. 29(2): p. 552-61.

129. Eberhardt, S., et al., *Cloning, sequencing, mapping and hyperexpression of the ribC gene coding for riboflavin synthase of Escherichia coli*. Eur J Biochem, 1996. 242(3): p. 712-9.
130. Illarionov, B., et al., *Riboflavin synthase of Escherichia coli. Effect of single amino acid substitutions on reaction rate and ligand binding properties*. J Biol Chem, 2001. 276(15): p. 11524-30.
131. Bown, D.H., et al., *Solution structures of 6,7-dimethyl-8-substituted-lumazines. Carbon-13 NMR evidence for intramolecular ether formation*. The Journal of Organic Chemistry, 1986. 51(13): p. 2461-2467.
132. Macheroux, P.G., S.; Hastings, J. W. *Bacterial, Luciferase: Bioluminescence Emission Using Lumazines as Substrates*. Flavins and Flavoproteins 1993, 1994: p. 839-842.
133. Plaut, G.W., R.L. Beach, and T. Aogaichi, *Studies on the mechanism of elimination of protons from the methyl groups of 6,7-dimethyl-8-ribityllumazine by riboflavin synthetase*. Biochemistry, 1970. 9(4): p. 771-85.
134. Illarionov, B., et al., *Presteady state kinetic analysis of riboflavin synthase*. J Biol Chem, 2003. 278(48): p. 47700-6.
135. Kelly, M.J., et al., *The NMR structure of the 47-kDa dimeric enzyme 3,4-dihydroxy-2-butanone-4-phosphate synthase and ligand binding studies reveal the location of the active site*. Proc Natl Acad Sci U S A, 2001. 98(23): p. 13025-30.
136. Bacher, A., et al., *Biosynthesis of riboflavin: structure and mechanism of lumazine synthase*. Biochem Soc Trans, 1996. 24(1): p. 89-94.
137. Ritsert, K., et al., *Studies on the lumazine synthase/riboflavin synthase complex of Bacillus subtilis: crystal structure analysis of reconstituted, icosahedral beta-subunit capsids with bound substrate analogue inhibitor at 2.4 Å resolution*. J Mol Biol, 1995. 253(1): p. 151-67.
138. Klinke, S., et al., *Structural and kinetic properties of lumazine synthase isoenzymes in the order Rhizobiales*. J Mol Biol, 2007. 373(3): p. 664-80.
139. Paterson, T. and H.C.S. Wood, *Deuterium exchange of C-methyl protons in 6,7-dimethyl-8-D-ribityl-lumazine, and studies of the mechanism of riboflavin biosynthesis*. J. Chem. Soc. D, 1969. 6: p. 290 - 291.
140. Brosi, R., et al., *Hindered rotation of a cofactor methyl group as a probe for protein-cofactor interaction*. J Am Chem Soc, 2010. 132(26): p. 8935-44.
141. Jorns, M.S., G.B. Sancar, and A. Sancar, *Identification of oligothymidylates as new simple substrates for Escherichia coli DNA photolyase and their use in a rapid spectrophotometric enzyme assay*. Biochemistry, 1985. 24(8): p. 1856-61.

GHS-Gefahrstoffkennzeichnung

Chemicals	H- und P-Sätze
2-Mercaptoethanol	H: 301-310-330-315-318-410 P: 280-273-302+352-304+340-305+351+338-309-310
Acetic acid	H: 226-314 P: 280-301+330+331-307+310-305+351+338
Acetone	H: 225-319-336 EUH066 P: 210-233-305+351+338
Acrylamide/bis-acrylamide (29 : 1), 40 %	H: 350-340-361f-301-372-332-312-319-315-317 P: 201-280-301+310-305+351+338-308+313
Agar	No safety data available
Agarose	No safety data available
Ammonium formate	H: 315-319-335 P: 261-305+351+338
Ammonium persulfate	H: 272-302-315-319-335-334-317 P: 280-305+351+338-302+352-304+341-342+311
Ammonium sulfate	No safety data available
Ampicillin	H: 315-317-319-334-335 P: 261-280-305+351+338-342+311
Biotin	No safety data available
Bromophenol Blue	No safety data available
Calcium chloride	H: 319 P: 305+351+338
Casein hydrolysate	No safety data available
Cobalt(II) chloride	H: 350i-341-360F-302-334-317-410 P: 201-281-273-308+313-304+340
Copper(II) chloride	H: 302-315-319-410 P: 260-273-302+352-305+351+338
Cyanocobalamin	No safety data available
D ₂ O 99.9 %	No safety data available
DMSO-d ₆ 99.9 %	No safety data available
dNTP mix	No safety data available
Dithiothreitol	H: 302-315-319 P: 302+352-305+351+338
EDTA	H: 319 P: 305+351+338
Ethanol	H: 225 P: 210
Ethidium bromide	H: 341-330-302 P: 281-302+352-305+351+338-304+340-309-310
Iron(III) chloride	H: 302-315-318-290 P: 280-302+352-305+351+338-313
Folic acid	No safety data available
Glucose	No safety data available
Glycerol	No safety data available
Glycine	No safety data available
Guanidinium chloride	H: 302-319-315 P: 305+351+338-302+352
Hepes	No safety data available

Hydrochloric Acid	H: 314-335 P: 260-301+330+331-303+361+353-305+351+338-405-501
Imidazole	H: 302-314-361d P: 280-301+330+331-305+351+338-309-310
IPTG (Isopropyl-1-thio-β-D-galactopyranoside)	No safety data available
Kanamycine	H: 360 P: 201-308+313
Magnesium Chloride	No safety data available
Manganese Chloride	H: 301-412 P: 273-301+310
Methanol	H: 225-331-311-301-370 P: 210-233-280-302+352
Magnesium sulfate	No safety data available
MOPS	No safety data available
Ammonium chloride	H: 302-319 P: 305+351+338
Nickel sulfate	H: 350i-341-360D-372-332-302-315-334-317-410 P: 201-280-273-308+313-342+311-302+352
4-Aminobenzoic acid	H: keine H-Sätze P: 260
Phenylmethanesulfonyl fluoride (PMSF)	H: 301-314 P: 280-305+351+338-310
Phosphoric acid	H: 314 P: 280-301+330+331-305+351+338-309+310
Potassium acetate	No safety data available
Potassium chloride	No safety data available
Potassium phosphate	No safety data available
Pyridoxamin hydrochloride	No safety data available
Ribose	No safety data available
Ribose 5-phosphate	No safety data available
Rubidium chloride	No safety data available
Sodium dodecyl sulfate (SDS)	H: 228-311-302-335-315-319 P: 210-280-304+340-305+351+338-309+310
Serva Blue G (Coomassie Brilliant Blue G-250)	No safety data available
Sodium azide	H: 300-400-410 P: 273-309-310
Sodium chloride	No safety data available
sodium citrate	No safety data available
Sodium hydroxide	H: 314 P: 280-301+330+331-309-310-305+351+338
Sodium phosphate	No safety data available
Sucrose	No safety data available
Tetramethylethylenediamine (TEMED)	H: 225-332-302-314 P: 210-233-280-301+330+331-305+351+338-309+310
Thiamin hydrochloride	No safety data available
Tris (Hydroxymethyl) aminomethane	H: 315-319-335 P: 261-305+351+338
Yeast extract	No safety data available
Zinc acetate	H: 302-410 P: 262-273

Acknowledgements

First and foremost, I would like to thank Professor Markus Fischer for providing me an opportunity to perform my PhD Study in Hamburg. It is a pleasure to work in this group. I would like to deeply acknowledge the H. Wilhelm Schaumann-Stiftung for financial support (scholarship and donation).

I would like to express my deep and sincere gratitude to Professor Adelbert Bacher for his ideas, support and fruitful discussions as well as the understanding, encouragement and personal guidance that have been always inspiring and motivating for me.

I am deeply grateful to Dr. Boris Illarionov, for introducing me to all the technics used and for priceless advice and insight throughout my work. His wisdom and patience provided a remarkable influence on my entire research.

I want to thank Dr. Wolfgang Eisenreich and Dr. Monika Joshi for essentially teaching me everything I know about NMR spectroscopy and its application in the present work, and for their detailed and constructive comments, helpfulness and for important support throughout this work. I would also like to thank Dr. Ilka Haase for kind support and advice.

I warmly thank Prof. Stefan Weber and PD Dr. Erik Schleicher of Albert-Ludwigs-Universität Freiburg, and Richard Brosi of Freie Universität Berlin for outstanding co-operation in the area of EPR and ENDOR spectroscopy. Their help and extensive discussions around my work have been very helpful for this study.

I would like to say a big thank you to everyone from the Department of Food Chemistry for all the help and friendship during my studies and for their support in the laboratory. And I would like to thank all my friends in Korea and in Germany.

Last but not least, I thank my family who have always believed in me and have supported me all the time. Without their support, encouragement and love I could never have completed my PhD studies. This work is dedicated to my parents.

Curriculum Vitae

Personal Details

Name; Ryuryun Kim
Date of Birth: 18. 07. 1982
Place of Birth; Po-Hang, South Korea
Nationality; South Korea

Education

- Jan. '08 – Present PhD Thesis at University of Hamburg, Hamburg, Germany
- Supervisor: Prof. Dr. Markus Fischer
 - Title: **Biosynthesis of Vitamin B₂ (Riboflavin). Studies on the Reaction Mechanism of Riboflavin Synthase.**
- Dec. '06 – Dec. '07 Technical University of Munich, Germany
Group of Prof. Dr. Adelbert Bacher : Biochemistry
- Mar. '05 – Feb. '07 Master of Science in Biochemistry, Chungnam National University,
Daejeon, Korea
- Supervisor: Prof. Chan-Yong Lee
 - Title: **Binding Properties of the Mutant Proteins of N-Terminal Domain of Riboflavin Synthase.**
- Mar. '01 – Feb. '05 Bachelor of Science in Biochemistry, Chungnam National
University, Daejeon, Korea
- Feb. '01 General Qualification for University Entrance,
Semyeong High School, Po-hang, South Korea

EIDESSTATTLICHE ERKLÄRUNG

Hiermit erkläre ich an Eides Statt, dass ich die vorliegende Dissertation „Biosynthesis of Vitamin B₂ (Riboflavin). Studies on the Reaction Mechanism of Riboflavin Synthase.“ selbstständig angefertigt und nur die von mir angegebenen Quellen und Hilfsmittel verwendet habe.

Ich erkläre außerdem, daß diese Dissertation weder in gleicher noch in anderer Form bereits in einem anderen Prüfungsverfahren vorgelegen hat. Es handelt sich hierbei um meinen ersten Promotionsversuch.

Hamburg, im März 2012